2018

Cellular Sheaves And Cosheaves For Distributed Topological Data Analysis

Hee Rhang Yoon
University of Pennsylvania, irishryoon@gmail.com

Cellular Sheaves And Cosheaves For Distributed Topological Data Analysis

Abstract
This dissertation proposes cellular sheaf theory as a method for decomposing data analysis problems. We present novel approaches to problems in pursuit and evasion games and topological data analysis, where cellular sheaves and cosheaves are used to extract global information from data distributed with respect to time, boolean constraints, spatial location, and density. The main contribution of this dissertation lies in the enrichment of a fundamental tool in topological data analysis, called persistent homology, through cellular sheaf theory. We present a distributed computation mechanism of persistent homology using cellular cosheaves. Our construction is an extension of the generalized Mayer-Vietoris principle to filtered spaces obtained via a sequence of spectral sequences. We discuss a general framework in which the distribution scheme can be adapted according to a user-specific property of interest. The resulting persistent homology reflects properties of the topological features, allowing the user to perform refined data analysis. Finally, we apply our construction to perform a multi-scale analysis to detect features of varying sizes that are overlooked by standard persistent homology.

Degree Type
Dissertation

Degree Name
Doctor of Philosophy (PhD)

Graduate Group
Applied Mathematics

First Advisor
Robert W. Ghrist

Subject Categories
Applied Mathematics

CELLULAR SHEAVES AND COSHEAVES
FOR DISTRIBUTED TOPOLOGICAL DATA ANALYSIS

Hee Rhang Yoon

A DISSERTATION

in

Applied Mathematics and Computational Science

Presented to the Faculties of the University of Pennsylvania
in
Partial Fulfillment of the Requirements for the
Degree of Doctor of Philosophy

2018

Supervisor of Dissertation

____

Robert W. Ghrist, Andrea Mitchell University Professor of Mathematics and Electrical and Systems Engineering

Graduate Group Chairperson

____

Charles L. Epstein, Thomas A. Scott Professor of Mathematics

Dissertation Committee
Robert W. Ghrist, Andrea Mitchell University Professor of Mathematics and Electrical and Systems Engineering
Jonathan Block, Professor of Mathematics
Alejandro Ribeiro, Rosenbluth Associate Professor of Electrical and Systems Engineering

To my teacher Jee-Yun Song

ACKNOWLEDGEMENTS

I would like to express my deepest gratitude to my advisor Robert Ghrist for every opportunity he provided for me. His dedication and creativity have truly been inspiring. Thank you, Rob, for your faith in me that has kept me grounded during low points of graduate school.

This work has benefited greatly from conversations with those who shared valuable insight. Thank you, Vin de Silva, Sanjeevi Krishnan, Vidit Nanda, Chad Giusti, Rachel Levanger, and Gregory Henselman, for your thoughts, suggestions, and questions. Special thanks to Darrick Lee for helping me refine drafts of this dissertation. I am greatly indebted to Justin Curry, whose insightful dissertation has been a continual source for learning.

Special thanks are due to my dissertation committee: Jonathan Block and Alejandro Ribeiro, for teaching me algebraic topology and showing me questions and perspectives in engineering.

I would like to express my gratitude to those who encouraged and guided me as I discovered the joy of mathematics at Swarthmore College: Janet Talvacchia, William Kronholm, Abram Lipman, Phil Everson, Aimee Johnson, Linda Chen, Deb Bergstrand, Stephen Maurer, Gene Klotz, Charles Grinstead, Ralph Gomez, and Don Shimamoto.

Finally, I thank my family for their unconditional support. Mom and dad, thank you for always believing in me. Thank you to my mother-in-law and father-in-law for their constant encouragement. Dan and Annie, you guys inspire me to relentlessly pursue my heart's desires. Paul, you made me laugh during difficult times. Madelyn and Watson, your presence in this world bring so much joy. Thank you, Jun, for making every day better.

ABSTRACT

CELLULAR SHEAVES AND COSHEAVES FOR DISTRIBUTED TOPOLOGICAL DATA ANALYSIS

Hee Rhang Yoon

Robert W. Ghrist

This dissertation proposes cellular sheaf theory as a method for decomposing data analysis problems. We present novel approaches to problems in pursuit and evasion games and topological data analysis, where cellular sheaves and cosheaves are used to extract global information from data distributed with respect to time, boolean constraints, spatial location, and density. The main contribution of this dissertation lies in the enrichment of a fundamental tool in topological data analysis, called persistent homology, through cellular sheaf theory. We present a distributed computation mechanism of persistent homology using cellular cosheaves. Our construction is an extension of the generalized Mayer-Vietoris principle to filtered spaces obtained via a sequence of spectral sequences. We discuss a general framework in which the distribution scheme can be adapted according to a user-specific property of interest. The resulting persistent homology reflects properties of the topological features, allowing the user to perform refined data analysis. Finally, we apply our construction to perform a multi-scale analysis to detect features of varying sizes that are overlooked by standard persistent homology.

Contents

List of Tables

List of Figures

Chapter 1

Introduction

1.1 An Introduction to Applied Topology

Applied topology is an extension of both the subject and the tools of topology. The subject of topology, in the context of data analysis, seeks an understanding of qualitative features such as shape, inconsistencies, and obstructions in data. The tools of topology allow one to combine locally gathered information or locally solved solutions to obtain global information. The tools are often used to study topological information, but they can also be applied to study questions that may not seem topological at first glance. Applied topology embodies both the subject and the tools of topology, and the degree of emphasis on the different aspects may vary depending on the application.

This dissertation focuses on two important aspects of applied topology: persistent homology and cellular (co)sheaf theory. Persistent homology is a fundamental tool in topological data analysis that extracts qualitative features of data and summarizes the information in a barcode. Its use has revealed interesting features in various problems in neuroscience [16], biology [22], sensor networks [25], and many other subjects. There are various great sources for an introduction to persistent homology, including the survey articles [7] and [14]. A selection of topics from persistent homology that are most closely relevant to this dissertation is provided in Chapter 2.

Cellular sheaf theory epitomizes the idea of extracting global information from local data, rendering itself an ideal candidate for distributed computation tools. Topics from cellular sheaf theory that are necessary for the understanding of this dissertation are provided in Chapter 2. A selection of applications of sheaf theory that emphasizes different aspects of topological information and distribution are included in Chapter 2 and Chapter 3. A rich introduction to cellular sheaf theory can be found in [10].

This dissertation uses the tool of sheaf theory to strengthen persistent homology, both in terms of the computation aspect (Chapter 4) and in terms of the information revealed (Chapter 3 and Chapter 5).

1.2 Contributions

The main contributions of this dissertation are the following.

In Chapter 3, novel sheaf theoretic approaches to variations of pursuit and evasion problems are proposed. Cellular sheaves and cosheaves are utilized to analyze data distributed with respect to time and boolean relations.

In Chapter 4, a distributed computation scheme for persistent homology is provided using cellular cosheaves. The generalized Mayer-Vietoris principle [5], phrased using the language of cellular (co)sheaf theory, provides a mechanism for computing homology in a distributed manner. Our construction addresses the question of relating the generalized Mayer-Vietoris sequences of filtered spaces. Let $X^1 \subseteq X^2 \subseteq \cdots \subseteq X^N$ be a filtration of a topological space. For each X^i, assume that there exists a finite open cover $\mathcal{U}^i = \{U^i_j\}_{j\in J}$ of X^i such that any triple intersection of members of $\mathcal{U}^i$ is trivial. Furthermore, assume that there is a filtration $U^1_j \subseteq U^2_j \subseteq \cdots \subseteq U^N_j$ for each $j \in J$. Then, we obtain the following exact sequences.

$$
\begin{array}{ccccccccc}
\cdots & \xrightarrow{f^1} & \bigoplus_{j\in J} H_n(U^1_j) & \longrightarrow & H_n(X^1) & \longrightarrow & \bigoplus_{j,k\in J} H_{n-1}(U^1_j \cap U^1_k) & \xrightarrow{g^1} & \cdots \\
\cdots & \xrightarrow{f^2} & \bigoplus_{j\in J} H_n(U^2_j) & \longrightarrow & H_n(X^2) & \longrightarrow & \bigoplus_{j,k\in J} H_{n-1}(U^2_j \cap U^2_k) & \xrightarrow{g^2} & \cdots \\
 & & \vdots & & \vdots & & \vdots & & \\
\cdots & \xrightarrow{f^N} & \bigoplus_{j\in J} H_n(U^N_j) & \longrightarrow & H_n(X^N) & \longrightarrow & \bigoplus_{j,k\in J} H_{n-1}(U^N_j \cap U^N_k) & \xrightarrow{g^N} & \cdots
\end{array}
$$

We can compute the homology of spaces X^i with field coefficients as the following.

$$\begin{aligned}
H_n(X^1) &\cong \operatorname{coker} f^1 \oplus \ker g^1 \\
H_n(X^2) &\cong \operatorname{coker} f^2 \oplus \ker g^2 \\
&\vdots \\
H_n(X^N) &\cong \operatorname{coker} f^N \oplus \ker g^N
\end{aligned}$$

We address the question of constructing the map $H_n(X^i) \to H_n(X^{i+1})$ induced by inclusion $X^i \hookrightarrow X^{i+1}$ from the direct sum decomposition of each homology. It turns out, the most naturally induced maps $\ker g^i \to \ker g^{i+1}$ and $\operatorname{coker} f^i \to \operatorname{coker} f^{i+1}$ are not enough to reconstruct the map $H_n(X^i) \to H_n(X^{i+1})$. We use spectral sequences to find the missing ingredient.

In Chapter 5, we provide a framework for multiscale persistence using the distributed computation scheme introduced in Chapter 4. Given data with some characteristic of interest such as density, proximity to a landmark, or time, this distributed computation scheme returns a barcode that reflects properties of its represented feature. We apply our method to a point cloud whose feature size is inversely proportional to the density of its constituent points. Our example illustrates the discerning power of this distributed computation method to detect significant features that are overlooked by the usual persistent homology method.

Chapter 2

Preliminaries

This chapter provides an introduction to the two main subjects of this dissertation: persistent homology (§2.1) and cellular sheaf theory (§2.2). While both persistent homology and sheaf theory have a rich literature, this chapter contains a selection of topics that are most closely relevant to this dissertation.

2.1 Persistent Homology

Persistent homology is a popular tool in applied topology that detects topological features from data in a robust manner. The subject plays a central role in Chapter 4 and Chapter 5 of this dissertation, where both its computation and the information conveyed are strengthened via cellular sheaf theory. In §2.1.1, we discuss some of the fundamental ideas of persistent homology. In §2.1.2, we summarize a generalization of persistent homology, called zigzag persistence. Morphisms of zigzag modules, introduced in §2.1.3, provide tools for comparing zigzag modules. The zigzag modules and their morphisms will be compared to cellular sheaves and sheaf morphisms in §2.2, and the comparison will provide an understanding of cellular sheaf cohomology that will be particularly useful in Chapter 5.

2.1.1 Persistent homology

Given some data, which is usually represented by a collection of points in some Euclidean space $\mathbb{R}^d$, information about the 'shape' of this data can provide insight into the underlying phenomenon that generates the data. Many data we encounter, however, come from a high dimensional space, and we can no longer rely on visualization or projection techniques to faithfully extract information about the shape of the dataset. Persistent homology, introduced by Edelsbrunner, Letscher, and Zomorodian [13] and extended by Carlsson and Zomorodian [28], uses tools from algebraic topology to infer global information about the shape of high dimensional datasets.

Given a space X, the topological properties of X can be summarized in a combinatorial way using the nerve of a covering.

Definition 1. Given an open covering $\mathcal{U} = \{U_i\}_{i \in I}$ of X, the **nerve of the covering**, denoted by $N_{\mathcal{U}}$, is a family of non-empty finite subsets $J \subseteq I$ such that

$$\bigcap_{j \in J} U_j \neq \emptyset.$$

An n-simplex of $N_{\mathcal{U}}$ corresponds to a non-empty intersection of $n+1$ members of $\mathcal{U}$. When discussing the nerve of a covering, we will often identify the nerve $N_{\mathcal{U}}$ with its geometric realization instead of its definition as an abstract simplicial complex. A particularly well-behaved covering $\mathcal{U}$ is called a good cover.

Definition 2. Given a topological space X, an open covering $\mathcal{U}$ of X is a **good cover** if every non-empty finite intersection of members of $\mathcal{U}$ is contractible.

When we have a good cover $\mathcal{U}$ of X, the nerve $N_{\mathcal{U}}$ captures the topology of X, as stated by the following Nerve Lemma.

Lemma 1 (Nerve Lemma [20], [4])**.** *Let X be a paracompact space and let $\mathcal{U}$ be a good cover of X. Then, the nerve of $\mathcal{U}$ is homotopic to the union of sets in $\mathcal{U}$.*

Let's switch our focus from understanding the topology of space X to 'topology' of some data set. Data is often represented as a point cloud.

Definition 3. A **point cloud** P is a finite set of points of some Euclidean space $\mathbb{R}^m$.

Our goal is to build an analogous combinatorial representation of the underlying space determined by a given point cloud. One of the most natural complexes one can build from a point cloud is a Čech complex.

Definition 4. Given a point cloud P in $\mathbb{R}^d$ and a parameter ϵ, let $\mathcal{U}_\epsilon$ denote the collection of ϵ-radius open balls centered at points of P. A **Čech complex** $\mathcal{C}^\epsilon$ with parameter ϵ is a simplicial complex whose k-simplices correspond to $(k+1)$-tuples of points from P whose $\epsilon/2$-radius balls have a nonempty intersection.

Note that the Čech complex is the nerve of $\mathcal{U}_{\epsilon/2}$. It follows from the Nerve Lemma that Čech complex $\mathcal{C}^\epsilon$ faithfully represents the topology of the union of open sets in $\mathcal{U}_{\epsilon/2}$. Constructing and storing a Čech complex, however, can be an expensive process, so we consider building other complexes that are still informative topological models.

Another effective method of approximating the topology of a point cloud is to build a Vietoris-Rips complex first introduced in [27].

Definition 5. The **Vietoris-Rips complex** $\mathcal{R}^\epsilon$ is an abstract simplicial complex whose k-simplices correspond to $(k+1)$-tuple of points from P that have pairwise distance $\leq \epsilon$.

For brevity, we will use the term "Rips complex" to refer to the Vietoris-Rips complex.

Note that a Rips complex is an example of a flag complex, i.e., once we determine the 1-skeleton, we can build the Rips complex by finding the maximal simplicial complex with the given 1-skeleton. Such property gives Rips complex a computational advantage over the Čech complex.

Even though Rips complexes are less expensive to compute and store, it is not immediately clear whether Rips complexes are reasonable substitutes for Čech complexes. The following theorem shows that Rips complexes are good approximations to Čech complexes.

Theorem 1 ([26]). *There exist inclusions*

$$\mathcal{R}^{\epsilon} \subset \mathcal{C}^{\epsilon'} \subset \mathcal{R}^{\epsilon'}$$

whenever $\frac{\epsilon'}{\epsilon} \geq \sqrt{\frac{2d}{d+1}}$.

Thus, given ϵ and ϵ' satisfying the conditions, a topological feature that exists in both $\mathcal{R}^{\epsilon}$ and $\mathcal{R}^{\epsilon'}$ must be a feature in $\mathcal{C}^{\epsilon'}$. Hence, it is important to study not only the topological features of $\mathcal{R}^{\epsilon}$ and $\mathcal{R}^{\epsilon'}$ individually, but also to examine which features of $\mathcal{R}^{\epsilon}$ persist to features in $\mathcal{R}^{\epsilon'}$. Studying such relations among features in different parameters lies at the heart of persistent homology.

Once we decide on which complex to build from a given point cloud P, we now face the question of choosing the parameter ϵ that will build the most informative model. However, it is impossible to know a priori which ϵ parameter leads to the most faithful model. Moreover, as we have seen in Theorem 1, studying the relations among features at various ϵ parameters can reveal crucial information. In fact, examining how features evolve and die across parameters is what allows us to discern true topological features from noise.

We thus consider an increasing family of parameters $(\epsilon_i)_{i=1}^{N}$ and build a complex $\mathbb{X}_i$ for each parameter ϵ_i. These complexes naturally have inclusion maps between each pair, leading to the sequence

$$\mathbb{X}_1 \hookrightarrow \mathbb{X}_2 \cdots \hookrightarrow \mathbb{X}_N.$$

One can apply the homology functor with coefficients in a field $\mathbb{K}$ to obtain the sequence of vector spaces

$$H_\bullet(\mathbb{X}_1) \to H_\bullet(\mathbb{X}_2) \cdots \to H_\bullet(\mathbb{X}_N). \tag{2.1}$$

The maps encode relations among homology classes of complexes. One might consider homology classes that live across a large range of parameters as significant features while features that live across a short range of parameters can be considered as noise.

For example, consider the sequence of complexes in Figure 2.1.

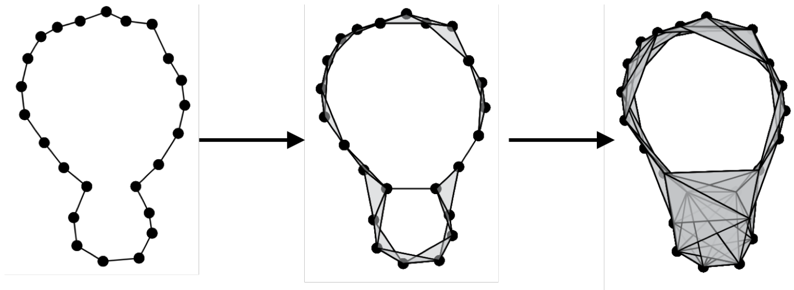

FIGURE 2.1: A sequence of Rips complexes

By applying the homology functor in dimension 1, one obtains the following sequence of vector spaces

$$\mathbb{K} \xrightarrow{\phi_1} \mathbb{K}^2 \xrightarrow{\phi_2} \mathbb{K}, \tag{2.2}$$

where the map ϕ_1 is represented by the matrix $\begin{bmatrix} 1 \\ 1 \end{bmatrix}$ and the map ϕ_2 is represented by the matrix $\begin{bmatrix} 1 & 0 \end{bmatrix}$. One can visualize maps ϕ_1 and ϕ_2 on the standard basis of each vector space as in Figure 2.2.

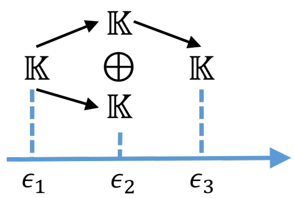

FIGURE 2.2: Visualization of maps between vector spaces

Recall that we are interested in studying the birth and death parameters of homological features. Examining Figure 2.2, we can see that there is one feature at parameter ϵ_1, two features at parameter ϵ_2, and one feature at parameter ϵ_3. However, we quickly run into some ambiguities when we attempt to make sense of the features while taking the maps ϕ_1 and ϕ_2 into account: Are there two features across parameters, namely one feature that is born at parameter ϵ_1 and persists until parameter ϵ_3, and another feature that is born at parameter ϵ_1 that persists until parameter ϵ_2? Does this contradict the fact that there is only one feature at parameter ϵ_1? How can we discuss birth and death times of features when it is not even clear how to determine features from the sequence?

In order to examine the sequence from Equation 2.1 in a systematic manner, we take advantage of the underlying algebraic structure as described by Zomorodian and Carlsson [28].

Definition 6. Let R be a commutative ring with unity. A **persistence module** $\mathcal{M}$ is a family of R-modules M^i with morphisms $\phi^i : M^i \to M^{i+1}$. A persistence module $\mathcal{M} = \{M^i, \phi^i\}$ is of **finite type** if each component module is finitely generated, and if the maps ϕ^i are isomorphisms for $i \geq m$ for some integer m.

Consider the following graded module

$$\alpha(\mathcal{M}) = \bigoplus_{i=1}^{\infty} M^i$$

over $R[t]$, where the action of t shifts the elements of the module up in degree. The above α establishes an equivalence of categories between category of persistence modules of finite type over R and the category of finitely generated non-negatively graded modules over $R[t]$.

Thus, in order to classify the persistence modules, we can instead classify finitely generated non-negatively graded modules over $R[t]$. Note that classifying such modules over $R[t]$, in general, is an extremely difficult problem. (Consider $R = \mathbb{Z}$).

However, when R is a field $\mathbb{K}$, then the graded ring $\mathbb{K}[t]$ is a principal ideal domain, and every ideal of $\mathbb{K}[t]$ has the form $t^n \cdot \mathbb{K}[t]$. By the Structure Theorem for finitely generated modules over principal ideal domains, we obtain the following Theorem.

Theorem 2 (Structure Theorem [28]). *Every graded module $\mathcal{M}$ over a graded PID over $\mathbb{K}[t]$ decomposes uniquely into the form*

$$\Big(\bigoplus_i t^{u_i}\mathbb{K}[t]\Big) \oplus \Big(\bigoplus_j t^{v_j}(\mathbb{K}[t]/(t^{w_j} \cdot \mathbb{K}[t]))\Big) \tag{2.3}$$

Let's revisit the sequence from Equation 2.1 and call it $\mathbb{V}$. Note that $\mathbb{V}$ is a persistence module of finite type. The Structure Theorem states that

$$\mathbb{V} \cong \Big(\bigoplus_i t^{u_i}\mathbb{K}[t]\Big) \oplus \Big(\bigoplus_j t^{v_j}(\mathbb{K}[t]/(t^{w_j} \cdot \mathbb{K}[t]))\Big).$$

In order to obtain such decomposition of the persistence module, we need to find a basis for this module $\mathbb{V}$ that is compatible with all the vector spaces, i.e., we need a change of basis so that all maps of Equation 2.1 become diagonal matrices with 1's and 0's on the diagonals. The Structure Theorem guarantees that there exists such change of basis.

Each free portion $t^{u_i}\mathbb{K}[t]$ corresponds to a homology class that is born at $H_\bullet(\mathbb{X}^{u_j})$. Each torsion portion $t^{v_j}(\mathbb{K}[t]/(t^{w_j} \cdot \mathbb{K}[t]))$ corresponds to a homology class that is born at $H_\bullet(\mathbb{X}^{v_j})$ and dies at $H_\bullet(\mathbb{X}^{v_j+w_j})$. Such birth and death times of homology classes of $H_\bullet(\mathbb{X};\mathbb{K})$ can be summarized using a set of intervals of the form (u_i, ∞) and $(v_j, v_j + w_j)$. Note that $(v_j, v_j + w_j)$ represents a homological feature born at parameter v_j that lasts until parameter $v_j + w_j - 1$.

One can visualize such birth and death times of homology classes using a barcode. Given a persistence module $\mathbb{V}$, a barcode, denoted *barcode*$(\mathbb{V})$ is a collection of bars that correspond to the intervals obtained from the decomposition of $\mathbb{V}$.

Let's return to the example persistence module from Equation 2.2. With the appropriate change of basis, we can express the persistence module with respect to the new basis as the following

$$\mathbb{K} \xrightarrow{\phi_1} \mathbb{K}^2 \xrightarrow{\phi_2} \mathbb{K},$$

where ϕ_1 is represented by the matrix $\begin{bmatrix} 1 \\ 0 \end{bmatrix}$ and the map ϕ_2 is represented by the matrix $\begin{bmatrix} 1 & 0 \end{bmatrix}$. The barcode for this persistence module is illustrated in Figure 2.3.

Given a persistence module

$$H_\bullet(\mathbb{X}_1) \to H_\bullet(\mathbb{X}_2) \cdots \to H_\bullet(\mathbb{X}_N),$$

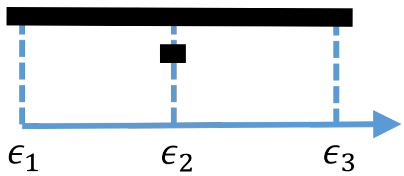

FIGURE 2.3: Barcode

the number of bars that span the parameter interval $[i, j]$ in $barcode(\mathbb{V})$ equals the rank of the map from $H_\bullet(\mathbb{X}^i)$ to $H_\bullet(\mathbb{X}^j)$ in the persistence module. For instance, in Figure 2.3, there is one interval spanning from ϵ_1 to ϵ_3, which equals the rank of the map $\phi_2 \circ \phi_1$.

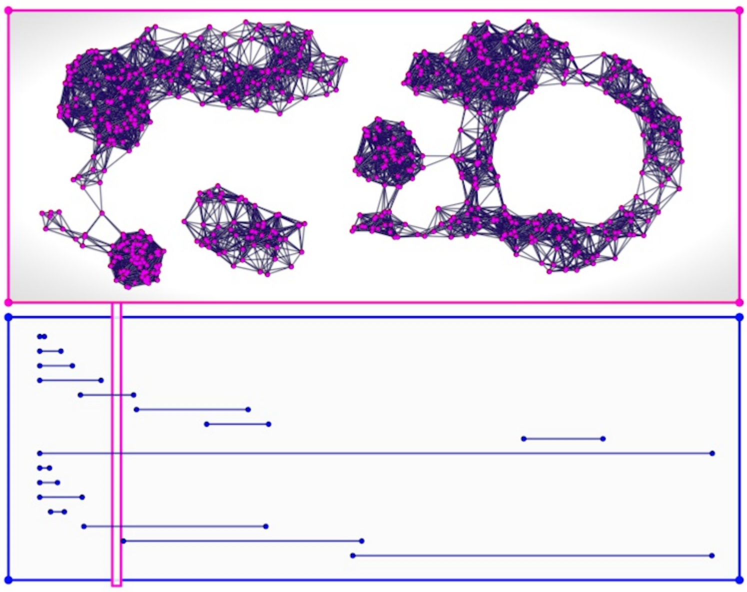

FIGURE 2.4: Point cloud and barcode

In general, when considering a wide range of ϵ parameter values, as illustrated in Figure 2.4, the long bars of the barcode capture significant features while the short bars correspond to noise. Barcodes, thus, provide qualitative means of distinguishing essential topological features from noise without requiring the user to select a particular value of parameter ϵ. Barcodes, or an equivalent visualization technique called persistence diagrams, are stable with respect to changes in input [9], and there exist efficient algorithms for computations [17]. For a survey of computation methods for persistent homology, we direct the reader to [23].

Remark. Throughout this dissertation, all homologies will be computed with respect to coefficients in a field $\mathbb{K}$.

2.1.2 Zigzag persistence

Persistent homology can be a powerful tool for studying topological features, but its usage depends on having a nested family of spaces. There are situations where it is natural to consider a sequence of spaces that have more interesting relations. Consider the following point cloud in Figure 2.5.

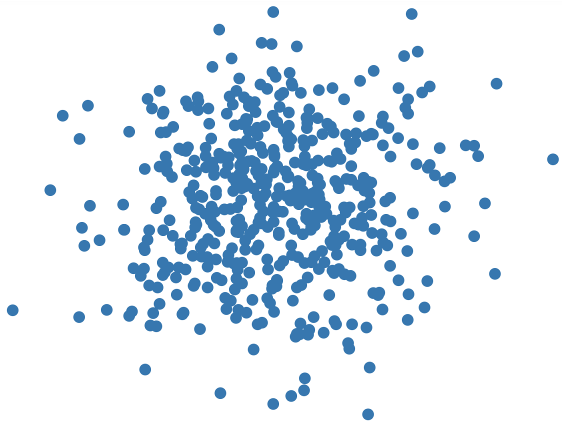

FIGURE 2.5: Point cloud with varying density

Let's say we are interested in studying how topological features change as we examine points with various density values. Note that there are various ways to estimate the density around a point p. For instance, one can count the number of points in an ϵ-neighborhood of p, or one can compute the distance to the k^{th} nearest point. Given a density estimate $\rho(p)$ for each point p, let $\mathbb{X}_1$ be a complex built among points whose density lies above the 25^{th} percentile, and let $\mathbb{X}_2$ be a complex built among points whose density lies below the the 75^{th} percentile. Note that there is no natural inclusion between the two complexes, making it difficult to compare the complexes $\mathbb{X}_1$ and $\mathbb{X}_2$. What one can do is to build a third complex $\mathbb{X}_{1,2}$ from points whose density lies above the 25^{th} percentile and below the 75^{th} percentile. Then, there are natural inclusion maps

$$\mathbb{X}_1 \hookleftarrow \mathbb{X}_{1,2} \hookrightarrow \mathbb{X}_2.$$

Applying the homology functor, we obtain the following sequence of vector spaces

$$H_\bullet(\mathbb{X}_1) \leftarrow H_\bullet(\mathbb{X}_{1,2}) \rightarrow H_\bullet(\mathbb{X}_2) \tag{2.4}$$

Studying the above sequence would reveal how topological features change as we filter data at different density levels. The work of de Silva and Carlsson [8] on zigzag persistence generalizes the theory of persistent homology to address such situations. For the purpose of this thesis, we will interpret certain cellular cosheaves as zigzag persistence to understand cellular cosheaf homology.

Definition 7. A **zigzag module** is a sequence of vector spaces over a field $\mathbb{K}$ and linear maps

$$V_1 \leftrightarrow V_2 \leftrightarrow \cdots \leftrightarrow V_n$$

where each $\leftrightarrow$ can represent either a forward map $\rightarrow$ or a backward map $\leftarrow$.

We call such a zigzag module $\mathbb{V}$ with n-number of vector spaces as having length n. Note that a persistence module is a zigzag module where all the maps are forward maps.

As we have done so with persistence modules, we would like a principled method of classifying such zigzag modules. We can show that zigzag modules have a nice decomposition into building blocks called interval modules.

Definition 8. An **interval module** with birth time b and death time d is written $\mathbb{I}(b,d)$, and defined as the zigzag module

$$0 \leftrightarrow \ldots 0 \leftrightarrow \mathbb{K} \overset{1}{\leftrightarrow} \mathbb{K} \overset{1}{\leftrightarrow} \ldots \overset{1}{\leftrightarrow} \mathbb{K} \leftrightarrow 0 \leftrightarrow \cdots \leftrightarrow 0,$$

where

$$\mathbb{I}(b,d)_i = \begin{cases} \mathbb{K} & \text{if } b \leq i \leq d \\ 0 & \text{otherwise.} \end{cases}$$

The linear maps are identity maps between adjacent pairs of $\mathbb{K}$, and zero maps otherwise.

The simplest form of Gabriel's Theorem tells us that any finite zigzag module can be described up to isomorphism.

Theorem 3 (Gabriel's Theorem, [12]). *A finite zigzag module $\mathbb{V}$ can be decomposed as*

$$\mathbb{V} \cong \bigoplus_{l=1}^{N} \mathbb{I}(b_l, d_l).$$

Given such decomposition, the zigzag persistence of $\mathbb{V}$ of length n is the multiset

$$Pers(\mathbb{V}) = \{[b_j, d_j] \subseteq \{1, \dots, n\} | j = 1, \dots, N\}.$$

Each interval $[b_j, d_j]$ corresponds to a homological feature that is born at parameter b_j and dies at parameter d_j. Thus, a long interval corresponds to a feature that is stable across varying parameter values. The set of intervals $Pers(\mathbb{V})$ can be represented pictorially as a barcode.

Zigzag persistence expands the subject of persistent homology by relaxing the requirement that a space needs to be filtered in one direction. Zigzag persistence is particularly important in this dissertation as it provides an interpretation of specific cellular sheaves and cosheaves. The correspondence between the specific cellular sheaves and zigzag persistence will be established in §2.2. Such perspective will be particularly useful in understanding certain properties of features in Chapter 5.

2.1.3 Morphisms of zigzag modules

Data often comes with multiple parameters that influence the analysis process, and a comparison framework across various parameters becomes useful in such situations. For example, the zigzag module

$$\mathbb{V} : H_\bullet(\mathbb{X}_1) \leftarrow H_\bullet(\mathbb{X}_{1,2}) \rightarrow H_\bullet(\mathbb{X}_2)$$

in Equation 2.4 was built from a sequence of complexes

$$\mathbb{X}_1 \hookleftarrow \mathbb{X}_{1,2} \hookrightarrow \mathbb{X}_2,$$

where each complex $\mathbb{X}_i$ was built from subsets P_i of point cloud P. Recall that building a complex from a set of points requires a proximity parameter ϵ. If we were to build a sequence of complexes on the same subsets P_i's using a larger proximity parameter ϵ', we would then obtain a different sequence of complexes

$$\mathbb{X}'_1 \hookleftarrow \mathbb{X}'_{1,2} \hookrightarrow \mathbb{X}'_2,$$

leading to a different zigzag module

$$\mathbb{V}' : H_\bullet(\mathbb{X}'_1) \leftarrow H_\bullet(\mathbb{X}'_{1,2}) \rightarrow H_\bullet(\mathbb{X}'_2).$$

A morphism of persistence modules allows us to compare the two different zigzag modules $\mathbb{V}$ and $\mathbb{V}'$.

Definition 9. Let $\mathbb{V}$ and $\mathbb{W}$ be zigzag modules such that the linear maps $V_i \leftrightarrow V_{i+1}$ and $W_i \leftrightarrow W_{i+1}$ are both forward or both backward maps for every i. A **morphism of zigzag modules** $\alpha : \mathbb{V} \rightarrow \mathbb{W}$ is a collection of linear maps $\alpha : \mathbb{V}_i \rightarrow \mathbb{W}_i$ that are compatible with the maps of $\mathbb{V}$ and $\mathbb{W}$.

The compatibility condition of the above definition refers to the fact that the following diagram commutes.

$$\begin{tikzcd}
V_1 \arrow[r, leftrightarrow] \arrow[d, "\alpha_1"] & V_2 \arrow[r, leftrightarrow] \arrow[d, "\alpha_2"] & \cdots \arrow[r, leftrightarrow] & V_n \arrow[d, "\alpha_n"] \\
W_1 \arrow[r, leftrightarrow] & W_2 \arrow[r, leftrightarrow] & \cdots \arrow[r, leftrightarrow] & W_n
\end{tikzcd}$$

For our example, the two sequence of complexes built on different proximity parameters are related by the following inclusion maps.

$$\begin{tikzcd}
\mathbb{X}_1 \arrow[d, hook] & \mathbb{X}_{1,2} \arrow[l, hook'] \arrow[r, hook] \arrow[d, hook] & \mathbb{X}_2 \arrow[d, hook] \\
\mathbb{X}'_1 & \mathbb{X}'_{1,2} \arrow[l, hook'] \arrow[r, hook] & \mathbb{X}'_2
\end{tikzcd}$$

Applying the homology functor results in the following morphism $\alpha : \mathbb{V} \to \mathbb{V}'$ of zigzag modules.

$$\begin{tikzcd}
H_\bullet(\mathbb{X}_1) \arrow[d] & H_\bullet(\mathbb{X}_{1,2}) \arrow[l] \arrow[r] \arrow[d] & H_\bullet(\mathbb{X}_2) \arrow[d] \\
H_\bullet(\mathbb{X}'_1) & H_\bullet(\mathbb{X}'_{1,2}) \arrow[l] \arrow[r] & H_\bullet(\mathbb{X}'_2)
\end{tikzcd}$$

Morphisms of persistence modules allow us to compare two different persistence modules $\mathbb{V}$ and $\mathbb{W}$. For example, if the vector spaces of $\mathbb{V}$ and $\mathbb{W}$ model the same data at different time points, then a morphism $\alpha : \mathbb{V} \to \mathbb{W}$ allows us to compare data across time.

In particular, when each $\alpha : \mathbb{V}_i \to \mathbb{W}_i$ is an isomorphism, then we call $\alpha : \mathbb{V} \to \mathbb{W}$ to be an isomorphism of zigzag modules. Given a zigzag module $\mathbb{V}$, the decomposition from Gabriel's Theorem (Theorem 3) is an isomorphism between $\mathbb{V}$ and the direct sum of interval modules $\bigoplus_{l=1}^{N} \mathbb{I}(b_l, d_l)$. Thus, if $\mathbb{V}$ and $\mathbb{V}'$ are isomorphic zigzag modules, then the two zigzag modules must have identical barcodes. Given a persistence module $\mathbb{V}$ of interest, efficient computation of an isomorphic persistence module $\mathbb{V}'$ would then lead to a faster computation of the barcode. In Chapter 4, we find the barcode of a persistence module $\mathbb{V}$ by computing an isomorphic persistence module in a distributed manner.

2.2 Cellular Sheaves and Cosheaves

Cellular sheaves and cosheaves are systematic tools for encoding local data and relations to extract global information. The practice of inferring global structure from local computations renders cellular sheaf theory well suited for distributed systems. This section provides a summary of topics from cellular sheaf theory that are utilized in Chapters 3, 4, and 5 of the dissertation. This section contains a collection of examples selected to communicate different intuitions and a variety of problems modeled via cellular sheaves. While some examples are substantial, many of the examples are fun and simple illustrations. The reader may safely skip the examples and move on to the next chapter.

We introduce cellular sheaves and cellular sheaf cohomology in §2.2.1 and §2.2.2. Sheaf morphisms in §2.2.3 are the main tools that allow us to study changes in global structure from local changes in data. In §2.2.4, we provide the machinery for examining the changes that occur when the base space evolves. An important connection between zigzag persistence and cellular sheaf cohomology is established in §2.2.5.

2.2.1 Cellular sheaves and cosheaves

A cellular sheaf is an assignment of algebraic structure to a cell complex. We direct the reader to [10] for a review of definitions involving cell complexes. Given a cell complex X, there is a cell category whose objects are the cells of X. Given a pair of cells τ and σ such that τ is a face of σ, this category assigns a unique morphism $\tau \to \sigma$. Let $\tau \trianglelefteq \sigma$ denote the face relation $\tau \subset \bar{\sigma}$.

Definition 10 ([24], [10])**.** A **cellular sheaf** $\mathcal{F}$ on a cell complex X with values in category D is a covariant functor from the associated cell category to D, i.e., $\mathcal{F}$ is a mapping that

- for each cell σ of X, assigns an object $\mathcal{F}(\sigma)$ in D, called local section of $\mathcal{F}$ on σ, and
- for each face relation $\tau \trianglelefteq \sigma$, assigns a restriction map $\mathcal{F}(\tau \trianglelefteq \sigma) : \mathcal{F}(\tau) \to \mathcal{F}(\sigma)$ such that
    - $\mathcal{F}(\tau \trianglelefteq \tau) : \mathcal{F}(\tau) \to \mathcal{F}(\tau)$ is the identity morphism for every cell τ, and
    - if $\rho \trianglelefteq \tau \trianglelefteq \sigma$, then $\mathcal{F}(\rho \trianglelefteq \sigma) = \mathcal{F}(\tau \trianglelefteq \sigma) \circ \mathcal{F}(\rho \trianglelefteq \tau)$.

Dually, a **cellular cosheaf** $\mathcal{G}$ on a cell complex X with values in category D is a contravariant functor from the associated cell category to D. The morphism $\mathcal{G}(\tau \trianglelefteq \sigma) : \mathcal{G}(\sigma) \to \mathcal{G}(\tau)$ assigned for each pair of cells with face relation $\tau \trianglelefteq \sigma$ is called an extension map.

In this thesis, we will mostly be studying sheaves and cosheaves with values in the category of vector spaces. We will occasionally examine sheaf of sets and cosheaf of sets, which have values in the category of sets.

Once we construct a cellular sheaf or a cosheaf on X, we want to use algebraic tools to extract useful information about our construction. One natural question to ask is whether there are elements of the local sections that are compatible with the restriction maps or the extension maps. Such is the idea of a global section. A global section of sheaf $\mathcal{F}$ on X, denoted $\mathcal{F}(X)$, is a collection of elements of local sections that are compatible with the restriction maps, i.e.,

$$\mathcal{F}(X) = \{\vec{s} \in \prod_{\sigma \in X} \mathcal{F}(\sigma) \quad | \quad s_\sigma = \mathcal{F}(\tau \trianglelefteq \sigma) s_\tau\}.$$

Given a cosheaf $\mathcal{G}$ on X, the global sections of $\mathcal{G}$ is given by

$$\mathcal{G}(X) = \bigoplus_{\sigma \in X} \mathcal{G}(\sigma) / \sim,$$

where $s_\sigma \in \mathcal{G}(\sigma)$ and $s_\tau \in \mathcal{G}(\tau)$ have equivalence relation $s_\sigma \sim s_\tau$ if

$$s_\tau = \mathcal{G}(\tau \trianglelefteq \sigma) s_\sigma.$$

The global section of cosheaf $\mathcal{G}$ is not a collection of compatible local sections. Rather, it is a collection of local sections where elements that are mapped from higher dimensional cells are identified. One might think that it's unnatural that the global sections on sheaves and cosheaves seem to have such different definitions. However, when the definitions are written in terms of limits and colimits [19], one can see that the definitions are dual to each other.

Definition 11. Given a sheaf $\mathcal{F}$ on X, the **global section** is

$$\mathcal{F}(X) := \varprojlim_{\sigma \in X} \mathcal{F}(\sigma).$$

Similarly, given a cohseaf $\mathcal{G}$ on X, the **global section** is

$$\mathcal{G}(X) := \underrightarrow{\operatorname{colim}}_{\sigma \in X} \mathcal{G}(\sigma).$$

Example 1. Recall the zigzag module from Equation 2.4. This zigzag module can be considered as a cosheaf on a cell complex as illustrated in Figure 2.6a. The local sections on the vertices are $H_\bullet(\mathbb{X}_1)$ and $H_\bullet(\mathbb{X}_2)$. The local section on the edge is $H_\bullet(\mathbb{X}_{1,2})$, and the extension maps are the morphisms induced by inclusion of complexes. Dually, one can construct a cellular sheaf $\mathcal{F}$ on the same cell complex as the following. Let the local sections on the vertices be $H_\bullet(\mathbb{X}_1)$ and $H_\bullet(\mathbb{X}_2)$, as before. Let the local section on the edge be $H_\bullet(\mathbb{X})$, where $\mathbb{X}$ is a complex built using all points of the point cloud P. Let the restriction maps be the morphisms $H_\bullet(\mathbb{X}_1) \to H_\bullet(\mathbb{X})$ and $H_\bullet(\mathbb{X}_2) \to H_\bullet(\mathbb{X})$ induced by the inclusion of complexes. Such sheaf $\mathcal{F}$ is illustrated in Figure 2.6b. The global section of this sheaf is a collection of homology classes $(s,t) \in H_\bullet(\mathbb{X}_1) \oplus H_\bullet(\mathbb{X}_2)$ such that s and t are mapped to the same homology class in $H_\bullet(\mathbb{X})$ via the restriction maps. Thus, the global section represents the homology classes that exist in both $\mathbb{X}_1$ and $\mathbb{X}_2$.

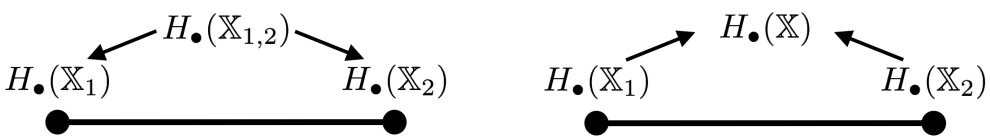

(A) Cosheaf (B) Sheaf

FIGURE 2.6: Zigzag modules as cellular cosheaves and sheaves

2.2.2 Cellular sheaf cohomology and cellular cosheaf homology

Homology and cohomology provide the algebraic tools to study cellular sheaves and cosheaves. Ideally, given a data system, we want to construct sheaves and cosheaves whose homology and cohomology reveal interesting information about the data. This section was written with the intention to communicate as much intuition about sheaf cohomology and cosheaf homology as possible. The examples, in particular, were chosen to convey various perspectives of sheaf cohomology and cosheaf homology. For the remainder of this thesis, we will assume that all our sheaves and cosheaves have values in vector spaces unless stated otherwise. Moreover, we will restrict ourselves to situations where cell complexes are compact.

Given a cellular sheaf $\mathcal{F}$ over a compact cell complex X, let

$$C^n(X,\mathcal{F}) = \bigoplus_{\dim\sigma=n} \mathcal{F}(\sigma).$$

Define $\partial^n : C^n(X,\mathcal{F}) \to C^{n+1}(X,\mathcal{F})$ by

$$\partial^n(s_\tau) = \sum_{\tau\trianglelefteq\sigma} [\tau:\sigma]\mathcal{F}(\tau\trianglelefteq\sigma)(s_\tau),$$

where $[\tau:\sigma]$ is the incidence number: for τ a codimension-1 face of σ, $[\tau:\sigma]=1$ if the attaching map of σ preserves the induced orientation from $\partial\sigma\to\tau$, and $[\tau:\sigma]=-1$ if orientation is reversed. If τ is not a codimension-1 face of σ, then $[\tau:\sigma]=0$. One can show that $\partial^{n+1}\circ\partial^n=0$, and obtain the following cochain complex

$$(C^\bullet\mathcal{F},\partial^\bullet) = 0 \to \bigoplus_{\dim\sigma=0}\mathcal{F}(\sigma) \xrightarrow{\partial^0} \bigoplus_{\dim\sigma=1}\mathcal{F}(\sigma) \xrightarrow{\partial^1} \bigoplus_{\dim\sigma=2}\mathcal{F}(\sigma) \xrightarrow{\partial^2} \cdots.$$

For brevity, we will denote the above cochain complex by $C^\bullet\mathcal{F}$.

Definition 12 ([24]). Given a cellular sheaf $\mathcal{F}$ on X, the **sheaf cohomology** of $\mathcal{F}$ is the cohomology of the cochain complex $C^\bullet\mathcal{F}$.

In other words, the sheaf cohomology in dimension n is $\ker\partial^n/\operatorname{im}\partial^{n-1}$. We will denote sheaf cohomology by $H^n(C^\bullet\mathcal{F})$.

Dually, given a cellular cosheaf $\mathcal{G}$ over a compact cell complex X, let

$$C_n(X,\mathcal{G}) = \bigoplus_{\dim\sigma=n}\mathcal{G}(\sigma),$$

and define $\partial_n : C_n(X, \mathcal{G}) \to C_{n-1}(X, \mathcal{G})$ by

$$\partial_n(s_\sigma) = \sum_{\tau \trianglelefteq \sigma} [\tau : \sigma] \mathcal{G}(\tau \trianglelefteq \sigma)(s_\sigma).$$

One can again show that $\partial_{n-1} \circ \partial_n = 0$ and obtain the following chain complex

$$(C_\bullet \mathcal{G}, \partial_\bullet) = \cdots \xrightarrow{\partial_3} \bigoplus_{\dim \sigma = 2} \mathcal{G}(\sigma) \xrightarrow{\partial_2} \bigoplus_{\dim \sigma = 1} \mathcal{G}(\sigma) \xrightarrow{\partial_1} \bigoplus_{\dim \sigma = 0} \mathcal{G}(\sigma) \xrightarrow{\partial_0} 0. \tag{2.5}$$

For brevity, we will denote the above chain complex by $C_\bullet \mathcal{G}$.

Definition 13. Given a cellular cosheaf $\mathcal{G}$ on X, the **cosheaf homology** of $\mathcal{G}$ is the homology of the chain complex $C_\bullet \mathcal{G}$.

Note that we have assumed our base space to be a compact cell complex X. A more general definition of cellular sheaf cohomology and cosheaf homology is introduced in [10]. We now provide a variety of examples that emphasize different interpretations of cellular sheaf cohomology and cosheaf homology.

One of the useful ways to think of $H^0(C^\bullet \mathcal{F})$ and $H_0(C_\bullet \mathcal{G})$ is to view them as the global sections of sheaf $\mathcal{F}$ and cosheaf $\mathcal{G}$ respectively.

Lemma 2. *Given a sheaf $\mathcal{F}$ on X,*

$$H^0(C^\bullet \mathcal{F}) = \mathcal{F}(X). \tag{2.6}$$

Given a cosheaf $\mathcal{G}$ on X,

$$H_0(C_\bullet \mathcal{G}) = \mathcal{G}(X). \tag{2.7}$$

This Lemma shows that global sections of sheaves and cosheaves are completely determined by local sections on the 0-cells and 1-cells. Recall from Definition 11 the limit and colimit definitions of global sections of sheaves and cosheaves. Then, Lemma 2 and Definition 11 implies that the global section on X is determined by the local sections on the 0 and 1 dimensional cells, i.e., two sheaves $\mathcal{F}$ and $\mathcal{F}'$ on X have the same global sections if the local sections and the maps agree on the 1-skeleton of X. In fact, one can show that for any sheaf $\mathcal{F}$ on X, the limit over X can be computed by the limit over the 1-skeleton of X.

Lemma 3. *Given a cell complex X, and $\mathcal{F}$ on X,*

$$\varprojlim_{\sigma \in X} \mathcal{F}(\sigma) = \varprojlim_{\substack{\sigma \in X, \\ \dim \sigma \leq 1}} \mathcal{F}(\sigma).$$

Dually, given a cosheaf $\mathcal{G}$ on X,

$$\underset{\sigma \in X}{\underrightarrow{\operatorname{colim}}}\, \mathcal{G}(\sigma) = \underset{\substack{\sigma \in X, \\ \dim \sigma \leq 1}}{\underrightarrow{\operatorname{colim}}}\, \mathcal{G}(\sigma).$$

The following selection of examples illustrate a few interpretations of sheaf cohomology and cosheaf homology.

Example 2. One natural way to interpret cosheaf homology is to consider it as an extension of homology in data. Homology with field coefficients detects the holes in the underlying space. Similarly, one can consider cosheaf homology as reading 'holes' in the data above the space. For example, consider a map $f : X \to \mathbb{R}$ illustrated in Figure 2.7. Let $\mathcal{V} = \{B, R\}$ be an open cover of $f(X)$. One can define a cosheaf $\mathcal{G}$ on the nerve $N_{\mathcal{V}}$ (Definition 1) as the following. For each $\sigma \in N_{\mathcal{V}}$, let $\mathcal{G}(\sigma)$ be the 0^{th} homology functor with field coefficients applied to the preimage of the corresponding set under f, i.e., $\mathcal{G}(v_B) = H_0(f^{-1}(B))$ and $\mathcal{G}(v_R) = H_0(f^{-1}(R))$. For $e_{BR} \in N_{\mathcal{V}}$, let $\mathcal{G}(e_{BR}) = H_0(f^{-1}(B \cap R))$. The extension maps are naturally induced. Such construction is a Leray cellular cosheaf [6]. Figure 2.8 illustrates the cosheaf $\mathcal{G}$.

The extension maps are each represented by the matrix $\begin{bmatrix} 1 & 1 \end{bmatrix}$. One can compute $H_1(C_\bullet \mathcal{F}) = \mathbb{K}$, which one can interpret as reading the hole in space X. The idea of sheaves and cosheaves as tools for summarizing homological and cohomological information among data is explored further in Chapter 4.

Example 3. Another valuable interpretation of sheaf cohomology is to consider it as detecting global inconsistencies in data. To make this idea concrete, we will first revisit

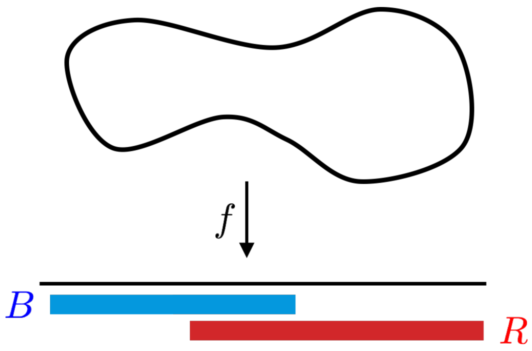

FIGURE 2.7: A map $f : X \to \mathbb{R}$ and a cover $\mathcal{V}$ of $f(X)$

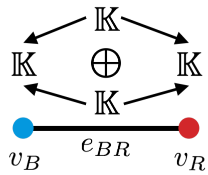

FIGURE 2.8: Visualization of cellular cosheaf

cohomology through the lens of detecting inconsistency, and we will extend the idea to sheaf cohomology. Let $\mathcal{F}$ be the constant sheaf on a 2-cell illustrated in Figure 2.9. Consider the local sections on the 0-cells as representing values for three different variables x, y, and z. Consider the local sections on the 1-cells xy, yz, and xz as representing the differences between values of adjacent 0-cells. For instance, $a \in \mathcal{F}(xy)$ implies that $y - x = a$. Thus, we can consider local sections on 1-cells as encoding relations among pairs of variables.

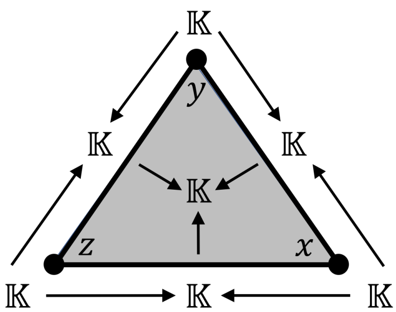

FIGURE 2.9: Constant sheaf on a 2-cell

The cochain complex for sheaf $\mathcal{F}$ is the following.

$$C^\bullet\mathcal{F} : 0 \to \mathbb{K}^3 \xrightarrow{\partial^0} \mathbb{K}^3 \xrightarrow{\partial^1} \mathbb{K} \to 0.$$

Now, consider $H^1(C^\bullet\mathcal{F}) = \ker\partial^1 / \operatorname{im}\partial^0$. Note that dimension of $\ker\partial^1$ is 2. A particular basis for $\ker\partial^1$ is illustrated in Figure 2.10 .

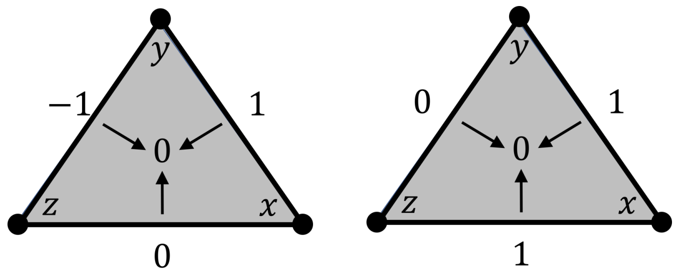

FIGURE 2.10: Basis elements of $\ker\partial^1$

Interpreting these basis of $\ker\partial^1$ as indicating relations among variables as we mentioned earlier, the first basis element on the left of Figure 2.10 corresponds to the system of equations

$$\begin{cases} y - x = 1 \\ z - y = -1 \\ z - x = 0, \end{cases}$$

and the second basis element on the right of Figure 2.10 corresponds to the equations

$$\begin{cases} y - x = 1 \\ z - y = 0 \\ z - x = 1. \end{cases}$$

If $(s_{xy}, s_{yz}, s_{xz}) \in \mathcal{F}(xy) \oplus \mathcal{F}(yz) \oplus \mathcal{F}(xz)$ is an element of $\ker\partial^1$, then the variables must satisfy the relations $s_{xy} + s_{yz} + s_{xz} = 0$, or $s_{xy} + s_{yz} = -s_{xz}$. What this implies is that given two equations corresponding to each element, the third equation is uniquely determined in a manner consistent with the map ∂^1. For instance, considering the first basis element of $\ker\partial^1$, any two equations, say $y - x = 1$ and $z - y = -1$ determines the third equation, $z - x = 0$. Thus, $\ker \partial^1$ represent relations among variables that are compatible with the restriction maps from 1-cells to 2-cells.

On the other hand, $\operatorname{im} \partial^0$ represents relations that can arise from actual data that are assigned to the variables. Then, $H^1(C^\bullet \mathcal{F}) = \ker \partial^1 / \operatorname{im} \partial^0$ represents the relations that cannot arise from the true values of the variables. For the example from Figure 2.9, one can check that $H^1(C^\bullet \mathcal{F}) = 0$, implying that any relations among variables compatible with the restriction map into 2-cells actually arises from data assignment of variables x, y, and z.

Example 4. Let's now consider a sheaf with nontrivial first cohomology. Consider the game of rock-paper-scissors. Let x represent rock, y represent paper, and z represent scissors. The pairwise relations among rock, paper, scissors can be represented by the following equations.

$$\begin{cases} y - x = 1 \\ z - y = 1 \\ x - z = 1 \end{cases}$$

One can represent such game via sheaf $\mathcal{F}$ illustrated in Figure 2.11.

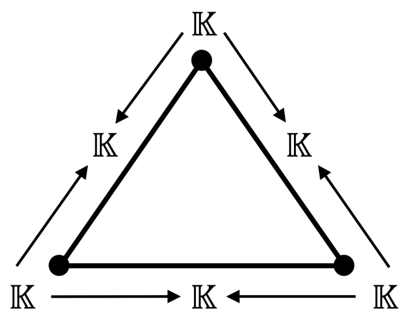

FIGURE 2.11: Game of rock-paper-scissors as a cellular sheaf

Then, $\ker \partial^1$ are elements $(s_{xy}, s_{yz}, s_{xz}) \in \mathcal{F}(xy) \oplus \mathcal{F}(yz) \oplus \mathcal{F}(xz)$ that satisfy $0 * s_{xy} + 0 * s_{yz} + 0 * s_{xz} = 0$, i.e., all the relations among variables represented by s_{xy}, s_{yz}, s_{xz} can be completely independent. Taking the quotient of $\ker \partial^1$ by $\operatorname{im} \partial^0$ then eliminates those relations that arises from data assignment to x,y, and z. Then, the fact that $H^1(C^\bullet \mathcal{F}) \neq 0$

implies that there exist relations among x, y, z that cannot be realized via values assigned to the variables, namely, the fact that there are partial orders among the variables, but the fact that there isn't a global ordering of the variables.

Example 5. With this perspective of $H^1(C^\bullet \mathcal{F})$ as an indicator of some form of structural inconsistency or impossibility, consider the example from Figure 2.12, where the restriction maps are both given by $\begin{bmatrix} 1 \\ 1 \end{bmatrix}$. Let x, y each be the variable represented by the 0-cells. The local section on the 1-cell can be represented by the following equations, each equation representing a component of $\mathbb{K}$.

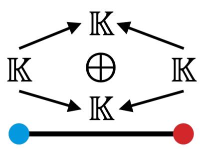

FIGURE 2.12: A cellular sheaf

$$\begin{cases} y - x = a \\ y - x = b \end{cases}$$

While the relation $y - x = a$ is possible for any value of a, it is impossible for data assigned to x and y to satisfy the above equations simultaneously if $a \neq b$. Such inconsistency in relations is reflected by the fact that $H^1(C^\bullet \mathcal{F}) \neq 0$.

2.2.3 Sheaf and cosheaf morphisms

We have so far seen that sheaf cohomology and cosheaf homology can reveal interesting information about data. Their real power, however, becomes even clearer when we compare cohomology and homology across different sheaves and cosheaves. Sheaf morphism is the tool that allows us to extract stable information from various sheaf constructions in Chapter 4 and Chapter 5.

Given multiple data systems encoded via different sheaves on a fixed base space, sheaf morphisms provide tools for transforming data from one system to another.

Definition 14 ([6]). Let $\mathcal{F}$ and $\mathcal{F}'$ be sheaves on X. A **sheaf morphism** $\phi : \mathcal{F} \to \mathcal{F}'$ is a transformation between local sections that respects restriction maps.

In other words, for each cell $\sigma \in X$, there exists a homomorphism $\phi|_\sigma : \mathcal{F}(\sigma) \to \mathcal{F}'(\sigma)$ such that for each face relation $\tau \trianglelefteq \sigma$, the following diagram commutes :

$$\begin{tikzcd}
\mathcal{F}(\tau) \arrow[r, "\phi|_\tau"] \arrow[d, "\mathcal{F}(\tau \trianglelefteq \sigma)"'] & \mathcal{F}'(\tau) \arrow[d, "\mathcal{F}'(\tau \trianglelefteq \sigma)"] \\
\mathcal{F}(\sigma) \arrow[r, "\phi|_\sigma"] & \mathcal{F}'(\sigma)
\end{tikzcd}$$

Thus, a sheaf morphism $\phi : \mathcal{F} \to \mathcal{F}'$ is a natural transformation from the functor $\mathcal{F}$ to $\mathcal{F}'$. Sheaf morphisms are useful tools of transforming data over a fixed base space. The dual notion **cosheaf morphism** can be defined analogously.
Given a sheaf morphism ϕ, let ϕ_n be the collection of morphisms $\phi|_\sigma$ on n-cells σ. Let ∂, ∂' be the coboundary maps of $\mathcal{F}, \mathcal{F}'$ respectively. Then, every square of the following diagram commutes.

$$\begin{tikzcd}
\cdots \bigoplus_{\dim \sigma = n-1} \mathcal{F}(\sigma) \arrow[r, "\partial^{n-1}"] \arrow[d, "\phi_{n-1}"] & \bigoplus_{\dim \sigma = n} \mathcal{F}(\sigma) \arrow[r, "\partial^{n}"] \arrow[d, "\phi_{n}"] & \bigoplus_{\dim \sigma = n+1} \mathcal{F}(\sigma) \cdots \arrow[d, "\phi_{n+1}"] \\
\cdots \bigoplus_{\dim \sigma = n-1} \mathcal{F}'(\sigma) \arrow[r, "\partial'^{n-1}"] & \bigoplus_{\dim \sigma = n} \mathcal{F}'(\sigma) \arrow[r, "\partial'^{n}"] & \bigoplus_{\dim \sigma = n+1} \mathcal{F}'(\sigma) \cdots
\end{tikzcd}$$

Since the sheaf morphism ϕ defines a cochain map $\phi^\bullet : C^\bullet\mathcal{F} \to C^\bullet\mathcal{F}'$, they induce moprphisms $H^n(\phi) : H^n(C^\bullet\mathcal{F}) \to H^n(C^\bullet\mathcal{F}')$ for every n. Similarly, a cosheaf morphism $\psi : \mathcal{G} \to \mathcal{G}'$ defines a chain map $\psi_\bullet : C_\bullet\mathcal{G} \to C_\bullet\mathcal{G}'$, which induces homomorphism $H_n(\psi) : H_n(C_\bullet\mathcal{G}) \to H_n(C_\bullet\mathcal{G}')$ for every n.

Lemma 4. *A sheaf morphism $\phi : \mathcal{F} \to \mathcal{F}'$ induces morphisms*

$$H^n(\phi) : H^n(C^\bullet\mathcal{F}) \to H^n(C^\bullet\mathcal{F}')$$

for every n. A cosheaf morphism $\psi : \mathcal{G} \to \mathcal{G}'$ induces morphisms

$$H_n(\psi) : H_n(C_\bullet \mathcal{G}) \to H_n(C_\bullet \mathcal{G}')$$

for every n.

The map $H^n(\phi)$ reveals the features of $H^n(C^\bullet \mathcal{F})$ that persist to $H^n(C^\bullet \mathcal{F}')$. One can extend this idea to a collection of sheaves $\mathcal{F}_1, \ldots, \mathcal{F}_k$ with sheaf morphisms $\phi_{i,i+1}$: $\mathcal{F}_i \to \mathcal{F}_{i+1}$ between adjacent pair of sheaves and examine the sequence of induced morphisms $H^n(C^\bullet \mathcal{F}_1) \to H^n(C^\bullet \mathcal{F}_2) \to \cdots \to H^n(C^\bullet \mathcal{F}_k)$.
In fact, a sheaf morphism between $\mathcal{F}_i$ and $\mathcal{F}_{i+1}$ does not have to be oriented in the direction of increasing indices. Consider a zigzag diagram of sheaf morphisms

$$\mathcal{F}_1 \leftrightarrow \mathcal{F}_2 \leftrightarrow \cdots \leftrightarrow \mathcal{F}_k$$

where each $\leftrightarrow$ between $\mathcal{F}_i$ and $\mathcal{F}_{i+1}$ represents either a sheaf morphism $\mathcal{F}_i \to \mathcal{F}_{i+1}$ or $\mathcal{F}_i \leftarrow \mathcal{F}_{i+1}$. Since each sheaf morphism induces a morphism of sheaf cohomology, the zigzag diagram of sheaf morphisms induces a zigzag module of sheaf cohomology:

$$H^n(C^\bullet \mathcal{F}_1) \leftrightarrow H^n(C^\bullet \mathcal{F}_2) \leftrightarrow \cdots \leftrightarrow H^n(C^\bullet \mathcal{F}_k)$$

for each n. The above zigzag module can be decomposed into interval modules, according to Theorem 3. We can represent the decomposition via barcodes, which then represents the birth and death of sheaf cohomology classes. Similarly, given a sequence of cosheaves and morphisms between each pair of cosheaves, one obtains a zigzag module of cosheaf homology :

$$H_n(C_\bullet \mathcal{G}_1) \leftrightarrow H_n(C_\bullet \mathcal{G}_2) \leftrightarrow \cdots \leftrightarrow H_n(C_\bullet \mathcal{G}_k).$$

Let's now consider a special kind of sheaf morphism. Let $\mathcal{F}, \mathcal{G}$, and $\mathcal{H}$ be cellular sheaves on X such that

$$0 \to \mathcal{F}(\sigma) \to \mathcal{G}(\sigma) \to \mathcal{H}(\sigma) \to 0$$

is exact for all $\sigma \in X$. We then say that

$$0 \to \mathcal{F} \to \mathcal{G} \to \mathcal{H} \to 0$$

is a short exact sequence of sheaves over X. This leads to a long exact sequence of sheaf cohomology

$$\cdots \to H^{n-1}(C^\bullet \mathcal{H}) \to H^n(C^\bullet \mathcal{F}) \to H^n(C^\bullet \mathcal{G}) \to H^n(C^\bullet \mathcal{H}) \to \cdots .$$

The following instance of long exact sequence comes in particularly handy when studying obstructions to extensions of local data. Let A be a subcomplex of X. Given a sheaf $\mathcal{G}$ on X, let $\mathcal{G}|_A$ be the restriction of $\mathcal{G}$ to A, and let $\mathcal{G}|_{X-A}$ be the complementary restriction of $\mathcal{G}$. Then, we have a short exact sequence of sheaves

$$0 \to \mathcal{G}|_{X-A} \to \mathcal{G} \to \mathcal{G}|_A,$$

which results in the following long exact sequence of sheaf cohomology.

$$0 \to H^0(C^\bullet \mathcal{G}|_{X-A}) \to H^0(C^\bullet \mathcal{G}) \xrightarrow{r} H^0(C^\bullet \mathcal{G}|_A) \xrightarrow{\delta} H^1(C^\bullet \mathcal{G}|_{X-A}) \to H^1(C^\bullet \mathcal{G}) \to \cdots$$

Given an element $s_A \in H^0(C^\bullet \mathcal{G}|_A)$, an extension of s_A to the entire complex X is an element $s \in H^0(C^\bullet \mathcal{G})$ such that $r(s) = s_A$. By exactness, $\operatorname{im} r = \ker \delta$. Thus, $s_A \in H^0(C^\bullet \mathcal{G}|_A)$ is extendable if and only if $\delta(s_A) = 0$. We can hence consider δ as representing obstruction to extending sections on A to global sections on X. One can address several interesting questions by using this obstruction.

The following examples were selected to illustrate the use of sheaf morphisms in detecting paradoxical information. The reader familiar with sheaf morphisms may safely skip the following examples and move on to §2.2.5.

Example 6. The long exact sequence of sheaf cohomology plays a central role in work by Abramsky, Barbosa, Kishida, Lal, and Mansfield [1] in detecting contextuality in physical systems. Contextuality is a foundational concept in quantum theory which states that the measurement result of an observable does not have a preset value, but the result depends on the specific experiments used to measure the observable. Qubits, or quantum bits, are 2-state quantum systems, such as the spin of a particle, photon polarization, and atomic orbitals. A qubit is an element of a 2-dimensional Hilbert space, and its state can be written as a unit vector $\begin{bmatrix} \alpha \\ \beta \end{bmatrix} \in \mathbb{C}^2$. It is commonly expressed as a superposition of its two states $|0\rangle$ and $|1\rangle$ using the Dirac notation

$$|\psi\rangle = \alpha|0\rangle + \beta|1\rangle$$

such that $\alpha, \beta \in \mathbb{C}$ and $|\alpha|^2 + |\beta|^2 = 1$. In order to know the state of the qubit, we make a measurement with respect to the standard basis $\{|0\rangle, |1\rangle\}$, which results in 0 with probability $|\alpha|^2$ and 1 with probability $|\beta|^2$. In fact, we can perform measurements with respect to any orthonormal basis $\{|v\rangle, |w\rangle\}$ as the following. We first express $|\psi\rangle$ with respect to this new basis as $|\psi\rangle = \alpha'|v\rangle + \beta'|w\rangle$. Then, our measurement will return v with probability $|\alpha'|^2$ and w with probability $|\beta'|^2$. An important aspect of measurement is that the measurement process alters the state. For instance, if the outcome of the measurement with respect to the standard basis returns 0, then α is changed to 1, and β is changed to 0.

Consider a system of two qubits, which reflects quantum states of several particles. Such system of two qubits has four states

$$|\psi\rangle = \alpha_{00}|0\rangle \otimes |0\rangle + \alpha_{01}|0\rangle \otimes |1\rangle + \alpha_{10}|1\rangle \otimes |0\rangle + \alpha_{11}|1\rangle \otimes |1\rangle,$$

where each $\alpha_{ij} \in \mathbb{C}$ and $\sum_{i,j} |\alpha_{ij}|^2 = 1$. Again, one can interpret each $|\alpha_{ij}|^2$ as the probability of obtaining a measurement outcome of i in the first qubit and j in the second qubit.

Suppose we have two qubits, $|\psi_1\rangle = \alpha|0\rangle + \beta|1\rangle$ and $|\psi_2\rangle = \alpha'|0\rangle + \beta'|1\rangle$. Interpreting the qubit expressions as probabilities of measurement outcomes, it seems quite reasonable to express the joint qubit as $|\psi_1\rangle \otimes |\psi_2\rangle = \alpha\alpha'|0\rangle \otimes |0\rangle + \alpha\beta'|0\rangle \otimes |1\rangle + \beta\alpha'|1\rangle \otimes |0\rangle + \beta\beta'|1\rangle \otimes |1\rangle$. However, there are two qubit states that cannot be decomposed as such individual states. A two qubit state $|\psi\rangle$ that can be expressed as $|\psi_1\rangle \otimes |\psi_2\rangle$ is called disentangled or separable. If $|\psi\rangle$ cannot be decomposed as such, then $|\psi\rangle$ is said to be entangled. For example, the following state

$$|\Phi^+\rangle = \frac{1}{\sqrt{2}}(|0\rangle \otimes |0\rangle + |1\rangle \otimes |1\rangle)$$

is entangled. Entanglement is a phenomenon that occurs from interactions of individual states which results in a correlation of the states even after being separated by a large distance.

Consider a scenario in which two agents, Alice and Bob, each have access to one qubit of an entangled 2-qubit state. Alice can perform measurements a_1 and a_2 on the first qubit, and Bob can perform measurements b_1 and b_2 on the second qubit. Note that the different measurements on each qubit refer to different sets of orthonormal basis. Assume that Alice and Bob communicate with each other the outcome of their measurements. The result can be summarized in a table that shows whether a particular outcome was observed or not. For example, Table 2.1 illustrates the Popescu-Rohrlich (PR) box.

A	B	$(0,0)$	$(0,1)$	$(1,0)$	$(1,1)$
a_1	b_1	1	0	0	1
a_1	b_2	1	0	0	1
a_2	b_1	1	0	0	1
a_2	b_2	0	1	1	0

TABLE 2.1: Popescu-Rohrlich (PR) box.

Each row represents the possible measurements made by Alice and Bob simultaneously. The ones indicate that a particular outcome (column) of a measurement (row) is possible, and the zeros indicate that a particular outcome is impossible.

In a classical system, the observables have a state, and the result of our measurements reflect this true state. In particular, the outcome should always reflect the physical truth, and hence should be independent of the measurements performed. However, this viewpoint fails to capture the nature of microphysical systems.

The PR box represented as a bundle is illustrated in Figure 2.13. The possible outcomes 0 and 1 are the fibers over the variables. We connect two outcomes with an edge when the outcomes can be measured together. A global section is a closed path that traverses the fibers exactly once.

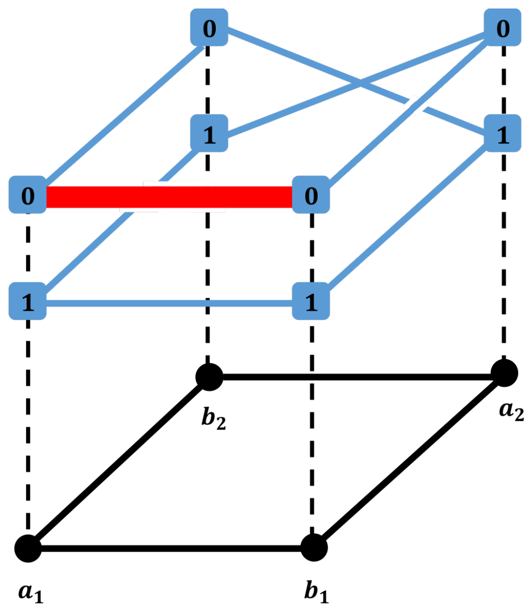

FIGURE 2.13: The PR box represented as a bundle

Logical contextuality refers to a system in which local assignment, as observed by each measurement, cannot be extended to a compatible global assignment. For example, the section $(a_1, b_1) = (0, 0)$, marked by the red edge in Figure 2.13, cannot be extended to a global section. Thus, PR box is logically contextual.

Strong contextuality refers to a system in which no global assignment is consistent with the measurement. One can see from Figure 2.13 that PR box is strongly contextual.

Abramsky et all formalized such bundle representation as a sheaf and examined the Čech cohomology of a sheaf [6] with respect to a particular cover $\mathcal{M}$ for indications of contextuality. We summarize their construction in terms of cellular sheaves on the nerve of the cover $N_{\mathcal{M}}$.

Let X be a finite set of variables. Let C_i be subsets of X, which is a collection of variables that can be measured together in one experiment. Assume that $\mathcal{M} = \{C_i\}$ is a cover of X that contains only the maximal measurements, i.e., if $C, C' \in \mathcal{M}$ and $C \subseteq C'$, then $C = C'$. Let O denote the set of possible values of each variable in X. Note that the possible values do not have to be uniform for all variables in X, but we will assume that such is the case for now. For the PR box example, $X = \{a_1, a_2, b_1, b_2\}$, and $\mathcal{M} = \{C_0, C_1, C_2, C_3\}$, where $C_0 = \{a_1, b_1\}, C_1 = \{a_1, b_2\}, C_2 = \{a_2, b_1\}$, and $C_3 = \{a_2, b_2\}$.

Let $N_{\mathcal{M}}$ be the nerve (Definition 1) of this covering $\mathcal{M}$. Construct a sheaf $\mathcal{F}$ of sets on $N_{\mathcal{M}}$ as the following. For each n-simplex $\sigma_{i_0,\ldots,i_n} \in N_{\mathcal{M}}$ that corresponds to an intersection of measurement contexts, $C_{i_0}, \ldots, C_{i_j}$, let $\mathcal{F}(\sigma_{i_0,\ldots,i_n})$ be the set of outcomes possible via every measurements C_{i_0} through C_{i_n}, i.e., if $x_0, \ldots, x_m$ are the variables that are being commonly observed by measurements $C_{i_0}, \ldots, C_{i_n}$, then

$$\mathcal{F}(\sigma_{i_0,\ldots,i_n}) = \{s \in O^{\{x_0,\ldots,x_m\}} | s \text{ is a possible outcome of each measurement } C_{i_0}, \ldots, C_{i_n}\}.$$

Given $\tau \trianglelefteq \sigma$, let the restriction map $\mathcal{F}(\tau \trianglelefteq \sigma) : \mathcal{F}(\tau) \to \mathcal{F}(\sigma)$ be the restriction $s \mapsto s|_{\sigma}$. The global section of $\mathcal{F}$ is an assignment of values of the variables that is compatible with the measurement context.

In order to compute cohomology of a sheaf, the authors turn the sheaf of sets $\mathcal{F}$ to a sheaf of R-modules $\mathcal{G}$ by applying the free functor $F_R : Set \to R\text{-}Mod$. By doing so, one obtains a sheaf $\mathcal{G}$ on $N_{\mathcal{M}}$ whose local section $\mathcal{G}(\sigma)$ is the free R-module generated by the set $\mathcal{F}(\sigma)$. Given $\tau \trianglelefteq \sigma$, the restriction maps $\mathcal{G}(\tau \trianglelefteq \sigma) : \mathcal{G}(\tau) \to \mathcal{G}(\sigma)$ is then induced by $\mathcal{F}(\tau \trianglelefteq \sigma)$ and the universal property of free R-modules.

Now that we have a sheaf with algebraic structure that allows us to take cohomology, given any vertex v of $N_{\mathcal{M}}$, one obtains the following long exact sequence.

$$0 \to H^0(C_\bullet \mathcal{G}|_{N_{\mathcal{M}}-v}) \to H^0(C_\bullet \mathcal{G}) \to H^0(C_\bullet \mathcal{G}|_v) \xrightarrow{\gamma} H^1(C_\bullet \mathcal{G}|_{N_{\mathcal{M}}-v}) \to H^1(C_\bullet \mathcal{G}) \to \cdots \tag{2.8}$$

Note that $\mathcal{G}|_v$ is simply the local section $\mathcal{G}(v)$.

Definition 15 ([1])**.** If there exists a vertex $v \in N_{\mathcal{M}}$ and a local section $s \in \mathcal{G}|_v$ such that $\gamma(s) \neq 0$, where γ is the connecting map from the long exact sequence in Equation 2.8, then the system is **cohomologically logically contextual**. If $\gamma(s) \neq 0$ for all local sections $s \in \mathcal{G}|_v$ for every $v \in N_{\mathcal{M}}$, then the system is **cohomologically strongly contextual**.

The following proposition uses cohomological obstructions to study contextuality.

Proposition 1 ([1])**.** *If a system is cohomologically logically contextual, then the system is logically contextual. If a system is cohomologically strongly contextual, then the system is strongly contextual.*

To illustrate Proposition 1, consider the PR box from Table 2.1. An illustration of sheaves $\mathcal{F}$ and $\mathcal{G}$ are provided in Figure 2.14. As the sheaf of sets $\mathcal{F}$, each local section should be considered as a set, and the arrows should be considered as morphisms of sets. As the sheaf of R-modules $\mathcal{G}$, the illustrated blue boxes should be considered as the generating basis, and the arrows should be considered as maps among basis elements that induce the restriction maps.

One can check that $\gamma(s) \neq 0$ for every local section $s \in \mathcal{G}(v)$ for every $v \in N_{\mathcal{V}}$. Thus, by Proposition 1, we conclude that PR box is a strongly contextual system. Indeed, considering Figure 2.14 as an illustration of sheaf of sets $\mathcal{F}$, one can see that no local section extends to a global section that traverses the fibers once.

Proposition 1 provides sufficient conditions for logical contextuality and strong contextuality, but not the necessary conditions. For example, one can visualize the Hardy model from table 2.2 to check that the model is logically contextual. However,

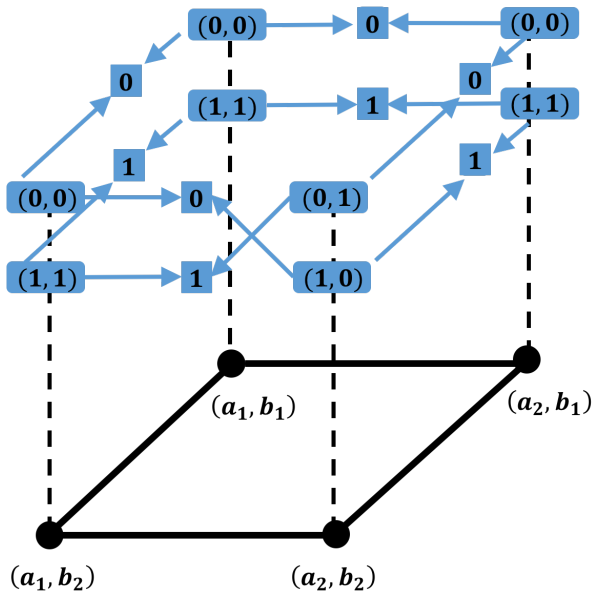

FIGURE 2.14: An illustration of cellular sheaves $\mathcal{F}$ and $\mathcal{G}$

one can check that $\gamma(s_0) = 0$ for all local sections of $\mathcal{G}$. This occurs because global sections of $\mathcal{G}$ read false positive global sections of the sheaf of sets $\mathcal{F}$. Given local section $s \in \mathcal{F}$ that does not extend to a global section in $\mathcal{F}$, it is possible for s to define a local section $s_0 \in \mathcal{G}$ that does admit a global extension in $\mathcal{G}$.

A	B	$(0,0)$	$(0,1)$	$(1,0)$	$(1,1)$
a_1	b_1	1	1	1	1
a_1	b_2	0	1	1	1
a_2	b_1	0	1	1	1
a_2	b_2	1	1	1	0

TABLE 2.2: Hardy model.

In the language of category theory, such false positives occur because the free functor $F_R : \mathit{Set} \to R\text{-}\mathit{Mod}$ we applied to obtain sheaf $\mathcal{G}$ from $\mathcal{F}$ doesn't preserve limits. The free functor, being the left adjoint of the forgetful functor, preserves colimits, while the forgetful functor, being the right adjoint of the free functor, preserves limits. Thus, $\mathcal{G}(X) = \varprojlim_{\sigma \in X} \mathcal{G}(\sigma)$ and $\mathcal{F}(X) = \varprojlim_{\sigma \in X} \mathcal{F}(\sigma)$ may differ.

Example 7. The following examples discuss a simple illustration of sheaf theoretic perspective on 2-coloring problems on a graph X: is it possible to color the vertices of X

using two colors, say red and blue, such that no two vertices connected by an edge have the same color?

There are a variety of sheaves and cosheaves one can build on X to approach the problem. We will provide a few examples of such sheaves and cosheaves, each of which emphasizes different aspects of graph coloring problems.

First of all, consider a sheaf of sets $\mathcal{F}$, whose local sections on each vertex is $\{r, b\}$, denoting the two possible colors. Let the local sections on edges be the set $\{rb, br\}$. To make sense of the local sections and restriction maps, assume that all edges of X are oriented. If a vertex v is the head of an edge e, then let $\mathcal{F}(v \trianglelefteq e)$ be the map of sets mapping r to rb and b to br. If a vertex w is the tail of an edge e, then let $\mathcal{F}(w \trianglelefteq e)$ be the map of sets mapping r to br and b to rb. An illustration of sheaf of sets $\mathcal{F}$ on two different graphs is provided in Figure 2.15.

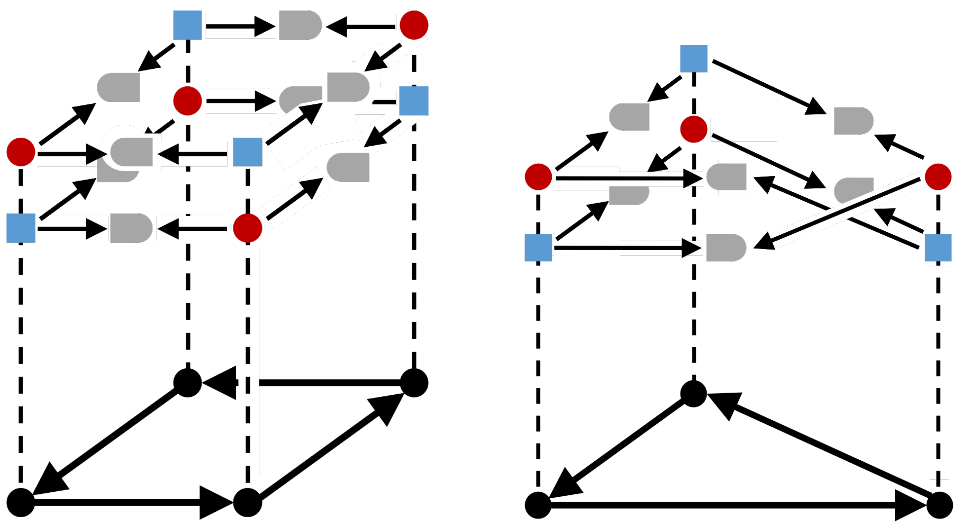

(A) Sheaves $\mathcal{F}$ and $\mathcal{G}$ on X

(B) Sheaves $\mathcal{F}$ and $\mathcal{G}$ on Y

FIGURE 2.15: Cellular sheaves $\mathcal{F}$ and $\mathcal{G}$ for 2-coloring problem

Since the sheaf $\mathcal{F}$ models the possible colors that can be assigned to each vertex, a global section of the sheaf $\mathcal{F}$ corresponds to a 2-coloring of the graph X. Thus a graph is 2-colorable if and only if the sheaf $\mathcal{F}$ has a global section. As it was the case in Example 6, we have very limited tools when it comes to sheaf of sets. Thus, we construct a sheaf of vector spaces $\mathcal{G}$ by applying the free functor from category of sets to category of $\mathbb{K}$-modules for field $\mathbb{K}$. Then, the local section $\mathcal{G}(\sigma)$ of $\sigma \in X$ is the vector space generated by the set $\mathcal{F}(\sigma)$, and the restriction maps $\mathcal{G}(v \trianglelefteq e)$ are induced by $\mathcal{F}(v \trianglelefteq e)$. One can consider Figure 2.15 as illustrating sheaf of vector spaces $\mathcal{G}$, where each set above $\sigma \in X$ represents a basis for $\mathcal{G}(\sigma)$.

One can use sheaf cohomology to determine whether a graph is 2-colorable or not, as stated in the following proposition.

Proposition 2. *A graph X is 2-colorable if and only if* $\dim H^0(C^\bullet \mathcal{G}) = 2$.

One can understand the construction of the sheaf $\mathcal{G}$ and Proposition 2 from the perspective of orientability of vector bundles. For example, given a base space S^1, the Möbius band can be considered as a vector bundle on S^1. Consider a similar construction on graph X, where each edge of X represents a half-twist of the band. Let $\pi : E \to X$ denote the resulting vector bundle. We then ask whether the resulting vector bundle is orientable or not. In fact, the sheaves in Figure 2.15 represent the orientation covers of vector bundles on graphs X and Y. Construct a sheaf of sets on X whose local sections are the choices of an orientation of fiber over each cell, and whose restriction maps reflect the maps of the orientations. This sheaf, in fact, coincides with sheaf of sets $\mathcal{F}$ introduced earlier.

Proposition 3. *Let E be a rank-n vector bundle on a connected manifold M. Then, the orientation cover O has either one or two connected components. Moreover, the following two statements are equivalent.*

- *The bundle E is orientable*
- *The manifold O is not connected*

Note that the number of connected components of O is reflected by the global section of sheaf $\mathcal{G}$. Since our sheaf $\mathcal{G}$ allows for construction of cohomology, we know from Lemma 2 that $H^0(C^\bullet \mathcal{G}) = \mathcal{G}(X)$. If $\dim H^0(C^\bullet \mathcal{G}) = 2$, this implies that manifold O has two connected components, implying that the bundle E is orientable. If $\dim H^0(C^\bullet \mathcal{G}) = 1$, then O is connected, and bundle E is not orientable.

So far, we have concluded that $\dim H^0(C^\bullet \mathcal{G})$ tells us whether a graph is colorable or not. Let's now go back to the language of graph theory and understand what $\dim H^1(C^\bullet \mathcal{G})$ represents. For starters, let's compare $H^0(C^\bullet \mathcal{G})$ on X and Y, as shown in Figure 2.15. Recall that the vector bundles were obtained by applying a half twist at each edge. Then, the vector bundle on X must be orientable, since we are applying this half twist even number of times, while the vector bundle on Y must be non-orientable since the half twist has been applied an odd number of times. This is, in fact reflected by the fact that $\dim H^0(C^\bullet \mathcal{G}) = 2$ on X and $\dim H^0(C^\bullet \mathcal{G}) = 1$ on Y. The fact that odd-length cycles is precisely what contributes to non-orientability of vector bundles is reflected in the language of graph theory in the following theorem that appears in one of the first textbooks on graph theory.

Theorem 4 ([18])**.** *A graph G is 2-colorable if and only if it has no odd-length cycles.*

Another way to approach such 2-coloring problem is to use a constant sheaf $\mathcal{C}$ on X whose local sections are $\mathcal{C}(\sigma) = \mathbb{F}_2$ for all $\sigma \in X$. Note that all restriction maps of $\mathcal{C}$ are the identity maps.

A graph X is 2-colorable if and only if it is bipartite, i.e., the vertices of X can be divided into disjoint sets U and V such that every edge connects between vertices in U and V. Then, whether or not a graph is colorable with two colors amounts to the following statement :

Proposition 4. *A graph X is 2-colorable if and only if the 1-cycle $(1, 1, \ldots, 1)$ of $\mathcal{C}$ lies in the image of $\partial^0 : C^0(C^\bullet \mathcal{C}) \to C^1(C^\bullet \mathcal{C})$, i.e., the homology class $[(1, 1, \ldots, 1)]$ is trivial in $H^1(C^\bullet \mathcal{C})$.*

2.2.4 Change of base spaces

So far, we discussed sheaf morphisms as tools for studying changes in sheaf $\mathcal{F}$ over a fixed base space. We can also ask ourselves how we might relate a sheaf on one space to a sheaf on another space. The ideas of pullback and pushforward allow us to address these questions.

Definition 16 ([10]). Let X and Y be cell complexes. Let $\mathcal{G}$ be a sheaf on Y, and let $f : X \to Y$ be a cellular map. The **pullback** or **inverse image sheaf** $f^*\mathcal{G}$ on X is defined as the following.

For $\sigma \in X$, the local section is $f^*\mathcal{G}(\sigma) = G(f(\sigma))$

If $\tau \trianglelefteq \sigma$, then the restriction map is $f^*\mathcal{G}(\tau \trianglelefteq \sigma) = \mathcal{G}(f(\tau) \trianglelefteq f(\sigma))$.

We can define the pullback of a cosheaf analogously.

Theorem 5 (Vietoris-Begle Mapping Theorem, [3]). *Let $f : X \to Y$ be a proper map between locally compact spaces with acyclic fibers. For any sheaf $\mathcal{G}$ on Y, the induced map*

$$f^* : H^n(C^\bullet \mathcal{G}) \to H^n(C^\bullet f^* \mathcal{G})$$

is an isomorphism for all n,

On the other hand, given a sheaf on Y, we can define a sheaf on X as the following.

Definition 17 ([10]). Let X and Y be cell complexes. Let $\mathcal{F}$ be a sheaf on X, and let $f : X \to Y$ be a cellular map. The **pushforward sheaf** $f_*\mathcal{F}$ on Y is defined as the following.

For $\sigma \in Y$, the local section is $f_*\mathcal{F}(\sigma) = \varprojlim_{f(\tau) \trianglerighteq \sigma} \mathcal{F}(\tau)$

If $\tau \trianglelefteq \sigma$, then the map $f_*\mathcal{F}(\tau) \to f_*\mathcal{F}(\sigma)$ is defined by the universal property of limits.

In other words, the local section $f_*\mathcal{F}(\sigma)$ is the global section of $\mathcal{F}$ over all cells τ such that $f(\tau) \trianglerighteq \sigma$.

To define the pushforward for a cosheaf $\mathcal{G}$ on X, let $f_*\mathcal{G}(\sigma) = \varinjlim_{f(\tau) \trianglerighteq \sigma} \mathcal{G}(\tau)$.

Example 8. One way to think of the pushforward sheaf is to consider it as a way of summarizing data over X as we simplify the base space via f. For example, consider the sheaf $\mathcal{F}$ on X illustrated in Figure 2.17a. A cellular map from X to Y is illustrated in Figure 2.16. The map $f : X \to Y$ is the cellular map defined by mapping 0-cell v to w.

The pushforward sheaf $f_*\mathcal{F}$ on Y is illustrated in Figure 2.17b. Note that $\mathcal{F}$ and $f_*\mathcal{F}$ have the same homologies for this particular example.

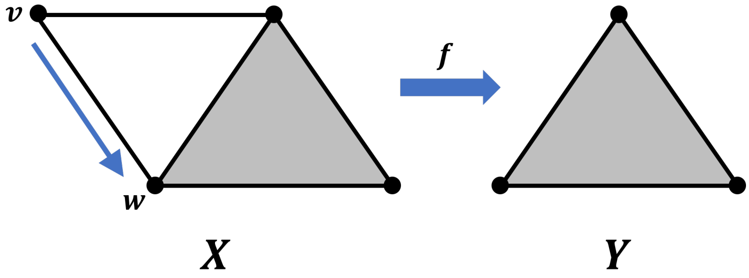

FIGURE 2.16: A cellular map $f : X \to Y$

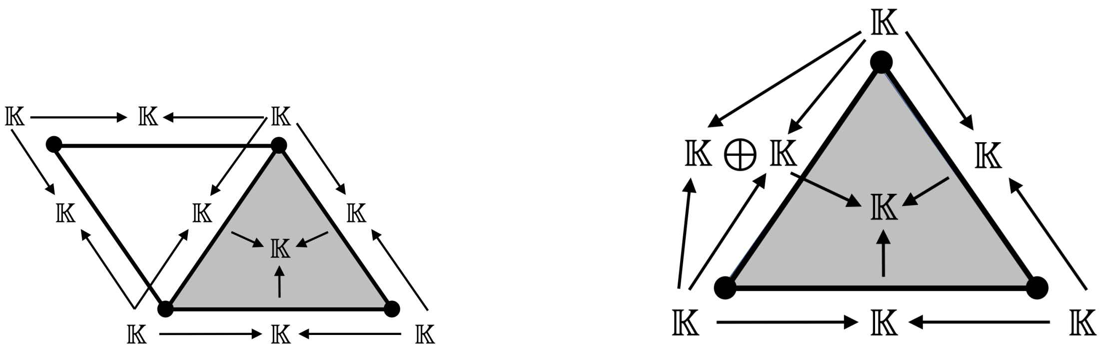

(A) Cellular sheaf $\mathcal{F}$ on X

(B) Cellular sheaf $f_*\mathcal{F}$ on Y

FIGURE 2.17: Cellular sheaf $\mathcal{F}$ on X and pushforward sheaf $f_*\mathcal{F}$ on Y

One should note that there are multiple kinds of pushforward of a sheaf. Considering a sheaf $\mathcal{F}$ as a functor from cell category to a category D, the pushforward $f_*\mathcal{F}$ is the right Kan extension of $\mathcal{F}$ along f. One can approach the pushforward by using a left Kan extension as well. The pushforward obtained by left Kan extension, denoted by $f_\dagger$, is called pushforward with open supports. Some calculated examples of pushforward sheaf, pushforward with open supports, pushfoward with compact supports, and their adjoint relations are described in detail in [10].

2.2.5 Sheaf cohomology, cosheaf homology, and zigzag modules

In previous sections, we have alluded to the fact that specific types of zigzag modules can be viewed as cellular sheaves or cosheaves and vice versa. Interpreting cellular sheaves (and cosheaves) as zigzag modules allows us to take advantage of Theorem 3 to decompose cellular sheaves in terms of simpler sheaves. Furthermore, such decomposition allows us to understand sheaf cohomology in terms of these simpler building blocks. Understanding the relations between sheaf cohomology and sheaf decomposition will play a crucial role in Chapter 5.

When our base space X is a compact subset of $\mathbb{R}$ with some cell structure, we can approach cellular sheaves and cellular cosheaves through the lens of zigzag modules. Indeed, given any sheaf $\mathcal{F}$ or cosheaf $\mathcal{G}$ on X, the local sections and the restriction or extension maps constitute a zigzag module. From Theorem 3, we know that such a finite zigzag module can be decomposed into a sum of interval modules $\mathbb{I}(b,d)$. Each of these interval modules $\mathbb{I}(b,d)$ are, in fact, indecomposable sheaves or cosheaves on X. Hence, we can decompose our sheaf or cosheaf into a direct sum of indecomposable sheaves and cosheaves. Such decomposition allows us to approach sheaf cohomology and cosheaf homology in terms of these simpler data structures.

For example, assume that a cellular sheaf $\mathcal{F}$ can be decomposed as a direct sum of indecomposable sheaves as illustrated in Figure 2.18.

$$
\begin{array}{ccccccccc}
 & & \mathbb{K} & \leftarrow & \mathbb{K} & \rightarrow & \mathbb{K} & & \\
\mathbb{K} & \rightarrow & \mathbb{K} & \leftarrow & \mathbb{K} & \rightarrow & \mathbb{K} & & \\
\mathbb{K} & \rightarrow & \mathbb{K} & \leftarrow & \mathbb{K} & \rightarrow & \mathbb{K} & \leftarrow & \mathbb{K} \\
 & & \mathbb{K} & \leftarrow & \mathbb{K} & \rightarrow & \mathbb{K} & \leftarrow & \mathbb{K} \\
\mathbb{K} & \rightarrow & \mathbb{K} & \leftarrow & \mathbb{K} & & & &
\end{array}
$$

FIGURE 2.18: A cellular sheaf $\mathcal{F}$ decomposed as a direct sum of indecomposable sheaves

Note that there are four types of indecomposable sheaves possible: sheaves $\mathcal{I}_{[-]}$ whose left and right most supports are 0-cells, sheaves $\mathcal{I}_{]-[}$ whose left and right most supports are 1-cells, sheaves $\mathcal{I}_{[-[}$ whose left most support is a 0-cell and the right most support is a 1-cell, and the sheaves $\mathcal{I}_{]-]}$ whose left most support is a 1-cell and the right most support is a 0-cell.

The following lemmas establish the connections between sheaves and barcodes of zigzag modules.

Lemma 5 ([10]). *The indecomposable sheaves $\mathcal{I}$ satisfy*

$$H^0(C^\bullet \mathcal{I}_{[-]}) = \mathbb{K}, \quad H^1(C^\bullet \mathcal{I}_{]-[}) = \mathbb{K}, \quad H^i(C^\bullet \mathcal{I}_{[-[}) = H^i(C^\bullet \mathcal{I}_{]-]}) = 0.$$

If sheaf $\mathcal{F}$ is decomposed as $\mathcal{F} \cong \bigoplus \mathcal{I}$, then $H^i(C^\bullet \mathcal{F}) \cong \oplus H^i(C^\bullet \mathcal{I})$. Thus, $\dim H^0(C^\bullet \mathcal{F})$ counts the number of bars of form $[-]$ in the decomposition, whereas $\dim H^1(C^\bullet \mathcal{F})$ counts the number of bars of form $]-[$ in the decomposition.

Analogously, a cosheaf $\mathcal{G}$ on X can be decomposed into a sum of indecomposable cosheaves $\mathcal{I}_{[-]}$, $\mathcal{I}_{]-[}$, $\mathcal{I}_{[-[}$, and $\mathcal{I}_{]-]}$.

Lemma 6 ([10]). *The indecomposable cosheaves $\mathcal{I}$ satisfy*

$$H_0(C_\bullet \mathcal{I}_{[-]}) = \mathbb{K}, \quad H_1(C_\bullet \mathcal{I}_{]-[}) = \mathbb{K}, \quad H_i(C_\bullet \mathcal{I}_{[-[}) = H_i(C_\bullet \mathcal{I}_{]-]}) = 0.$$

Thus, if cosheaf $\mathcal{G}$ can be decomposed as $\mathcal{G} \cong \bigoplus \mathcal{I}$, then $H_i(C_\bullet \mathcal{G}) \cong \oplus H_i(C_\bullet \mathcal{I})$. The connections between sheaves and barcodes of zigzag modules established by Lemma 5 and Lemma 6 is the key to enriching the persistent homology barcodes in Chapter 5.

The cellular sheaf theory introduced in this chapter will be used to establish distributed systems for a variety of applications, where the distribution can occur with respect to time, sensing modalities, spatial relations, density estimates, and other properties of interest. The sheaf morphisms will allow us to examine such distributed systems that undergo changes with respect to factors such as time, base spaces, and other parameters in the system. In Chapter 4, cellular sheaf theory and persistent homology come together to produce a distributed computation scheme of persistent homology. In Chapter 5, the correspondence between cellular sheaves and zigzag persistence further strengthens persistent homology by enriching the information conveyed via barcodes.

Chapter 3

Distributed Systems for Pursuit and Evasion

The local to global nature of sheaf theory makes it a suitable tool for distributed data analysis. This chapter discusses applications of cellular sheaves and cosheaves to variations of problems in pursuit and evasion. These novel applications highlight the utility of information distribution and collation with respect to particular aspects of the problem. In §3.1 we use cellular sheaves to encode evader's information at different time points. We propose a necessary and sufficient condition for determining whether an evasion path exists over a given time interval. In §3.2 we consider a variation of pursuit and evasion problems where a teamwork of pursuers is required to capture an evader. Information available to each team of pursuers is then collated via cellular sheaves to determine if an evader can hide from the team of pursuers that is specified by a boolean expression. While these applications are constructed in the context of pursuit and evasion problems, they allude to further applications of cellular sheaf theory to time varying data, propositional logic, and many more.

3.1 Pursuit and Evasion

We consider a variation of a pursuit and evasion game. Suppose that a collection of mobile sensors (or pursuers) with minimal sensing abilities wanders in a bounded domain. The sensors are minimal in the sense that they do not know their location coordinates. However, the sensors can detect objects (other sensors and evaders) that are within a certain distance from them. The goal of the sensors is to capture evaders, where capture occurs when an evader is in a sensed region. An interesting topological question, then, is whether we can determine if an evader can successfully hide from the pursuers, given only the connectivity information conveyed by the sensors.

To mathematically formulate the problem, let $D \subset \mathbb{R}^d$ be a bounded domain where pursuers (or sensors) and evaders can move around. Let $S \subset D \times [0, 1]$ denote the regions that sensors occupy over the time interval $[0, 1]$, and let $E = S^c$, which represents the possible areas an evader can hide. An evasion path is a section $s : [0, 1] \to E$ of the time projection map $\pi : E \to [0, 1]$. The question of interest is whether there is a necessary and sufficient condition for the existence of an evasion path.

An approach by de Silva and Ghrist [25] gives a partial answer to this question by providing the necessary condition to the existence of an evasion path. Adams and Carlsson [2] phrase an equivalent condition in the language of zigzag persistence, hence allowing the necessary condition to be computed in a streamlining fashion. They also provide an example illustrating the fact that it is impossible to find a necessary and sufficient condition from connectivity of sensors alone. Curry [10] rephrases Adams and Carlsson's approach in the language of cellular cosheaves obtained from studying Reeb graph of $\pi : E \to [0, 1]$. The author found such sheaf theoretic approach to be particularly helpful, so we will begin our discussion in a similar framework.

Note that a necessary and sufficient condition to a very general pursuit and evasion problem is provided by Ghrist and Krishnan [15] using positive (co)homology and positive variant of Alexander Duality. The goal of this section is to further explore the sheaf theoretic viewpoint phrased by Curry and to provide a variant of cellular sheaf that gives a necessary and sufficient condition for the existence of an evasion path given $\pi : E \to [0, 1]$.

3.1.1 Sheaf theoretic viewpoint of pursuit and evasion

Let $\pi : E \to [0,1]$ be a cellular map that projects the escape region to the time axis. Let $R(E)$ denote the Reeb graph of π. We then obtain a cellular map $R(E) \to [0,1]$. For the remainder of this chapter, we will take the projection map π to denote $\pi : R(E) \to [0,1]$. Let X denote $[0,1]$ with the given cell structure. The vertices of X correspond to discrete time points, say $t_0, \ldots, t_K$, and edges of X correspond to intervals between consecutive time points.

We present a summary of the construction by Adams and Carlsson and the counterexample for the construction using sheaf theoretic language as expressed by Curry. Let $\pi : R(E) \to [0,1]$ be the cellular map illustrated in Figure 3.1a. Let $\mathcal{C}$ be the constant sheaf of vector spaces on $R(E)$. One can then construct a sheaf $\mathcal{G}$ on $X = [0,1]$ by taking the pushforward sheaf (Definition 17) of $\mathcal{C}$, i.e., $\mathcal{G} = \pi_* \mathcal{C}$. The sheaf $\mathcal{G}$ on X is illustrated in Figure 3.1b.

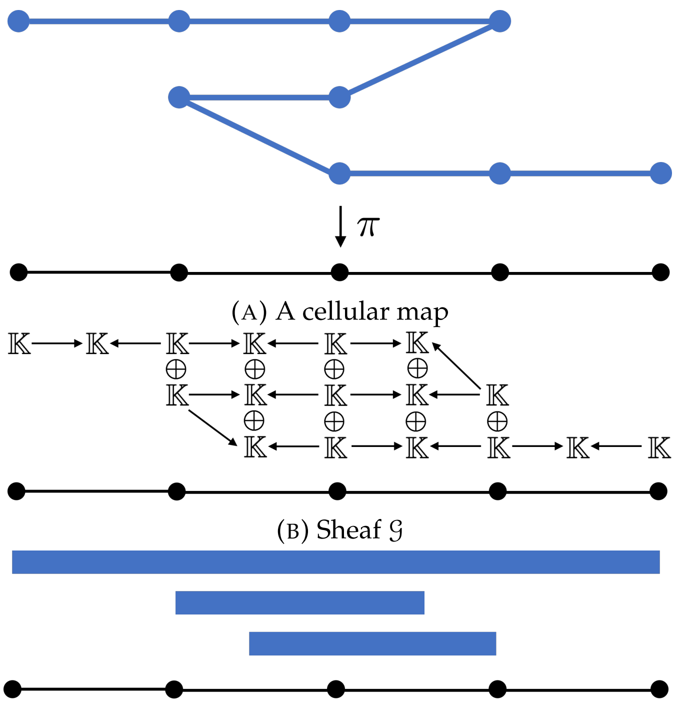

(A) A cellular map

(B) Sheaf $\mathcal{G}$

(C) Barcode

FIGURE 3.1: A counterexample cellular map and sheaf

Considering the sheaf $\mathcal{G}$ as a zigzag persistence module, Adams and Carlsson show that if there exits an evasion path, then there exists a full length interval in the barcode. The example in Figure 3.1b illustrates the fact that the existence of a full length interval in the barcode is not sufficient condition for an evasion path to exist. The barcode, illustrated in Figure 3.1c, show that there exists a full length interval. However, from Figure 3.1a, we can see that it is not possible for an evader to escape unless the evader is allowed to travel back in time.

In order to resolve this issue, Curry proposes a new sheaf on X by linearizing the sheaf of sections. When such a sheaf is constructed for the example in Figure 3.1a, we no longer detect the full length bar in its barcode decomposition. However, Curry also provides a counterexample, illustrated in Figure 3.2a, showing how a non-escape path can lead to a full length interval in the barcode, illustrated in 3.2b.

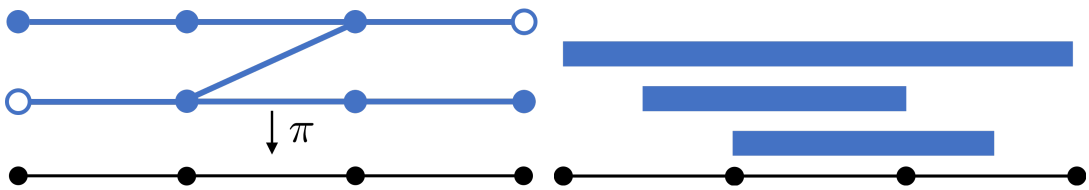

(A) Cellular map (B) Barcode

FIGURE 3.2: Counterexample by Curry

We provide another sheaf construction on X whose existence of a full length barcode provides a necessary and sufficient condition for the existence of an escape path. For each vertex v_i of X, let $\mathcal{F}(v_i)$ be the vector space generated by the set $\pi^{-1}(v_i)$. For example, if $\pi^{-1}(v_i)$ consists of three components, say a, b, c, then let $\mathcal{F}(v_i)$ be the vector space with basis denoted by $\vec{e}_a, \vec{e}_b, \vec{e}_c$. For each edge $e_{i,i+1}$ connecting the vertex v_i on the left and v_{i+1} on the right, let $\mathcal{F}(e_{i,i+1}) = \mathcal{F}(v_{i+1})$. To define the restriction maps, given $v_{i+1} \trianglelefteq e_{i,i+1}$, let $\mathcal{F}(v_{i+1} \trianglelefteq e_{i,i+1}) : \mathcal{F}(v_{i+1}) \to \mathcal{F}(e_{i,i+1})$ be the identity map. Given $v_i \trianglelefteq e_{i,i+1}$, we will define $\mathcal{F}(v_i \trianglelefteq e_{i,i+1})$ on the basis vectors of $\mathcal{F}(v_i)$ as the following. Let $\vec{e}^i_1, \ldots, \vec{e}^i_n$ be the basis vectors of $\mathcal{F}(v_i)$ each representing the cells $a^i_1, \ldots, a^i_n$ of $\pi^{-1}(v_i)$, and let $\vec{e}^{i+1}_1, \ldots, \vec{e}^{i+1}_m$ be the basis vectors of $\mathcal{F}(e_{i,i+1}) = \mathcal{F}(v_{i+1})$ each representing the cells $a^{i+1}_1, \ldots, a^{i+1}_m$ of $\pi^{-1}(v_{i+1})$. For each component a^i_j of $\pi^{-1}(v_i)$, let $a^{i+1}_{j_1}, \ldots, a^{i+1}_{j_k}$ be the elements of $\pi^{-1}(v_{i+1})$ that are connected to a^i_j via an edge in $R(E)$. Then, define

$\mathcal{F}(v_i \trianglelefteq e_{i,i+1})$ to be the linear transformation that maps $\vec{e}^{\,i}_j$ to $\vec{e}^{\,i+1}_{j_1} + \cdots + \vec{e}^{\,i+1}_{j_k}$, i.e., the morphism $\mathcal{F}(v_i \trianglelefteq e_{i,i+1})$ maps $\vec{e}^{\,i}_j$ to $\vec{e}^{\,i+1}_l$ if it's possible for an evader to move from a^i_j to a^{i+1}_l in $R(E)$. Note that if there are no evasion paths possible from a^i_j, then $\mathcal{F}(v_i \trianglelefteq e_{i,i+1})$ maps $\vec{e}^{\,i}_j$ to the zero vector.

Once we define sheaf $\mathcal{F}$ of vector spaces, we obtain the following cochain complex

$$0 \to C^0\mathcal{F} \xrightarrow{\partial} C^1\mathcal{F} \to 0,$$

where $C^0\mathcal{F} = \bigoplus_v \mathcal{F}(v)$. By construction, for every $v_{i+1} \trianglelefteq e_{i,i+1}$, the restriction map $\mathcal{F}(v_{i+1} \trianglelefteq e_{i,i+1})$ is an identity map. Thus, if $\gamma \in \ker \partial$ and $v_0, \ldots, v_K$ are the vertices of X, then by construction, γ can be expressed as the following

$$\gamma = \gamma_0 + \gamma_1 + \cdots + \gamma_K, \tag{3.1}$$

where $\gamma_0 \in \mathcal{F}(v_0)$, $\gamma_1 \in \mathcal{F}(v_1), \ldots, \gamma_K \in \mathcal{F}(v_K)$, and $\gamma_{i+1} = \mathcal{F}(v_i \trianglelefteq e_{i,i+1})(\gamma_i)$ for every i.

Lemma 7. *$H^0(C^\bullet\mathcal{F}) \cong \mathcal{F}(v_0)$.*

Proof. Given $\gamma \in H^0(C^\bullet\mathcal{F})$, recall from Equation 3.1 the expression of

$$\gamma = \gamma_0 + \gamma + 1 + \cdots + \gamma_K.$$

Define $f : H^0(C^\bullet\mathcal{F}) \to \mathcal{F}(v_0)$ by

$$f(\gamma) = \gamma_0.$$

Note that this map f is linear.

We will show that f is an isomorphism. Given $\gamma_0 \in \mathcal{F}(v_0)$, let $\gamma_1 \in \mathcal{F}(v_1), \ldots,$ $\gamma_K \in \mathcal{F}(v_K)$ be defined by the following

$$\begin{aligned}
\gamma_1 &= \mathcal{F}(v_0 \trianglelefteq e_{0,1})(\gamma_0) \\
\gamma_2 &= \mathcal{F}(v_1 \trianglelefteq e_{1,2})(\gamma_1) \\
&\vdots \\
\gamma_K &= \mathcal{F}(v_{K-1} \trianglelefteq e_{K-1,K})(\gamma_{K-1}).
\end{aligned}$$

Let

$$\gamma' = \gamma_0 + \gamma_1 + \cdots + \gamma_K.$$

Then, $f(\gamma') = \gamma_0$. So f is surjective.

To show that f is injective, assume that $f(\gamma) = 0$, i.e., $\gamma_0 = 0$. Then, by Equation 3.1, $\gamma_i = 0$ for all i, and $\gamma = 0$. Thus, f is injective.

Thus, f is an isomorphism. □

A useful conclusion from Lemma 7 is that we can find an explicit basis for $H^0(C^\bullet\mathcal{F})$ as the collection of standard basis vectors $\vec{e}_j^{\,0}$'s of $\mathcal{F}(v_0)$, i.e., given a standard basis vector $\vec{e}_j^{\,0}$ of $\mathcal{F}(v_0)$, define $\vec{e}_j^{\,i} \in \mathcal{F}(v_i)$ by

$$\begin{aligned}
\vec{e}_j^{\,1} &= \mathcal{F}(v_0 \trianglelefteq e_{0,1})(\vec{e}_j^{\,0}) \\
\vec{e}_j^{\,2} &= \mathcal{F}(v_1 \trianglelefteq e_{1,2})(\vec{e}_j^{\,1}) \\
&\vdots \\
\vec{e}_j^{\,K} &= \mathcal{F}(v_{K-1} \trianglelefteq e_{K-1,K})(\vec{e}_j^{\,K-1}).
\end{aligned}$$

Then, the collection of vectors of form

$$e'_j = \vec{e}_j^{\,0} + \vec{e}_j^{\,1} + \cdots + \vec{e}_j^{\,K} \tag{3.2}$$

form a basis of $H^0(C^\bullet\mathcal{F})$. Note that each such vector e'_j represents an evasion path starting at component a_j^0 of $\pi^{-1}(v_0)$.

Example 9. Let's now revisit the Reeb graph from Figure 3.3a. The sheaf $\mathcal{F}$ on X is illustrated in Figure 3.3b.

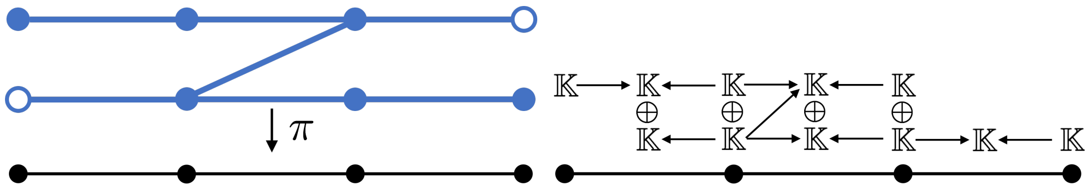

(A) A cellular map (B) Sheaf $\mathcal{F}$

FIGURE 3.3: A cellular map and sheaf

The basis for $H^0(C^\bullet\mathcal{F})$ and the corresponding escape path are illustrated in Figures 3.4a and 3.4b.

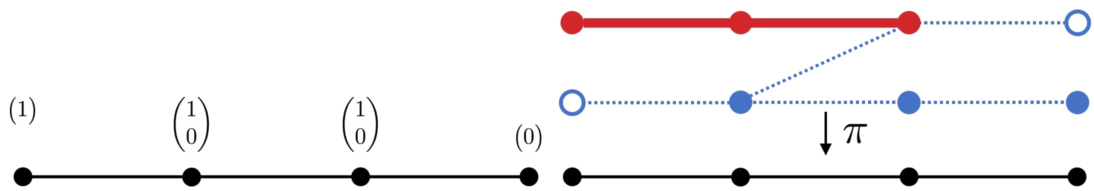

(A) (B)

FIGURE 3.4: A basis vector of $H^0(C^\bullet\mathcal{F})$ and its representing escape path

Example 10. Consider the escape region illustrated in Figure 3.5a. It's corresponding sheaf $\mathcal{F}$ is illustrated in Figure 3.5b.

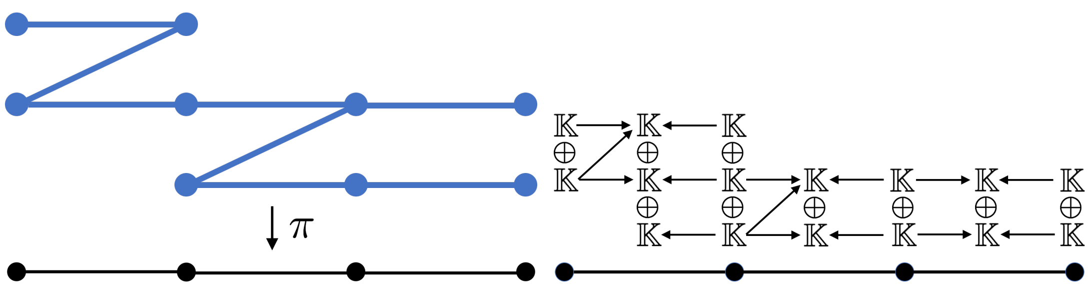

(A) A cellular map (B) Sheaf $\mathcal{F}$

FIGURE 3.5: A cellular map and sheaf

The two basis vectors of $H^0(C^\bullet\mathcal{F})$ are illustrated in Figures 3.6a and 3.6c. The escape paths they represent are illustrated in Figures 3.6b and 3.6d. Note from Figures 3.6b and

3.6d that the escape paths represent all possible movements starting from a particular node at time t_0.

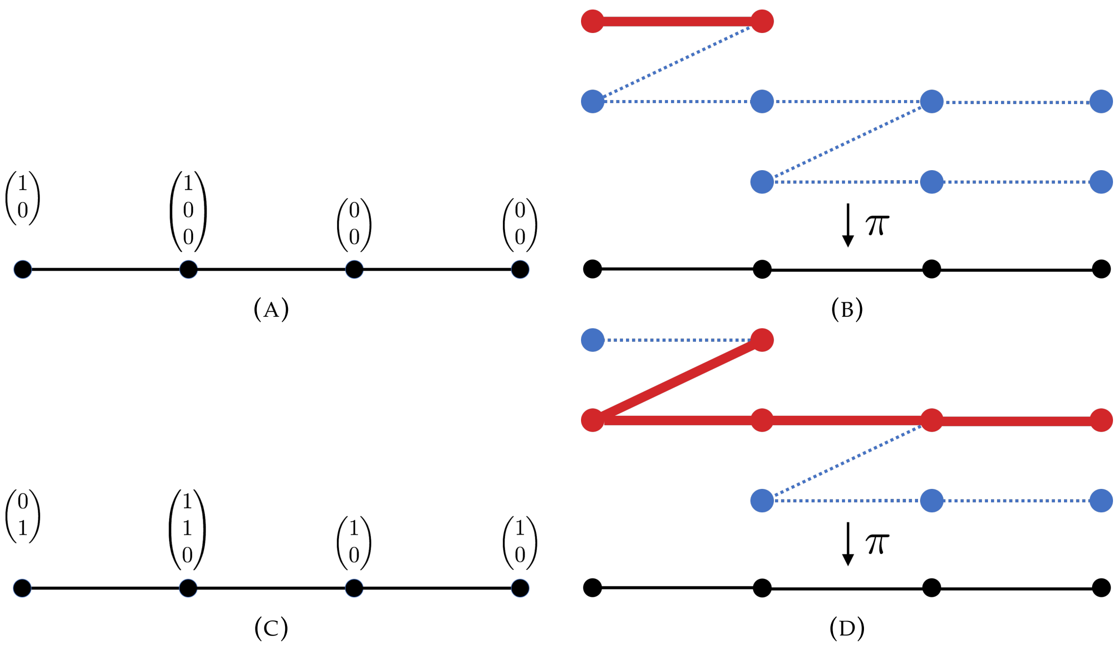

FIGURE 3.6: Basis vectors of $H^0(C^\bullet \mathcal{F})$ and the corresponding escape paths

Note that each component of $H^0(C^\bullet \mathcal{F})$ corresponds to a possible escape path that starts at a particular node at time t_0. The escape paths that emerge from an intermediate time point are not detected by $H^0(C^\bullet \mathcal{F})$. However, the sheaf cohomology $H^0(C^\bullet \mathcal{F})$ fails to distinguish escape paths that continue to the end from the ones that don't.

From previous examples, we have seen that while $H^0(C^\bullet \mathcal{F})$ detects possible escape paths, it fails to distinguish the true escape paths from the ones that disappear in an intermediate time point. To address this issue, we use persistent homology.

Recall the sheaf of vector spaces $\mathcal{F}$ on the graph X. Let $\mathcal{G}$ be a sheaf on X such that $\mathcal{G}(v_K) = \mathcal{F}(v_K)$ for the very last vertex v_K of X and $\mathcal{G}(\sigma) = 0$ for any other cell σ of X.

Define a sheaf morphism $\phi : \mathcal{F} \to \mathcal{G}$ as the following. Let $\phi_{v_K} : \mathcal{F}(v_K) \to \mathcal{G}(v_K)$ be the identity morphism. For all other cells σ of X, let ϕ_σ be the zero map.

The induced morphism $H^0(\phi) : H^0(C^\bullet \mathcal{F}) \to H^0(C^\bullet \mathcal{G})$ then checks whether an escape path emerging at time t_0, as read by $H^0(C^\bullet \mathcal{F})$, continues until the final time t_K.

The image of the induced morphism $H^0(\phi)$ then correspond to escape paths beginning at t_0 and ending at time t_K. The following Lemma makes this statement formal.

Lemma 8. *An escape path exists in $R(E)$ if and only if $\dim(\mathrm{im} H^0(\phi)) \neq 0$.*

Proof. If there exists an escape path in $R(E)$, say starting at node a_j^0 at time t_0, let $\vec{e}_j^{\,0}$ be the standard basis vector of $\mathcal{F}(v_0)$ that represents this node. Recall from Equation 3.2 that one can find an explicit basis $e_j' = \vec{e}_j^{\,0} + \vec{e}_j^{\,1} + \cdots + \vec{e}_j^{\,K}$ of $H^0(C^\bullet\mathcal{F})$. Since e_j' represents all escape paths starting at node j, we know that $\vec{e}_j^{\,K} \in \mathcal{F}(v_K)$ is nontrivial. In fact, $H^0(\phi)[e_j'] = \vec{e}_j^{\,K}$, so $\dim(\mathrm{im}\, H^0(\phi)) \neq 0$.

On the other hand, assume that no escape path exists. For any node a_j^0 at time t_0, let $\vec{E}_j^{\,0}$ be the standard basis vector of $\mathcal{F}(v_0)$ that represents this node. Again, we can find an explicit basis $e_j' = \vec{e}_j^{\,0} + \vec{e}_j^{\,1} + \cdots + \vec{e}_j^{\,K}$ of $H^0(C^\bullet\mathcal{F})$. Since there are no escape paths, we know that $\vec{e}_j^{\,K} = 0$. Then, $\mathrm{im}\, H^0(\phi)$ must be trivial, and $\dim(\mathrm{im}\, H^0(\phi)) = 0$. $\square$

An equivalent formulation of Lemma 8 can be obtained by considering the sheaf $\mathcal{F}$ as a zigzag module. Then, $\dim(\mathrm{im}\, H^0(\phi)) \neq 0$ if and only if the barcode decomposition of $\mathcal{F}$ contains a full-length bar. Note that by construction, every backwards map $\mathcal{F}(v_{i+1} \trianglelefteq e_{i,i+1})$ is an identity map. Thus, instead of examining the sheaf $\mathcal{F}$ as a zigzag module, one can consider the following persistence module

$$\mathbb{V}_{\mathcal{F}} : \mathcal{F}(v_0) \xrightarrow{\mathcal{F}(v_0 \trianglelefteq v_1)} \mathcal{F}(v_1) \xrightarrow{\mathcal{F}(v_1 \trianglelefteq v_2)} \cdots \xrightarrow{\mathcal{F}(v_{K-1} \trianglelefteq v_K)} \mathcal{F}(v_K),$$

where $\mathcal{F}(v_i \trianglelefteq v_{i+1}) : \mathcal{F}(v_i) \to \mathcal{F}(v_{i+1})$ is the restriction map $\mathcal{F}(v_i \trianglelefteq e_{i,i+1})$ from earlier. Then, a full length bar exists in the barcode decomposition of $\mathcal{F}$ is and only if there exists a full length bar in the barcode decomposition of $\mathbb{V}_{\mathcal{F}}$.

Corollary 1. *Given $\mathcal{F}$ on X, the barcode of $\mathbb{V}_{\mathcal{F}}$ contains a full length bar if and only if there exists an escape path in $R(E)$.*

Example 11. Recall the escape regions from Figure 3.3a. The sheaf $\mathcal{F}$ illustrated in Figure 3.3b gives rise to the following persistence module illustrated in Figure 3.7a.

$$\begin{tikzcd}
\mathbb{K} \arrow[r] & \mathbb{K} \arrow[r] & \mathbb{K} & \\
& \oplus & \oplus & \\
& \mathbb{K} \arrow[r] \arrow[uur] & \mathbb{K} \arrow[r] & \mathbb{K}
\end{tikzcd}$$

(A) Persistence module from sheaf $\mathcal{F}$

(B) Barcode

FIGURE 3.7: Persistence module and barcode

The barcode of this persistence module, illustrated in Figure 3.7b, lacks a full length interval, implying that there is no escape path in Figure 3.3a.

On the other hand, consider the escape region from Figure 3.5a. The associated sheaf, illustrated in Figure 3.5b, results in a persistence module illustrated in Figure 3.8a, and its barcode illustrated in Figure 3.8b contains a full length interval, implying the fact that there exists an escape path.

$$\begin{tikzcd}
\mathbb{K} \arrow[r] & \mathbb{K} & & \\
\oplus & \oplus & & \\
\mathbb{K} \arrow[r] \arrow[uur] & \mathbb{K} \arrow[r] & \mathbb{K} \arrow[r] & \mathbb{K} \\
& \oplus & \oplus & \oplus \\
& \mathbb{K} \arrow[r] \arrow[uur] & \mathbb{K} \arrow[r] & \mathbb{K}
\end{tikzcd}$$

(A) Persistence module from sheaf $\mathcal{F}$

(B) Barcode

FIGURE 3.8: Persistence module and barcode

3.2 Boolean Pursuit and Evasion

Consider a variation of a pursuit and evasion problem, where the domain D is now a graph or a grid. Assume that the pursuers know their exact coordinates on D. Moreover, assume that the pursuers are divided into teams of different colors, say red, blue, and yellow. Specific teamwork is required for a pursuer to be captured. For example, an evader can be captured if both the red and blue pursuers are at the same location as the evader, or if both the blue and yellow pursuers are at the same location.

Such rule for combination of sensors required for capture will be called a capture criterion. Let $p = \{p_1, \ldots, p_M\}$ be the collection of different colored team of pursuers.

For the remainder of this section, we will refer to each p_i, which is a collection of pursuers belonging to a same colored team, as one pursuer. For example, if p_i is a collection of red pursuers, we will refer to p_i as the red pursuer.

Let P_i be a binary variable. One can think of $P_i = 1$ as indicating that an evader is sensed by pursuer p_i and $P_i = 0$ as indicating that the evader is not sensed by p_i.

A capture criterion can be written as

$$C = T_1 \vee T_2 \vee \cdots \vee T_K,$$

where each $T_i = P_{i_1} \wedge \cdots \wedge P_{i_M}$ denotes the teams of pursuers required for capture. For example, the following capture criterion

$$C = (P_R \wedge P_B) \vee (P_R \wedge P_Y) \tag{3.3}$$

indicates that capture occurs if both red and blue pursuers are present or if both red and yellow pursuers are present.

For each node $x \in D$, the variables P_i are assigned a value depending on whether x is sensed by pursuer p_i. Let C_x denote the value of expression C for the node x. Then, $C_x = 1$ if an evader at node x is captured by pursuers, and $C_x = 0$ if the evader at node x can escape.

Given a coverage criterion C, our goal is to determine the nodes $x \in D$ that do not satisfy C, i.e., we want to find the nodes $x \in D$ such that $C_x = 0$. Note that $\neg C_x = 1$ if $C_x = 0$ and $\neg C_x = 0$ if $C_x = 1$. So let

$$E = \neg C$$

be the escape criterion. If $E_x = 1$, then an evader at node x can escape, and if $E_x = 0$, then an evader at node x cannot escape.

For the capture criterion $C = (P_R \wedge P_B) \vee (P_R \wedge P_Y)$ from Equation 3.3, the corresponding escape criterion is

$$E = (\neg P_R \vee \neg P_B) \wedge (\neg P_R \vee \neg P_Y).$$

Since every propositional formula can be written in a conjunctive normal form, we can equivalently write the escape criterion as

$$E = \neg P_R \vee (\neg P_B \wedge \neg P_Y).$$

Since each pursuer p_i knows the exact nodes of D that are covered by p_i, the pursuer also knows the nodes of D that remain undetected by pursuer p_i. From each pursuer's knowledge of the uncovered region, we can use sheaves and cosheaves to determine if it's possible for an evader to hide.

3.2.1 Boolean capture via sheaves and cosheaves of sets

In this section, we construct sheaves and cosheaves that allow us to determine if it's possible for an evader to hide given an escape criterion. We assume that the escape criterion is given in either conjunctive normal form or disjunctive normal form.

Escape criterion in disjunctive normal form

Assume that we are given an escape criterion of the form

$$E = E_1 \vee E_2 \vee \cdots \vee E_K,$$

where each E_i has the form $E_i = \neg P_{i_0} \wedge \cdots \wedge \neg P_{i_n}$.

We first define the base space. Given M number of pursuers, let X be a $(M-1)$-simplex. Each vertex of X corresponds to a pursuer p_i, so label such vertex by v_{p_i}. For each n-simplex σ of X, label σ by its vertices. For example, if $v_{p_{i_0}}, \ldots, v_{p_{i_{n+1}}}$ are the vertices of σ, then label σ by $\sigma_{p_{i_0},\ldots,p_{i_{n+1}}}$.

We will now construct a cosheaf $\mathcal{S}$ of sets on X that encodes the region remaining undetected by the pursuers. For each vertex v_{p_i} of X, let $\mathcal{S}(v_{p_i})$ be the set of nodes of D that are not detected by the pursuer p_i. For each $\sigma_{p_{i_0},\ldots,p_{i_{n+1}}}$, let $\mathcal{S}(\sigma_{p_{i_0},\ldots,p_{i_{n+1}}}) = \bigcap_{j=0}^{n+1} \mathcal{S}(v_{p_{i_j}})$, the set of nodes of D that are not detected by any of the pursuers $p_{i_0}, \ldots, p_{i_{n+1}}$. Let the extension maps be the inclusion of sets.

For example, let D be a graph that is covered by three pursuers as illustrated in Figure 3.9. The base space X and the labels of its simplices are illustrated in Figure 3.10a. The cosheaf $\mathcal{S}$ on X is illustrated in Figure 3.10b. Note that even though Figure 3.10b shows the graph D as local sections, the local sections of $\mathcal{S}$ are just the sets corresponding to the colored nodes of the graph D.

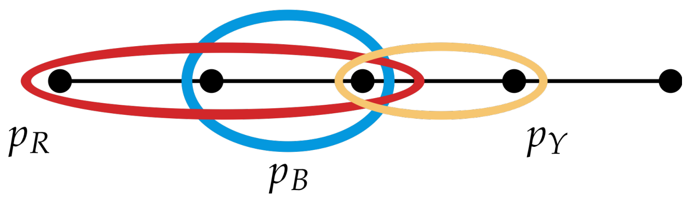

FIGURE 3.9: Domain D with pursuers.

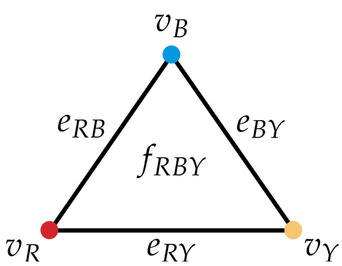

(A) Labels of simplices of base space X

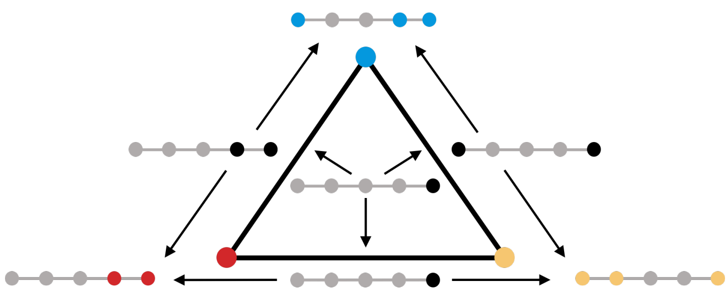

(B) Cosheaf of sets $\mathcal{S}$ encoding the nodes not occupied by pursuers.

FIGURE 3.10: Cosheaf of sets $\mathcal{S}$ on base space X

Assume that the escape criterion is

$$E = \neg P_R \vee (\neg P_B \wedge \neg P_Y). \tag{3.4}$$

Note that $\mathcal{S}(v_R)$ represents the two nodes that are not detected by the red sensors, and $\mathcal{S}(e_{BY})$ represents the two nodes that are not detected by both the blue sensors and the yellow sensors. The nodes that satisfy the escape criterion are the nodes that are in either $\mathcal{S}(v_R)$ or $\mathcal{S}(e_{BY})$. We can find such nodes by computing the colimit of the following diagram.

$$
\begin{tikzcd}
 & \mathcal{S}(e_{RB}) \arrow[r] & \mathcal{S}(v_R) \\
\mathcal{S}(f_{RBY}) \arrow[ur] \arrow[r] \arrow[dr] & \mathcal{S}(e_{RY}) \arrow[ur] & \\
 & \mathcal{S}(e_{BY}) &
\end{tikzcd}
\tag{3.5}
$$

The above diagram is illustrated in Figure 3.11.

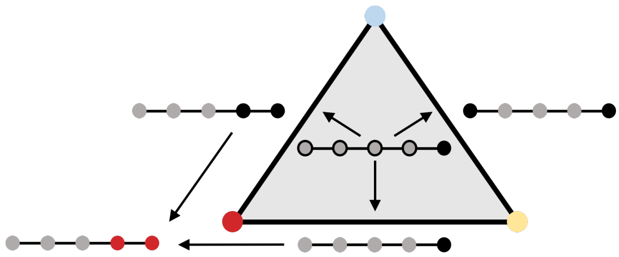

FIGURE 3.11: Diagram for colimit.

Note that the resulting colimit is the local section of $\mathcal{S}$ on the subset $\{v_R, e_{BY}, e_{RY}, e_{RB}, f_{RBY}\}$ of X. This local section is the set representing the nodes in Figure 3.12.

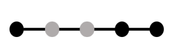

FIGURE 3.12: Local section of $\mathcal{S}$ on $\{v_R, e_{BY}, e_{RY}, e_{RB}, f_{RBY}\}$.

In general, given an escape criterion of the form

$$E = E_1 \vee E_2 \vee \cdots \vee E_K,$$

where each E_i has the form $E_i = \neg P_{i_0} \wedge \cdots \wedge \neg P_{i_n}$, the local sections $\mathcal{S}(\sigma_{p_{i_0},\ldots,p_{i_n}})$ on $\sigma_{p_{i_0},\ldots,p_{i_n}}$ represent the escape nodes that satisfy the criterion E_i. An escape node satisfying E is an escape node satisfying any of the criteria E_i's. The set of nodes satisfying

E can then be computed by

$$\varinjlim_{\tau \in S} \mathcal{S}(\tau),$$

where S is the collection of cells

$$S = \{\tau | \sigma_{p_{i_0},\ldots,p_{i_n}} \trianglelefteq \tau \trianglelefteq F \text{ for some } i\},$$

where F is the top dimensional cell in X and $\sigma_{p_{i_0},\ldots,p_{i_n}}$ is the cell corresponding to the escape criterion E_i.

Escape criterion in conjunctive normal form

The escape criterion can be equivalently expressed in its dual form

$$E = E^1 \wedge \cdots \wedge E^K,$$

where each E^i is a disjunction $E^i = \neg P_{i_0} \vee \cdots \vee \cdots \neg P_{i_n}$. In such cases, a dual construction of $\mathcal{S}$ can come in handy. While the local sections of cosheaf $\mathcal{S}$ on higher dimensional simplices encoded intersection relations of lower dimensional simplices, a dual construction would encode union relations instead of intersection relations.

On the same base space X, construct a sheaf $\hat{\mathcal{S}}$ as the following. Let $\hat{\mathcal{S}}(v_{p_i})$ be the set of nodes on D that are not detected by pursuer p_i as before. On each $\sigma_{p_{i_0},\ldots,p_{i_{n+1}}}$ of X, let $\hat{\mathcal{S}}(\sigma_{p_{i_0},\ldots,p_{i_{n+1}}}) = \bigcup_{j=0}^{n+1} \hat{\mathcal{S}}(v_{p_{i_j}})$. Let the restriction maps be inclusion maps of sets.

Recall the example illustrated in Figure 3.9. The sheaf $\hat{\mathcal{S}}$ for this example is illustrated in Figure 3.13.

The escape criterion in Equation 3.4 can be expressed in the following conjunctive normal form

$$E = (\neg P_R \vee \neg P_B) \wedge (\neg P_R \vee \neg P_Y).$$

The local section $\hat{\mathcal{S}}(e_{RB})$ denotes the set of nodes that satisfy the criterion $\neg P_R \vee \neg P_B$, and $\hat{\mathcal{S}}(e_{RY})$ represents the nodes that satisfy the criterion $\neg P_R \vee \neg P_Y$. The nodes that

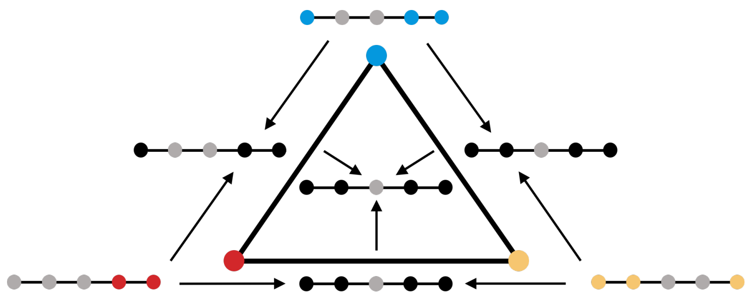

FIGURE 3.13: Sheaf $\hat{\mathcal{S}}$.

satisfy the escape criterion E are nodes that are present in both $\hat{\mathcal{S}}(e_{RB})$ and $\hat{\mathcal{S}}(e_{RY})$. Such nodes can be computed as the limit of diagram 3.6.

$$\begin{tikzcd} \hat{\mathcal{S}}(e_{RB}) \arrow[r] & \hat{\mathcal{S}}(f_{RBY}) \\ \hat{\mathcal{S}}(e_{RY}) \arrow[ur] & \end{tikzcd} \tag{3.6}$$

The diagram is illustrated in Figure 3.14. The nodes that satisfy the escape criterion then, are the local sections of the sheaf $\hat{\mathcal{S}}$ on the subset $\{e_{RB}, e_{RY}, f_{RBY}\}$.

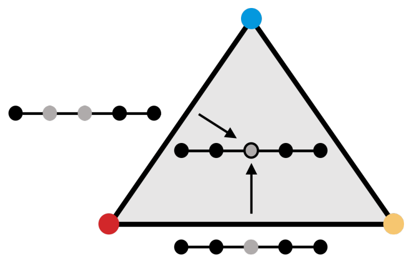

FIGURE 3.14: Diagram for limit.

In general, given an escape criterion in the conjunctive normal form

$$E = E^1 \wedge \cdots \wedge E^K,$$

where each E^i is a disjunction $E^i = \neg P_{i_0} \vee \cdots \vee \cdots \neg P_{i_n}$, the local section $\hat{\mathcal{S}}(\sigma_{p_{i_0},\ldots,p_{i_n}})$ on $\sigma_{p_{i_0},\ldots,p_{i_n}}$ represents the escape nodes that satisfy the criterion E^i. An escape node satisfying E is an escape node satisfying every criteria E^i. Such escape nodes can be computed by

$$\varprojlim_{\tau \in S} \hat{\mathcal{S}}(\tau),$$

where S is the collection of cells

$$S = \{\tau | \sigma_{p_{i_0},\ldots,p_{i_n}} \trianglelefteq \tau \trianglelefteq F \text{ for some } i\},$$

where F is the top dimensional cell in X and $\sigma_{p_{i_0},\ldots,p_{i_n}}$ is the cell corresponding to escape criterion E^i.

3.2.2 Boolean algebra via sheaves of vector spaces

We now present a different construction, one that allows us to take advantage of algebraic structure. Assume that an escape criterion is given in the conjunctive normal form

$$E = E^1 \wedge \cdots \wedge E^K,$$

where each E^i is a disjunction $E^i = \neg P_{i_0} \vee \cdots \vee \neg P_{i_n}$. We will construct a sheaf of vector spaces that can be used to determine if an evader can hide from the escape criterion E.

To start, let's assume a simpler escape criterion

$$E = \neg P_0 \vee \cdots \vee \neg P_i.$$

Recall the cosheaf of sets $\mathcal{S}$ constructed in §3.2.1. Let $\mathcal{V}$ be a cosheaf on X obtained from $\mathcal{S}$ by applying the free functor from category for sets to category of $\mathbb{K}$-modules, where $\mathbb{K}$ is a field, i.e., for every $\sigma \in X$, let $\mathcal{V}(\sigma)$ be the vector space generated by the set $\mathcal{S}(\sigma)$. Note that the extension maps of $\mathcal{S}$ also define the extension maps of $\mathcal{V}$.

One can visualize $\mathcal{V}$ using the same picture as $\mathcal{S}$. For example, recall the locations of pursuers on D from Figure 3.9. Figure 3.10b, which represents a picture for $\mathcal{S}$, also visualizes the cosheaf $\mathcal{V}$ on X. The nodes illustrated on $\sigma \in X$ can be interpreted as the basis for vector space $\mathcal{V}(\sigma)$.

For a concrete example, assume that our escape criterion is

$$E = \neg P_B \vee \neg P_Y,$$

which represents the fact that if a node is not detected by a blue pursuer or it's not detected by a yellow pursuer, then it's possible for an evader on the node to escape. Recall that the nodes that satisfy this escape criterion is computed by the colimit of the following diagram, which is the local section of $\mathcal{S}(\bar{e}_{BY})$ on the closed cell $\bar{e}_{BY}$ with vertices v_B and v_Y.

$$\begin{tikzcd} \mathcal{S}(e_{BY}) \arrow[r] \arrow[dr] & \mathcal{S}(v_B) \\ & \mathcal{S}(v_Y) \end{tikzcd}$$

Analogously, the local section of $\mathcal{V}(\bar{e}_{BY})$ on the closed cell $\bar{e}_{BY}$ is the colimit of the following diagram.

$$\begin{tikzcd} \mathcal{V}(e_{BY}) \arrow[r] \arrow[dr] & \mathcal{V}(v_B) \\ & \mathcal{V}(v_Y) \end{tikzcd}$$

Note that since the free functor is left adjoint to the forgetful functor, the free functor preserves colimits. Thus, $\mathcal{V}(\bar{e}_{BY})$ is the vector space generated by $\mathcal{S}(\bar{e}_{BY})$, i.e., $\mathcal{V}(\bar{e}_{BY})$ is the vector space generated by nodes that are escapable, and $\dim \mathcal{V}(\bar{e}_{BY})$ equals the number of escape nodes.

In general, given an escape criterion

$$E = \neg P_0 \vee \cdots \vee \neg P_i,$$

the vector space generated by the escape nodes is the local section of $\mathcal{V}$ on the closed cell $\overline{\sigma}_{p_0,\ldots,p_i}$.

Let's now consider the general case in which an escape criterion is given by

$$E = E^1 \wedge \cdots \wedge E^K,$$

where each E^i is a disjunction $E^i = \neg P_{i_0} \vee \cdots \vee \neg P_{i_n}$.

From the above construction of cosheaf $\mathcal{V}$, we know how to compute the number of escape nodes that satisfy each E^i. Our job now is to find the number of escape nodes that satisfy every E^i.

For example, assume that we are given the escape criterion

$$E = (\neg P_R \vee \neg P_B) \wedge (\neg P_R \vee \neg P_Y).$$

Then, the escape nodes satisfying $\neg P_R \vee \neg P_B$ can be found as $\mathcal{V}(\bar{e}_{RB})$, the local section over the closed cell $\bar{e}_{RB}$ whose vertices are v_R and v_B. Similarly, the escape nodes satisfying $\neg P_R \vee \neg P_Y$ can be found as $\mathcal{V}(\bar{e}_{RY})$, the local section over the closed cell $\bar{e}_{RY}$.

To find the vector space generated by escape nodes satisfying the escape criterion E, construct a sheaf on a new base space X' as the following. Let X' be the complete graph on K number of vertices, where K is the number of disjunctive clauses in the escape criterion. In our example, we have two such clauses, $E^1 = \neg P_R \vee \neg P_B$ and $E^2 = \neg P_R \vee \neg P_Y$, so X' is a graph with two vertices connected by an edge. Each vertex of X' correspond to one disjunctive clause, so label each vertex of X' by v_{E^i} to indicate the fact that it corresponds to the clause E^i.

Construct a sheaf $\mathcal{S}'$ on X' by $\mathcal{S}'(v_{E^i}) = \mathcal{S}(\overline{\sigma}_{E^i})$ for each $E^i = \neg P_{i_0} \vee \cdots \vee \neg P_{i_n}$, where $\mathcal{S}$ is the sheaf of sets constructed in §3.2.1, and $\overline{\sigma}$ is the closed cell $\overline{\sigma}_{p_{i_0},\ldots,p_{i_n}}$ of X. On every edge e of X', let $\mathcal{S}'(e)$ be the set of all nodes in domain D. Let the restriction maps be the inclusion of sets. Let $\mathcal{V}_{\mathcal{S}'}$ be the sheaf of vector spaces on X' obtained from $\mathcal{S}'$ by applying the free functor. Then, for every vertex v_{E^i} of X', the local section $\mathcal{V}_{\mathcal{S}'}(v_{E^i})$ is the vector space generated by $\mathcal{S}(\overline{\sigma}_{E^i})$, i.e.,

$$\mathcal{V}_{\mathcal{S}'}(v_{E^i}) = \mathcal{V}(\overline{\sigma}_{E^i}),$$

where $\mathcal{V}$ is the sheaf of vector spaces obtained from sheaf of sets $\mathcal{S}$. Note that for each edge e of X', the local section $\mathcal{V}_{\mathcal{S}'}(e)$ is the vector space generated by all nodes of domain D.

Figure 3.15 provides a visualization of the sheaves $\mathcal{S}'$ and $\mathcal{V}_{\mathcal{S}'}$ constructed for Figure 3.9 and the escape criterion

$$E = (\neg P_R \vee \neg P_B) \wedge (\neg P_R \vee \neg P_Y).$$

Note that $E^1 = \neg P_R \vee \neg P_B$ and $E^2 = \neg P_R \vee \neg P_Y$. As the sheaf of sets $\mathcal{S}'$, the nodes of graph D on a cell of X' should be considered as a set, and the arrows should be considered as a map of sets. As the sheaf of vector spaces $\mathcal{V}_{\mathcal{S}'}$, the illustrated nodes of D should be considered as the generating basis, and the arrows should be considered as maps among basis vectors that induce maps of vector spaces.

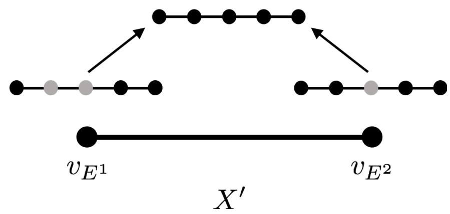

FIGURE 3.15: Visualization of sheaves $\mathcal{S}'$ and $\mathcal{V}_{\mathcal{S}'}$

The dimension of 0th sheaf cohomology of $\mathcal{V}_{\mathcal{S}'}$ gives the number of escape nodes.

Theorem 6. *$H^0(C^\bullet \mathcal{V}_{\mathcal{S}'})$ is the vector space generated by escape nodes satisfying escape criterion E.*

The proof of Theorem 6 depends on the commutativity of various limits and colimits specific to this construction. We establish some Lemmas before proving Theorem 6.

Let X^* be the $K-1$ simplex that has X' as its 1-skeleton. We will first construct a sheaf of sets $\mathcal{A}^*$ on X^* whose global section equals the set of nodes that satisfy the escape criterion E. For each $v_{E^i} \in X^*$, let $\mathcal{A}^*(v_{E^i}) = \mathcal{S}'(v_{E^i})$, the set of nodes that satisfy the escape criterion E^i. For each $\sigma_{E^{i_0},\ldots,E^{i_j}} \in X^*$ that has $v_{E^{i_0}},\ldots,v_{E^{i_j}}$ as its vertices, let

$$\mathcal{A}^*(\sigma_{E^{i_0},\ldots,E^{i_j}}) = \mathcal{A}^*(v_{E^{i_0}}) \cup \cdots \cup \mathcal{A}^*(v_{E^{i_j}}).$$

Let the restriction maps be the inclusion of sets. By construction, the global section $\mathcal{A}^*(X^*)$ is the set of nodes that satisfy the escape criterion E.

Recall that the global section $\mathcal{A}^*(X^*)$ is defined as

$$\mathcal{A}^*(X^*) = \varprojlim_{\sigma \in X^*} \mathcal{A}^*(\sigma).$$

Moreover, recall from Lemma 3 that the above limit can be computed over the 1-skeleton of X^*, which is X'. Let $\mathcal{A}$ be the sheaf on X' such that for every $\sigma \in X'$, the local section $\mathcal{A}(\sigma) = \mathcal{A}^*(\sigma)$. Given $v \trianglelefteq e$, the restriction maps $\mathcal{A}(v \trianglelefteq e) = \mathcal{A}^*(v \trianglelefteq e)$. Then, by Lemma 3,

$$\mathcal{A}(X') = \mathcal{A}^*(X^*),$$

so $\mathcal{A}(X')$ is the set of nodes that satisfy the escape criterion E.

For our example, the sheaf $\mathcal{A}$ is illustrated in Figure 3.16.

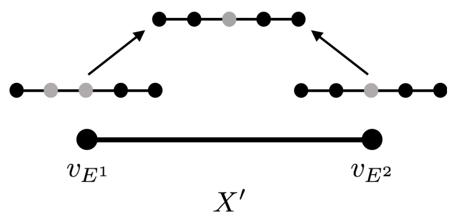

FIGURE 3.16: Illustration of sheaf $\mathcal{A}$

Let $\mathcal{V}_{\mathcal{A}}$ denote the sheaf of vector spaces on X' obtained by applying the free functor to $\mathcal{A}$.

Lemma 9. $H^0(C^\bullet \mathcal{V}_{\mathcal{A}}) = H^0(C^\bullet \mathcal{V}_{\mathcal{S}'})$.

Proof. Let's compare the cochain complexes of the two sheaves.

$$C^\bullet \mathcal{V}_{\mathcal{A}} : C^0 \mathcal{V}_{\mathcal{A}} \xrightarrow{\partial^0_{\mathcal{A}}} C^1 \mathcal{V}_{\mathcal{A}} \to 0$$

$$C^\bullet \mathcal{V}_{\mathcal{S}'} : C^0\mathcal{V}_{\mathcal{S}'} \xrightarrow{\partial^0_{\mathcal{S}'}} C^1\mathcal{V}_{\mathcal{S}'} \to 0$$

By construction, $\mathcal{V}_{\mathcal{A}}(v) = \mathcal{V}_{\mathcal{S}'}(v)$ for every vertex $v \in X'$, so $C^0\mathcal{V}_{\mathcal{A}} = C^0\mathcal{V}_{\mathcal{S}'}$. For each edge $e \in X'$, note that there is an inclusion of sets from $\mathcal{A}(e)$ to $\mathcal{S}'(e)$ since $\mathcal{S}'(e)$ is the set of all nodes in domain D while $\mathcal{A}(e)$ is a subset of the nodes in D. Then, $\mathcal{V}_{\mathcal{A}}(e)$ is a subspace of the space $\mathcal{V}_{\mathcal{S}'}(e)$. Thus, there exists an inclusion map $i : C^1\mathcal{V}_{\mathcal{A}} \to C^1\mathcal{V}_{\mathcal{S}'}$. So far, we have the following diagram.

$$\begin{tikzcd}
C^0\mathcal{V}_{\mathcal{A}} = C^0\mathcal{V}_{\mathcal{S}'} \arrow[r, "\partial^0_{\mathcal{A}}"] \arrow[dr, "\partial^0_{\mathcal{S}'}"'] & C^1\mathcal{V}_{\mathcal{A}} \arrow[d, "i"] \\
& C^1\mathcal{V}_{\mathcal{S}'}
\end{tikzcd}$$

Then, $\ker \partial^0_{\mathcal{A}} = \ker \partial^0_{\mathcal{S}'}$. Thus, $H^0(C^\bullet\mathcal{V}_{\mathcal{A}}) = H^0(C^\bullet\mathcal{V}_{\mathcal{S}'})$.

$\square$

Note that $\mathcal{A}$ is a copoduct of sheaf of sets $\mathcal{J}_i$, where each sheaf $\mathcal{J}_i$ is defined as the following. For each node n_i of domain D and each cell $\sigma \in X'$, the local section $\mathcal{J}_i(\sigma)$ is defined as the following.

$$\mathcal{J}_i(\sigma) = \begin{cases} \{n_i\} & \text{if } n_i \in \mathcal{A}(\sigma) \\ \emptyset & \text{if } n_i \notin \mathcal{A}(\sigma) \end{cases}$$

If $\mathcal{J}_i(v) = \{n_i\}$ for some vertex v of X', then $\mathcal{J}_i(e) = \{n_i\}$ for all edges e that have v as a face, and the restriction map $\mathcal{J}_i(v \trianglelefteq e) = \mathcal{J}_i(v) \to \mathcal{J}_i(e)$ is the identity map. We can write $\mathcal{A}$ as the coproduct.

$$\mathcal{A} = \coprod_{n_i \in D} \mathcal{J}_i.$$

For our example sheaf of sets $\mathcal{A}$, illustrated in Figure 3.16, the sheaf $\mathcal{A}$ as a coproduct is illustrated in Figure 3.17. In Figure 3.17, each $\{a\}$, $\{b\}$, $\{c\}$, $\{d\}$, and $\{e\}$ corresponds to a node of D from left to right.

For the remainder of this chapter, we will use *Free* to denote the free functor from category of sets to category of vector spaces.

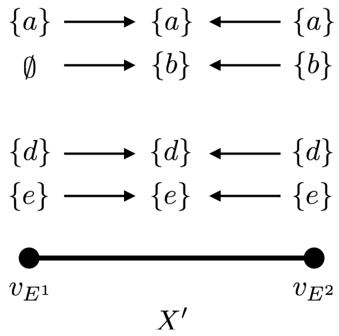

FIGURE 3.17: Sheaf $\mathcal{A}$ as a coproduct $\mathcal{A} = \coprod_{n_i \in D} \mathfrak{J}_i$

Lemma 10. *$Free(\varprojlim_{\sigma \in X'} \mathfrak{J}_i(\sigma)) = \varprojlim_{\sigma \in X'} Free(\mathfrak{J}_i(\sigma))$ for every $n_i \in D$.*

Proof. In general, free functors do not preserve limits. In our case, the Lemma holds true because the sheaves $\mathfrak{J}_i$ are simple enough. Recall that for every $\sigma \in X'$, the local section $\mathfrak{J}_i(\sigma)$ is either a set with one element $\{n_i\}$ or the empty set. We consider two cases.

Case 1: If $\mathfrak{J}_i(v) = \{n_i\}$ for every vertex $v \in X'$, then $\mathfrak{J}_i(e) = \{n_i\}$ for every edge $e \in X'$ as well. Moreover, $\varprojlim_{\sigma \in X'} \mathfrak{J}_i(\sigma) = \{n_i\}$, and $Free(\varprojlim_{\sigma \in X'} \mathfrak{J}_i(\sigma)) = \mathbb{K}$ is a one dimensional vector space. On the other hand, $Free(\mathfrak{J}_i(\sigma)) = \mathbb{K}$ for every $\sigma \in X'$, and $Free(\mathfrak{J}_i)$ is the constant sheaf on X'. Thus, $\varprojlim_{\sigma \in X'} Free(\mathfrak{J}_i(\sigma)) = \mathbb{K}$.

Case 2: If $\mathfrak{J}_i(v) = \emptyset$ for some vertex $v \in X'$, then $\varprojlim_{\sigma \in X'} \mathfrak{J}_i(\sigma) = \emptyset$, and $Free(\varprojlim_{\sigma \in X'} \mathfrak{J}_i(\sigma))$ is the trivial vector space. On the other hand, $Free(\mathfrak{J}_i(v))$ is the trivial vector space for some vertex $v \in X'$, and $\varprojlim_{\sigma \in X'} Free(\mathfrak{J}_i(\sigma))$ is trivial as well.

Thus, the Lemma holds for every sheaf $\mathfrak{J}_i$.

□

Lemma 11. $\coprod_{n_i \in D} \varprojlim_{\sigma \in X'} Free(\mathfrak{J}_i(\sigma)) = \varprojlim_{\sigma \in X'} \coprod_{n_i \in D} Free(\mathfrak{J}_i(\sigma)).$

Proof. Note that coproducts and limits do not commute in general.

Let $\mathcal{F}$ denote the sheaf $\mathcal{F} = \coprod_{n_i \in D} Free(\mathfrak{J}_i)$. Note that the coproduct is, in fact, a direct sum in the category of vector spaces, so we can write the sheaf $\mathcal{F}$ as $\mathcal{F} = \bigoplus_{n_i \in D} Free(\mathfrak{J}_i)$.

We know that

$$\varprojlim_{\sigma \in X'} \coprod_{n_i \in D} Free(\mathcal{I}_i(\sigma)) = \varprojlim_{\sigma \in X'} \mathcal{F}(\sigma) = H^0(C^\bullet \mathcal{F}) = \ker \partial^0,$$

where $\partial^0 : C^0\mathcal{F} \to C^1\mathcal{F}$ is the boundary map of the cochain complex. The cochain complex is

$$\bigoplus_{v \in X'} \bigoplus_{n_i \in D} Free(\mathfrak{J}_i(v)) \xrightarrow{\partial^0} \bigoplus_{e \in X'} \bigoplus_{n_i \in D} Free(\mathfrak{J}_i(e)),$$

which can be expressed equivalently as

$$\bigoplus_{n_i \in D} \bigoplus_{v \in X'} Free(\mathfrak{J}_i(v)) \xrightarrow{\partial^0} \bigoplus_{n_i \in D} \bigoplus_{e \in X'} Free(\mathfrak{J}_i(e)).$$

For each $n_i \in D$, let $C^\bullet Free(\mathfrak{J}_i)$ denote the cochain complex

$$C^\bullet Free(\mathfrak{J}_i) : \bigoplus_{v \in X'} Free(\mathfrak{J}_i(v)) \xrightarrow{\partial_i^0} \bigoplus_{e \in X'} Free(\mathfrak{J}_i(e)).$$

Then,

$$\begin{aligned} \ker \partial^0 &= \bigoplus_{n_i \in D} \ker \partial_i^0 \\ &= \bigoplus_{n_i \in D} \varprojlim_{\sigma \in X'} Free(\mathfrak{J}_i(\sigma)) \\ &= \coprod_{n_i \in D} \varprojlim_{\sigma \in X'} Free(\mathfrak{J}_i(\sigma)). \end{aligned}$$

The second equality follows from the fact that $\ker \partial_i^0 = H^0(C^\bullet Free(\mathcal{I}_i)) = \varprojlim_{\sigma \in X'} Free(\mathcal{I}_i)$. Thus, the Lemma holds true.

□

We are now ready to prove Theorem 6.

Proof of Theorem 6. From Lemma 9, we know that $H^0(C^\bullet \mathcal{V}_{\mathcal{S}'}) = H^0(C^\bullet \mathcal{V}_{\mathcal{A}})$. We also know that $\mathcal{A}(X')$ is the set of nodes that satisfy the escape criterion E. We will thus show that $H^0(C^\bullet \mathcal{V}_{\mathcal{A}}) = Free(\mathcal{A}(X'))$.

Recall that $\mathcal{A}$ is a coproduct of sheaf of sets $\mathfrak{J}_i$:

$$\mathcal{A} = \coprod_{n_i \in D} \mathfrak{J}_i.$$

Then,

$$\begin{aligned}
Free(A(X')) &= Free(\varprojlim_{\sigma \in X'} \coprod_{n_i \in D} \mathfrak{J}_i(\sigma)) \\
&= Free(\coprod_{n_i \in D} \varprojlim_{\sigma \in X'} \mathfrak{J}_i(\sigma)) \\
&= \coprod_{n_i \in D} Free(\varprojlim_{\sigma \in X'} \mathfrak{J}_i(\sigma)) \\
&= \coprod_{n_i \in D} \varprojlim_{\sigma \in X'} Free(\mathfrak{J}_i(\sigma)) \\
&= \varprojlim_{\sigma \in X'} \coprod_{n_i \in D} Free(\mathfrak{J}_i(\sigma)) \\
&= \varprojlim_{\sigma \in X'} Free(\coprod_{n_i \in D} \mathfrak{J}_i(\sigma)) \\
&= \varprojlim_{\sigma \in X'} Free(\mathcal{A}(\sigma)) \\
&= H_0(C^\bullet \mathcal{V}_A)
\end{aligned}$$

The second equality follows from the fact that sheaf $\mathcal{A}$ can be considered as a bifunctor $\mathcal{A} : Po(X') \times D \to Set$, where $Po(X')$ is the indexing poset of X' and D is the set of nodes. Then, $\mathcal{A}(\sigma, n_i) = \mathfrak{J}_i(\sigma)$. Since $Po(X')$ is a connected category, then $\coprod_{n_i \in D} \varprojlim_{\sigma \in X'} \mathfrak{J}_i(\sigma) = \varprojlim_{\sigma \in X'} \coprod_{n_i \in D} \mathfrak{J}_i(\sigma)$ follows from the commutativity of coproducts and connected limits.

The third equality follows from the fact that free functors preserve colimits, and hence coproducts. The fourth equality follows from Lemma 10. The fifth equality follows from Lemma 11. The sixth equality follows again from the fact that free functors preserve colimits. The last two equalities follow from definition. $\square$

This chapter introduced various constructions of cellular sheaves and cosheaves for summarizing globally consistent data from information distributed with respect to different properties. The cellular sheaf constructed in §3.1 collated information distributed over time. It's construction alludes to the possibility of sheaves as tools for studying time varying data. On the other hand, in §3.2, we introduced cellular sheaves and cosheaves that extract information satisfying a particular boolean expression. A natural question that follows §3.2 is to determine the existence of an evasion path given mobile pursuers and evaders with boolean capture condition.

As this chapter illustrated, the construction of cellular sheaves and cosheaves depend on the nature of the distribution of information, and it is the author's belief that cellular sheaves have great potential to model various kinds of distribution system. In Chapter 4 and Chapter 5, we will construct cellular cosheaves that collate information distributed with respect to coordinate location. In fact, our construction generalizes to model information distributed with respect to any user specific function.

Chapter 4

Distributed Topological Data Analysis

In this chapter, cellular sheaf theory is used to assemble information distributed with respect to properties of interest. Such a distribution system, when combined with persistent homology, provides the necessary tools to address the following question:

Given a large point cloud P can we compute persistent homology on P by combining persistence modules from the subsets of the points P?

We discuss a distributed computation method for homology using Leray cellular cosheaves in §4.1. The heart of this dissertation provides an affirmative answer to the above question by constructing a distributed persistent homology computation mechanism which is provided in §4.2. As discussed in Chapter 5, our construction not only provides an efficient computation mechanism for large point clouds but also enriches the information conveyed via barcodes.

4.1 Distributed Computation of Homology

We summarize the distributed homology computation method for topological spaces by Curry, Ghrist and Nanda [11] and adapt it for a distributed homology computation of Rips complexes built from a point cloud. The original constructions by Leray [6] and Serre [21] are phrased in the language of sheaf cohomology in [11] as the following.

Remark. Throughout this chapter, we assume:

- a cover $\mathcal{V}$ of a space is an open cover consisting of finitely many sets, and
- every homology is computed with coefficients in a field $\mathbb{K}$.

Let $f : X \to Y$ be a continuous map of topological spaces, and let $\mathcal{V}$ be a cover of $f(X) \subset Y$. Let $N_{\mathcal{V}}$ denote the nerve of $\mathcal{V}$ (Definition 1). Given an n-simplex $\sigma \in N_{\mathcal{V}}$, we will let U_σ be the corresponding $(n+1)$-intersection of members of $\mathcal{V}$. The Leray cellular cosheaf $\mathcal{L}_n$ associated to the map f and cover $\mathcal{V}$ is a cosheaf on $N_{\mathcal{V}}$ defined as the following. Given $\sigma \in N_{\mathcal{V}}$, let $\mathcal{L}_n(\sigma) = H_n(f^{-1}(U_\sigma))$, the homology of the preimage with coefficients in a field $\mathbb{K}$. Let $\mathcal{L}_n(\sigma \trianglelefteq \tau)$ be the map induced by inclusion $f^{-1}(U_\tau) \hookrightarrow f^{-1}(U_\sigma)$. The following can be obtained from a basic spectral sequence argument as shown, for example, in Theorem 5.7 of [11].

Theorem 7. *([11]) Let $f : X \to Y$ be continuous. Let $\mathcal{V}$ be a cover of the image $f(X) \subset Y$ with one-dimensional nerve $N_{\mathcal{V}}$. Then, for each $n \in \mathbb{N}$,*

$$H_n(X) \cong H_0(C_\bullet \mathcal{L}_n) \oplus H_1(C_\bullet \mathcal{L}_{n-1}).$$

Note that the above special case of the Leray spectral sequence coincides with the generalized Mayer-Vietoris principle [6].

We now address a problem of interest in topological data analysis. Given a point cloud P, our goal is to compute the homology of a Rips complex $\mathcal{R}^\epsilon$ built with respect to some parameter ϵ in a distributed manner using Rips complexes built on subsets of P. Note that while we focus our attention on Rips complexes, the following construction can be easily generalized for computations involving other complexes built on P.

Let $f : P \to \mathbb{R}^d$ be any map, and for any ϵ, let $\mathcal{R}^\epsilon$ be the Rips complex built on P. Let $\mathcal{V}$ be a cover of $f(P)$. For each n-simplex $\sigma \in N_{\mathcal{V}}$, let $U_\sigma \subset \mathbb{R}^d$ be the corresponding intersection of members of $\mathcal{V}$. Let $\mathcal{R}^\epsilon_\sigma$ denote the Rips complex built on points of $f^{-1}(U_\sigma)$ for proximity parameter ϵ.

Remark. We will use the following terminologies throughout the remainder of this dissertation:

- we will refer to the collection $\coprod_{\dim\sigma=n} \mathcal{R}^{\epsilon}_{\sigma}$ as the "Rips complexes over the n-simplices of $N_{\mathcal{V}}$", and
- we will refer to the entire collection $\coprod_{\sigma\in N_{\mathcal{V}}} \mathcal{R}^{\epsilon}_{\sigma}$ as the "Rips system".

Define a cosheaf $\mathcal{F}^{\epsilon}_{n}$ on $N_{\mathcal{V}}$ as the following. For each $\sigma \in N_{\mathcal{V}}$, let $\mathcal{F}^{\epsilon}_{n}(\sigma) = H_n(\mathcal{R}^{\epsilon}_{\sigma})$, the n^{th} homology with coefficients in a field $\mathbb{K}$. For $\sigma \trianglelefteq \tau$, let $\mathcal{F}^{\epsilon}_{n}(\sigma \trianglelefteq \tau)$ be the map induced by inclusion $\mathcal{R}^{\epsilon}_{\tau} \hookrightarrow \mathcal{R}^{\epsilon}_{\sigma}$.

A proof similar to that of Theorem 7 can be used to obtain the following isomorphism. The proof is reconstructed in order to clarify ideas in §4.2.2.

Lemma 12. *Let P be a point cloud, and let $f : P \to \mathbb{R}^d$ be any map. Let $\mathcal{V}$ be a cover of $f(P)$ such that $N_{\mathcal{V}}$ is one-dimensional. Assume that the Rips system is a covering of $\mathcal{R}^{\epsilon}$. Then,*

$$H_n(\mathcal{R}^{\epsilon}) \cong H_0(C_{\bullet}\mathcal{F}^{\epsilon}_{n}) \oplus H_1(C_{\bullet}\mathcal{F}^{\epsilon}_{n-1}). \tag{4.1}$$

Proof. Consider the following commutative diagram.

$$\begin{tikzcd}
\vdots & \vdots \arrow[d] & \vdots \arrow[d] & \vdots \arrow[d] & \vdots \\
0 & C_2(\mathcal{R}^{\epsilon}) \arrow[l] \arrow[d] & \bigoplus_{v\in N_{\mathcal{V}}} C_2(\mathcal{R}^{\epsilon}_{v}) \arrow[l, "j_2"'] \arrow[d] & \bigoplus_{e\in N_{\mathcal{V}}} C_2(\mathcal{R}^{\epsilon}_{e}) \arrow[l, "e_2"'] \arrow[d] & 0 \arrow[l] \\
0 & C_1(\mathcal{R}^{\epsilon}) \arrow[l] \arrow[d] & \bigoplus_{v\in N_{\mathcal{V}}} C_1(\mathcal{R}^{\epsilon}_{v}) \arrow[l, "j_1"'] \arrow[d] & \bigoplus_{e\in N_{\mathcal{V}}} C_1(\mathcal{R}^{\epsilon}_{e}) \arrow[l, "e_1"'] \arrow[d] & 0 \arrow[l] \\
0 & C_0(\mathcal{R}^{\epsilon}) \arrow[l] & \bigoplus_{v\in N_{\mathcal{V}}} C_0(\mathcal{R}^{\epsilon}_{v}) \arrow[l, "j_0"'] & \bigoplus_{e\in N_{\mathcal{V}}} C_0(\mathcal{R}^{\epsilon}_{e}) \arrow[l, "e_0"'] & 0 \arrow[l]
\end{tikzcd} \tag{4.2}$$

The leftmost column is a chain complex of $\mathcal{R}^{\epsilon}$, the middle column is a chain complex of the Rips complexes over the vertices $\bigoplus_{v\in N_{\mathcal{V}}} \mathcal{R}^{\epsilon}_{v}$, and the rightmost column is the chain complex of the Rips complexes over the edges $\bigoplus_{e\in N_{\mathcal{V}}} \mathcal{R}^{\epsilon}_{e}$. The maps $j_n : \bigoplus_{v\in N_{\mathcal{V}}} C_n(\mathcal{R}^{\epsilon}_{v})$ are each collections of inclusion maps. The maps $e_n : \bigoplus_{e\in N_{\mathcal{V}}} C_n(\mathcal{R}^{\epsilon}_{e}) \to \bigoplus_{v\in N_{\mathcal{V}}} C_n(\mathcal{R}^{\epsilon}_{v})$ are also collections of inclusion maps that take the incidence numbers into account : if

$\gamma \in \bigoplus_{e \in N_{\mathcal{V}}} C_n(\mathcal{R}^{\epsilon}_e)$ and v_1, v_2 are the faces of e, then $e_n(\gamma) = [v_1 : e]\gamma + [v_2 : e]\gamma$, where $[v_1 : e]\gamma \in C_n(\mathcal{R}^{\epsilon}_{v_1})$ and $[v_2 : e]\gamma \in C_n(\mathcal{R}^{\epsilon}_{v_2})$.

When the Rips system covers $\mathcal{R}^{\epsilon}$, every row of Diagram 4.2 is exact. Hence, taking the spectral sequence with respect to the horizontal maps results in a trivial page. One can then show that the following spectral sequence converges to the homology of $\mathcal{R}^{\epsilon}$.

$$\begin{tikzcd}
\vdots \arrow[d] & \vdots \arrow[d] \\
\bigoplus_{v \in N_{\mathcal{V}}} C_2(\mathcal{R}^{\epsilon}_v) \arrow[d] & \bigoplus_{e \in N_{\mathcal{V}}} C_2(\mathcal{R}^{\epsilon}_e) \arrow[l, "e_2"'] \arrow[d] \\
\bigoplus_{v \in N_{\mathcal{V}}} C_1(\mathcal{R}^{\epsilon}_v) \arrow[d] & \bigoplus_{e \in N_{\mathcal{V}}} C_1(\mathcal{R}^{\epsilon}_e) \arrow[l, "e_1"'] \arrow[d] \\
\bigoplus_{v \in N_{\mathcal{V}}} C_0(\mathcal{R}^{\epsilon}_v) & \bigoplus_{e \in N_{\mathcal{V}}} C_0(\mathcal{R}^{\epsilon}_e) \arrow[l, "e_0"']
\end{tikzcd} \tag{4.3}$$

Taking the homology with respect to the vertical maps, we obtain the following page.

$$\begin{tikzcd}
\vdots \arrow[d, dash, dashed] & \vdots \arrow[d, dash, dashed] \\
\bigoplus_{v \in N_{\mathcal{V}}} H_2(\mathcal{R}^{\epsilon}_v) \arrow[d, dash, dashed] & \bigoplus_{e \in N_{\mathcal{V}}} H_2(\mathcal{R}^{\epsilon}_e) \arrow[l, "\partial_2"'] \arrow[d, dash, dashed] \\
\bigoplus_{v \in N_{\mathcal{V}}} H_1(\mathcal{R}^{\epsilon}_v) \arrow[d, dash, dashed] & \bigoplus_{e \in N_{\mathcal{V}}} H_1(\mathcal{R}^{\epsilon}_e) \arrow[l, "\partial_1"'] \arrow[d, dash, dashed] \\
\bigoplus_{v \in N_{\mathcal{V}}} H_0(\mathcal{R}^{\epsilon}_v) & \bigoplus_{e \in N_{\mathcal{V}}} H_0(\mathcal{R}^{\epsilon}_e) \arrow[l, "\partial_0"']
\end{tikzcd} \tag{4.4}$$

One can check that the n^{th} row of Diagram 4.4 coincides with the chain complex

$$C_{\bullet}\mathcal{F}^{\epsilon}_n : \bigoplus_{v \in N_{\mathcal{V}}} \mathcal{F}^{\epsilon}_n(v) \leftarrow \bigoplus_{e \in N_{\mathcal{V}}} \mathcal{F}^{\epsilon}_n(e)$$

of cosheaf $\mathcal{F}_n^{\epsilon}$. Taking the homology with respect to the horizontal maps in Diagram 4.4 then results in the following cosheaf homologies.

$$\begin{array}{ccc} \vdots & & \vdots \\ \vdots & & \vdots \\ H_0(C_\bullet \mathcal{F}_2^{\epsilon}) & \text{------} & H_1(C_\bullet \mathcal{F}_2^{\epsilon}) \\ \vdots & & \vdots \\ H_0(C_\bullet \mathcal{F}_1^{\epsilon}) & \text{------} & H_1(C_\bullet \mathcal{F}_1^{\epsilon}) \\ \vdots & & \vdots \\ H_0(C_\bullet \mathcal{F}_0^{\epsilon}) & \text{------} & H_1(C_\bullet \mathcal{F}_0^{\epsilon}) \end{array} \tag{4.5}$$

As noted earlier, the spectral sequence converges to the homology $H_n(\mathcal{R}^{\epsilon})$. Thus,

$$H_n(\mathcal{R}^{\epsilon}) \cong H_0(C_\bullet \mathcal{F}_n^{\epsilon}) \oplus H_1(C_\bullet \mathcal{F}_{n-1}^{\epsilon})$$

$\square$

While Lemma 12 can be considered as an analogue to Lemma 7, note that Lemma 12 contains an additional condition that the Rips system must cover $\mathcal{R}^{\epsilon}$. An analogous condition was not necessary in Lemma 7 because the collection of pre-images $f^{-1}(U_\sigma)$ formed a cover of the space X by construction. The following lemma allows us to bound the parameter ϵ for which the Rips system provides a covering of $\mathcal{R}^{\epsilon}$ without having to build $\mathcal{R}^{\epsilon}$.

Lemma 13. *Let P be a point cloud, and let $f : P \to \mathbb{R}^d$ be any map. Let $\mathcal{V}$ be a cover of $f(P)$ such that $N_{\mathcal{V}}$ is one-dimensional. There exists a constant K such that*

$$H_n(\mathcal{R}^{\epsilon}) \cong H_0(C_\bullet \mathcal{F}_n^{\epsilon}) \oplus H_1(C_\bullet \mathcal{F}_{n-1}^{\epsilon}) \tag{4.6}$$

for every $\epsilon < K$.

Proof. We first specify K. In the following proof, we let the minimum over an empty set to be ∞.

For each $p \in P$, if there exists an unique set $U \in \mathcal{V}$ such that $f(p) \in U$, then let

$$K_p = \min_{\{q | f(q) \notin U\}} d(p,q). \tag{4.7}$$

If there are two sets of the cover, say $U, W \in \mathcal{V}$ such that $f(p) \in U \cap W$, then first let

$$k_p^1 = \min_{\{q | f(q) \notin U \cup W\}} d(p,q), \tag{4.8}$$

and let

$$k_p^2 = \min_{\substack{\{q,q' | d(p,q) < k_p^1, \quad f(q) \notin U, \\ d(p,q') < k_p^1, \quad f(q') \notin W\}}} d(q,q'). \tag{4.9}$$

Let

$$K_p = \min\{k_p^1, k_p^2\}.$$

Let $K = \min_{p \in P} K_p$. Assume $\epsilon < K$. We will now show that Equation 4.6 holds by showing that the Rips system covers $\mathcal{R}^\epsilon$. Let ω be a simplex of $\mathcal{R}^\epsilon$. We can express ω in terms of its vertices as $\omega = (v_0, \ldots, v_l)$. The fact that $\omega \in \mathcal{R}^\epsilon$ implies that for any two vertices v_i and v_j of ω, the pairwise distance $d(v_i, v_j) < \epsilon$. We will show that there exists some $U_\sigma \in \mathcal{V}$ such that $f(v_0), \ldots, f(v_l) \in U_\sigma$, which implies that $\omega \in \mathcal{R}^\epsilon_\sigma$.

If there exists a vertex, say v_0 of ω, such that v_0 has a unique set U with $f(v_0) \in U$, then by construction, $K < K_{v_0}$, where $K_{v_0} = \min_{\{q|f(q) \notin U\}} d(v_0, q)$ from Equation 4.7. Thus, for any other vertex v of ω, we have $d(v_0, v) < \epsilon < K_{v_0}$, and hence, $f(v) \in U$ as well. Thus, $f(v_0), \ldots, f(v_l) \in U$.

On the other hand, assume that for every vertex v of ω there exist two sets $U_v, W_v \in \mathcal{V}$ such that $f(v) \in U_v \cap W_v$. Without loss of generality, assume that $f(v_0) \in U \cap W$. Note that for any other vertex v of ω, we have

$$d(v_0, v) < \epsilon < K_{v_0} \leq k_{v_0}^1, \tag{4.10}$$

where $k^1_{v_0}$ is given by Equation 4.8. By Equation 4.8, the above inequality implies that

$$f(v) \in U \cup W \tag{4.11}$$

for every $v \in \omega$. In fact, we can show that either $f(v_0), \ldots, f(v_l) \in U$ or $f(v_0), \ldots, f(v_l) \in W$. Assume not. Then there exist distinct vertices, say v_1 and v_2, such that $f(v_1) \notin U$ and $f(v_2) \notin W$. By construction, $d(v_0, v_1) < \epsilon < k^1_{v_0}$, and $d(v_0, v_2) < \epsilon < k^1_{v_0}$. By definition of $k^2_{v_0}$ from Equation 4.9, we know that $k^2_{v_0} \geq d(v_1, v_2)$. However, this contradicts the fact that $d(v_1, v_2) < \epsilon < k^2_{v_0}$. Thus, it must be the case that $f(v_0), \ldots, f(v_l) \in U$ or $f(v_0), \ldots, f(v_l) \in W$, and ω is covered by some subcomplex $\mathcal{R}^\epsilon_\sigma$. Thus, the Rips system covers $\mathcal{R}^\epsilon$, and Lemma 13 follows from Lemma 12.

□

Example 12. Let $P \subset \mathbb{R}^2$ be a point cloud, as illustrated in Figure 4.1. Let $f : P \to \mathbb{R}$ be a projection map to the horizontal coordinate. Let $f(P)$ be covered by intervals V_B, V_Y, V_R illustrated in Figure 4.1.

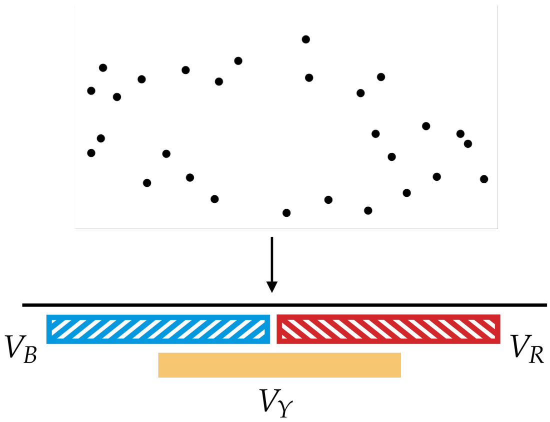

FIGURE 4.1: Point cloud P, projection map $f : P \to \mathbb{R}$, and a covering $\mathcal{V}$ of $f(P)$.

Let's compute $H_1(\mathcal{R}^\epsilon)$ for some parameter ϵ. The Rips complex $\mathcal{R}^\epsilon$ and the Rips system over the nerve $N_\mathcal{V}$ are illustrated in Figure 4.2a and 4.2b. Let v_B, v_Y, v_R denote the vertices of $N_\mathcal{V}$ that each corresponds to the intervals V_B, V_Y, V_R. Let e_{BY} and e_{YR} denote the edges of $N_\mathcal{V}$ that correspond to the intervals $V_B \cap V_Y$ and $V_Y \cap V_R$.

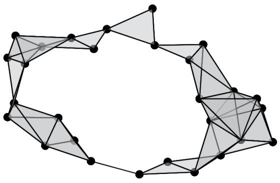

(A) Rips complex $\mathcal{R}^\epsilon$

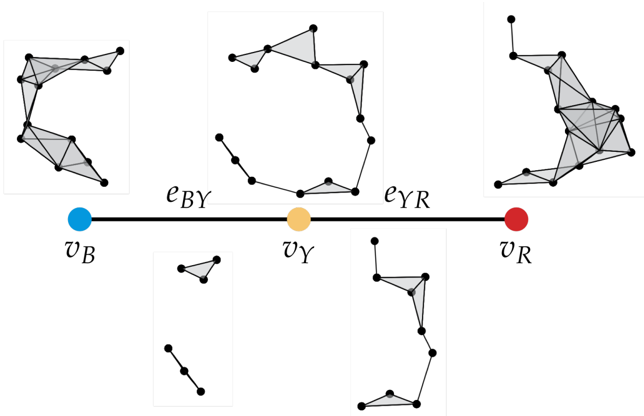

(B) Rips system over the nerve $N_\mathcal{V}$

FIGURE 4.2: Rips complex and the associated Rips system

Since we are interested in computing $H_1(\mathcal{R}^\epsilon)$, we need to build two cosheaves, $\mathcal{F}_0^\epsilon$ and $\mathcal{F}_1^\epsilon$, from the Rips system. Cosheaf $\mathcal{F}_1^\epsilon$ is trivial since none of the Rips subcomplexes of the Rips system have non-trivial 1-cycles. The local sections of $\mathcal{F}_0^\epsilon$ on e_{BY} is $\mathcal{F}_0^\epsilon(e_{BY}) = \mathbb{K} \oplus \mathbb{K}$. The local section of $\mathcal{F}_0^\epsilon$ on any other simplex of $N_\mathcal{V}$ is $\mathbb{K}$. The extension maps are given by $\mathcal{F}_0^\epsilon(v_B \trianglelefteq e_{BY}) = \mathcal{F}_0^\epsilon(v_Y \trianglelefteq e_{BY}) = \begin{bmatrix} 1 & 1 \end{bmatrix}$. All other extension maps are the identity maps. The two relevant cosheaves are illustrated in Figure 4.3a and 4.3b.

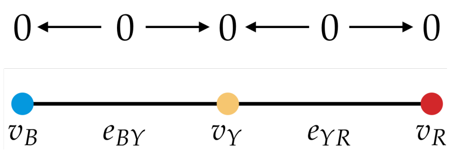

(A) Cosheaf $\mathcal{F}_1^\epsilon$

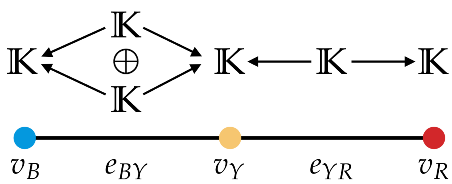

(B) Cosheaf $\mathcal{F}_0^\epsilon$

FIGURE 4.3: The two relevant cosheaves for computing $H_1(\mathcal{R}^\epsilon)$

One can verify that Equation 4.1 holds by computing

$$H_0(C_\bullet \mathcal{F}_1^\epsilon) = 0, \quad H_1(C_\bullet \mathcal{F}_0^\epsilon) = \mathbb{K}. \tag{4.12}$$

Example 13. Let's now consider a larger epsilon parameter ϵ'. Considering such a case will allow us to clarify the difference between $H_0(C_\bullet \mathcal{F}_1^\epsilon)$ and $H_1(C_\bullet \mathcal{F}_0^\epsilon)$. The Rips complex $\mathcal{R}^{\epsilon'}$ and the Rips system are illustrated in Figure 4.4a and 4.4b.

The cosheaf $\mathcal{F}_1^{\epsilon'}$ has trivial local sections except for $\mathcal{F}_1^{\epsilon'}(v_Y) = \mathbb{K}$. Cosheaf $\mathcal{F}_0^{\epsilon'}$ is

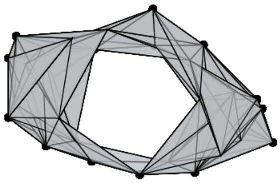

(A) Rips complex $\mathcal{R}^{\epsilon'}$

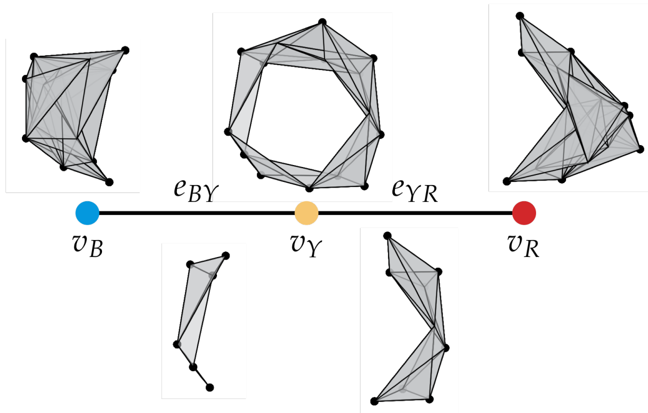

(B) Rips system over the nerve $N_{\mathcal{V}}$

FIGURE 4.4: Rips complex and the associated Rips system

a constant cosheaf with local sections $\mathbb{K}$ everywhere. The cosheaves $\mathcal{F}_1^{\epsilon'}$ and $\mathcal{F}_0^{\epsilon'}$ are illustrated in Figure 4.5a and 4.5b. One can compute

$$H_0(C_\bullet \mathcal{F}_1^{\epsilon'}) = \mathbb{K}, \quad H_1(C_\bullet \mathcal{F}_0^{\epsilon'}) = 0. \tag{4.13}$$

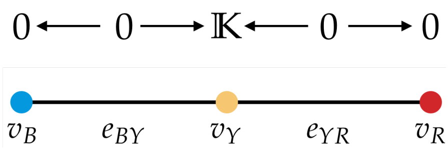

(A) Cosheaf $\mathcal{F}_1^{\epsilon'}$

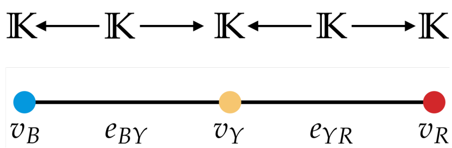

(B) Cosheaf $\mathcal{F}_0^{\epsilon'}$

FIGURE 4.5: The two relevant cosheaves for computing $H_1(\mathcal{R}^{\epsilon'})$

Let's compare the cosheaf homologies from Equation 4.12 and Equation 4.13 for the two parameters $\epsilon < \epsilon'$. Note that both $H_1(\mathcal{R}^{\epsilon}) = \mathbb{K}$ and $H_1(\mathcal{R}^{\epsilon'}) = \mathbb{K}$. In Example 12, the nonzero component appeared in $H_1(C_\bullet \mathcal{F}_0^{\epsilon})$, while for the larger ϵ' parameter, the nonzero component appears in $H_0(C_\bullet \mathcal{F}_1^{\epsilon'})$. The reason for such a difference becomes apparent when we compare the Rips systems from Figures 4.2b and 4.4b. In Figure 4.4b, one can see that the Rips complex $\mathcal{R}^{\epsilon}_{v_Y}$ contains a non-trivial 1-cycle, while in Figure 4.2b, there is no such 1-cycle contained in any of the complexes $\mathcal{R}^{\epsilon}_{\sigma}$ for $\sigma \in N_{\mathcal{V}}$. In fact, $H_0(C_\bullet \mathcal{F}_n^{\epsilon})$ reads non-trivial n-cycles that exist in $\mathcal{R}^{\epsilon}_{\sigma}$ for some $\sigma \in N_{\mathcal{V}}$. On the other hand, $H_1(C_\bullet \mathcal{F}_{n-1}^{\epsilon})$ reads non-trivial n-cycles of $\mathcal{R}^{\epsilon}$ that are not cycles of $H_n(\mathcal{R}^{\epsilon}_{\sigma})$

for any $\sigma \in N_{\mathcal{V}}$.

4.2 Distributed Computation of Persistent Homology

In §4.1, we computed the homology of a Rips complex from homologies of subcomplexes. A natural question that arises is whether we can leverage such a construction to compute persistence modules in a distributed manner.

Constructing the Rips complexes on a point cloud P for increasing parameter values $(\epsilon_i)_{i=1}^N$ results in the following sequence of Rips complexes and inclusion maps.

$$\mathcal{R}^1 \xhookrightarrow{\iota^1} \mathcal{R}^2 \xhookrightarrow{\iota^2} \dots \xhookrightarrow{\iota^{N-1}} \mathcal{R}^N$$

Applying the homology functor of dimension n with coefficients in a field $\mathbb{K}$, we obtain the persistence module

$$\mathbb{V} : H_n(\mathcal{R}^1) \xrightarrow{\iota^1_*} H_n(\mathcal{R}^2) \xrightarrow{\iota^2_*} \dots \xrightarrow{\iota^{N-1}_*} H_n(\mathcal{R}^N). \tag{4.14}$$

Assume that we have a map $f : P \to \mathbb{R}^d$ and a covering $\mathcal{V}$ that satisfies the conditions of Lemma 12. Hence, we have the following isomorphisms

$$H_n(\mathcal{R}^i) \cong H_0(C_\bullet \mathcal{F}^i_n) \oplus H_1(C_\bullet \mathcal{F}^i_{n-1}) \tag{4.15}$$

for every i and n. Can we construct a persistence module

$$\mathbb{V}_\Psi : H_0(C_\bullet \mathcal{F}^1_n) \oplus H_1(C_\bullet \mathcal{F}^1_{n-1}) \xrightarrow{\Psi^1} \cdots \xrightarrow{\Psi^{N-1}} H_0(C_\bullet \mathcal{F}^N_n) \oplus H_1(C_\bullet \mathcal{F}^N_{n-1})$$

that is isomorphic to the persistence module $\mathbb{V}$ from Equation 4.14?

In §4.2.1, we show that the most naturally induced cosheaf morphisms $H_0(\phi^i_n) : H_0(C_\bullet \mathcal{F}^i_n) \to H_0(C_\bullet \mathcal{F}^{i+1}_n)$ and $H_1(\phi^i_{n-1}) : H_1(C_\bullet \mathcal{F}^i_{n-1}) \to H_1(C_\bullet \mathcal{F}^{i+1}_{n-1})$ are not enough to construct a persistence module isomorphic to $\mathbb{V}$. In §4.2.2 we construct the missing ingredient $\psi^i : H_1(C_\bullet \mathcal{F}^i_{n-1}) \to H_0(C_\bullet \mathcal{F}^{i+1}_n)$ using spectral sequences. For the interested reader, we provide an alternate construction of the missing map ψ^i using long exact sequences in Appendix A. In §4.2.3, we construct the persistence module

$$\mathbb{V}_\Psi : H_0(C_\bullet \mathcal{F}_n^1) \oplus H_1(C_\bullet \mathcal{F}_{n-1}^1) \xrightarrow{\Psi^1} \cdots \xrightarrow{\Psi^{N-1}} H_0(C_\bullet \mathcal{F}_n^N) \oplus H_1(C_\bullet \mathcal{F}_{n-1}^N).$$

In §4.2.4, we show that the constructed persistence module $\mathbb{V}_\Psi$ is isomorphic to the persistence module $\mathbb{V}$.

For §4.2.1 and §4.2.2, we limit our attention to the situation with two parameters $\epsilon_i < \epsilon_{i+1}$ in order to simplify notations. In §4.2.3 and §4.2.4, we come back to considering the entire family of parameters $(\epsilon_i)_{i=1}^N$ as we construct $\mathbb{V}_\Psi$.

4.2.1 Cosheaf morphisms

Given two parameters $\epsilon_i < \epsilon_{i+1}$, let $\mathcal{R}_\sigma^i$ and $\mathcal{R}_\sigma^{i+1}$ each denote the Rips complexes built on $f^{-1}(U_\sigma)$ for the two parameters. Let $\mathcal{F}_n^i$ and $\mathcal{F}_n^{i+1}$ be the cosheaves on $N_\mathcal{V}$ obtained by applying the n^{th} homology functor to the Rips system for the two parameters. Note that for every $\sigma \in N_\mathcal{V}$, there exists an inclusion map $\mathcal{R}_\sigma^i \hookrightarrow \mathcal{R}_\sigma^{i+1}$. Such inclusion maps induce maps $\mathcal{F}_n^i(\sigma) \to \mathcal{F}_n^{i+1}(\sigma)$ for every σ that are compatible with the extension maps. Let $\phi_n^i : \mathcal{F}_n^i \to \mathcal{F}_n^{i+1}$ be the resulting cosheaf morphism. Recall from Lemma 4 that cosheaf morphisms induce morphisms in cosheaf homology. In particular, the cosheaf morphisms ϕ_n^i and ϕ_{n-1}^i induce the following morphisms

$$\begin{aligned} H_0(\phi_n^i) &: H_0(C_\bullet \mathcal{F}_n^i) \to H_0(C_\bullet \mathcal{F}_n^{i+1}), \\ H_1(\phi_{n-1}^i) &: H_1(C_\bullet \mathcal{F}_{n-1}^i) \to H_1(C_\bullet \mathcal{F}_{n-1}^{i+1}). \end{aligned} \tag{4.16}$$

The maps $H_0(\phi_n^i)$ and $H_1(\phi_{n-1}^i)$ can be used to construct a persistence module

$$\mathbb{V}_{\Psi^i} : H_0(C_\bullet \mathcal{F}_n^i) \oplus H_1(C_\bullet \mathcal{F}_{n-1}^i) \xrightarrow{\Psi^i} H_0(C_\bullet \mathcal{F}_n^{i+1}) \oplus H_1(C_\bullet \mathcal{F}_{n-1}^{i+1})$$

by

$$\Psi^i(u, v) = (H_0(\phi_n^i)(u), H_1(\phi_{n-1}^i)(v)).$$

However, the resulting persistence module $\mathbb{V}_{\Psi^i}$ cannot be isomorphic to the persistence module of interest $\mathbb{V} : H_n(\mathcal{R}^i) \xrightarrow{\iota_*^i} H_n(\mathcal{R}^{i+1})$. Recall from Definition 9 that if $\mathbb{V}_{\Psi^i}$ and $\mathbb{V}$ were isomorphic persistence modules, then there would exist isomorphisms Φ^i and Φ^{i+1} such that the following diagram commutes.

$$\begin{array}{ccc} H_0(C_\bullet \mathcal{F}_n^i) \oplus H_1(C_\bullet \mathcal{F}_{n-1}^i) & \xrightarrow{\Phi^i} & H_n(\mathcal{R}^i) \\ \downarrow \Psi^i & & \downarrow \iota_*^i \\ H_0(C_\bullet \mathcal{F}_n^{i+1}) \oplus H_1(C_\bullet \mathcal{F}_{n-1}^{i+1}) & \xrightarrow{\Phi^{i+1}} & H_n(\mathcal{R}^{i+1}) \end{array} \tag{4.17}$$

However, one can check that Diagram 4.17 fails to commute for any isomorphisms Φ^i and Φ^{i+1} by examining Examples 12 and 13. Let $\mathcal{R}^i$ denote the Rips complex built on parameter ϵ^i from Example 12, and let $\mathcal{R}^{i+1}$ denote the Rips complex built on parameter ϵ^{i+1} from Example 13. Let's say we are interested in computing $\mathbb{V} : H_1(\mathcal{R}^i) \to H_1(\mathcal{R}^{i+1})$. Recall from Equations 4.12 and 4.13 that the relevant cosheaf homologies are

$$H_0(C_\bullet \mathcal{F}_1^i) = 0, \quad H_1(C_\bullet \mathcal{F}_0^i) = \mathbb{K},$$

$$H_0(C_\bullet \mathcal{F}_1^{i+1}) = \mathbb{K}, \quad H_1(C_\bullet \mathcal{F}_0^{i+1}) = 0.$$

Let $s \in H_1(C_\bullet \mathcal{F}_0^i)$ which represents the non-trivial 1-cycle in Figure 4.2a, i.e., $\Phi^i(s)$ is the non-trivial 1-cycle illustrated in Figure 4.2a. Then, $\iota_*^i \circ \Phi^i(s)$ must be the non-trivial 1-cycle represented in Figure 4.4a. On the other hand, with our current construction of Ψ^i, we have $\Psi^i(s) = 0$, and hence, $\Phi^{i+1} \circ \Psi^i(s) = 0$ for any isomorphism Φ^{i+1}. Thus, Diagram 4.17 cannot commute.

To understand why the diagram fails to commute, note that elements of $H_0(C_\bullet \mathcal{F}_n^i)$ correspond to homology classes of $H_n(\mathcal{R}^i)$ that can be represented by a cycle γ such that $\gamma \in H_n(\mathcal{R}_\sigma^i)$ for some $\sigma \in N_\mathcal{V}$. Elements of $H_1(C_\bullet \mathcal{F}_{n-1}^i)$ correspond to homology classes of $H_n(\mathcal{R}^i)$ that cannot be represented by such cycles. As one can see from Examples 12 and 13, as we increase the parameter from ϵ^i to ϵ^{i+1}, a cycle in $H_1(C_\bullet \mathcal{F}_{n-1}^i)$ can become homologous to a cycle in $H_0(C_\bullet \mathcal{F}_n^{i+1})$. However, the current definition of Ψ^i fails to take such subtlety into account. In order for the Diagram 4.17 to commute, Ψ^i must map an element of $H_1(C_\bullet \mathcal{F}^i_{n-1})$ to $H_0(C_\bullet \mathcal{F}^{i+1}_n)$.

4.2.2 Connecting morphism via spectral sequences

In this section, we will construct a map $\psi^i : H_1(C_\bullet \mathcal{F}^i_{n-1}) \to H_0(C_\bullet \mathcal{F}^{i+1}_n)$ that is required to define a map Ψ^i that makes Diagram 4.17 commute. Recall from Equation 4.16 that $H_0(\phi^i_n)$ and $H_1(\phi^i_{n-1})$ denote the morphisms on cosheaf homology induced by cosheaf morphisms $\phi^i_n : \mathcal{F}^i_n \to \mathcal{F}^{i+1}_n$. Before constructing ψ^i, we will show that there exists a morphism $\delta^i : \ker H_1(\phi^i_{n-1}) \to \operatorname{coker} H_0(\phi^i_n)$ using a spectral sequence type argument.

The importance of the morphism δ^i is that it extends to a map $\psi^i : H_1(C_\bullet \mathcal{F}^i_{n-1}) \to H_0(C_\bullet \mathcal{F}^{i+1}_n)$ (Lemma 14), which, along with $H_0(\phi^i_n)$, and $H_1(\phi^i_{n-1})$, can construct a persistence module isomorphic to $\mathbb{V} : H_n(\mathcal{R}^i) \xrightarrow{\iota^i_*} H_n(\mathcal{R}^{i+1})$ (§4.2.4).

Theorem 8. *Let P be a point cloud, and let $f : P \to \mathbb{R}^d$ be any map. Let $\mathcal{V}$ be a cover of $f(P) \subset \mathbb{R}^d$ such that $N_\mathcal{V}$ is at most one dimensional. Cosheaf morphisms ϕ^i_n, ϕ^i_{n-1} induce a morphism $\delta^i : \ker H_1(\phi^i_{n-1}) \to \operatorname{coker} H_0(\phi^i_n)$.*

Proof. Consider the following commutative diagram. Let $\iota^i_n : \bigoplus_{v \in N_\mathcal{V}} C_n(\mathcal{R}^i_v) \to \bigoplus_{v \in N_\mathcal{V}} C_n(\mathcal{R}^{i+1}_v)$ denote the collection of inclusion maps of the Rips complexes over the vertices of $N_\mathcal{V}$, and let $\kappa^i_n : \bigoplus_{e \in N_\mathcal{V}} C_n(\mathcal{R}^i_e) \to \bigoplus_{e \in N_\mathcal{V}} C_n(\mathcal{R}^{i+1}_e)$ denote the collection of inclusion maps of the Rips complexes over the edges of $N_\mathcal{V}$. Let $e^i_n : \bigoplus_{e \in N_\mathcal{V}} C_n(\mathcal{R}^i_e) \to \bigoplus_{v \in N_\mathcal{V}} C_n(\mathcal{R}^i_v)$ denote the collection of inclusion maps. The maps ∂'s denote the boundary maps. Note that the front and back faces of the cube are the 0^{th} pages of the spectral sequence 4.3 for parameters ϵ^i and ϵ^{i+1} respectively.

$$
\begin{tikzcd}
 & {} & & {} \\
{} & \bigoplus\limits_{v\in N_{\mathcal{V}}} C_n(\mathcal{R}_v^{i+1}) \arrow[dd, "\partial"] & {} & \bigoplus\limits_{e\in N_{\mathcal{V}}} C_n(\mathcal{R}_e^{i+1}) \arrow[ll, "e_n^{i+1}"] \arrow[dd, "\partial"] \\
\bigoplus\limits_{v\in N_{\mathcal{V}}} C_n(\mathcal{R}_v^{i}) \arrow[ur, "\iota_n^i"] \arrow[dd, "\partial"] & & \bigoplus\limits_{e\in N_{\mathcal{V}}} C_n(\mathcal{R}_e^{i}) \arrow[ll, "e_n^i"] \arrow[ur, "\kappa_n^i"] \arrow[dd, "\partial"] & \\
 & \bigoplus\limits_{v\in N_{\mathcal{V}}} C_{n-1}(\mathcal{R}_v^{i+1}) \arrow[dd] & & \bigoplus\limits_{e\in N_{\mathcal{V}}} C_{n-1}(\mathcal{R}_e^{i+1}) \arrow[ll, "e_{n-1}^{i+1}"] \arrow[dd] \\
\bigoplus\limits_{v\in N_{\mathcal{V}}} C_{n-1}(\mathcal{R}_v^{i}) \arrow[ur, "\iota_{n-1}^i"] \arrow[d] & & \bigoplus\limits_{e\in N_{\mathcal{V}}} C_{n-1}(\mathcal{R}_e^{i}) \arrow[ll, "e_{n-1}^i"] \arrow[ur, "\kappa_{n-1}^i"] \arrow[d] & \\
{} & {} & {} & {}
\arrow[from=1-2, to=2-2]
\arrow[from=1-4, to=2-4]
\arrow[from=2-1, to=3-1]
\arrow[from=2-3, to=3-3]
\end{tikzcd}
\tag{4.18}
$$

Computing the homology with respect to the boundary maps ∂, we obtain the following diagram. The maps denoted by ∂_n's in Diagram 4.19 now refers to the boundary maps of the chain complexes $C_\bullet\mathcal{F}_n^i$ of the respective cosheaves. Note that the front and back faces of the cube are the E_1 pages of the spectral sequences illustrated in Diagram

4.4.

$$\begin{tikzcd}
& \bigoplus\limits_{v\in N_{\mathcal{V}}} H_n(\mathcal{R}_v^{i+1}) \arrow[dd, dash, dashed] & & \bigoplus\limits_{e\in N_{\mathcal{V}}} H_n(\mathcal{R}_e^{i+1}) \arrow[ll, "\partial_n^{i+1}"'] \arrow[dd, dash, dashed] \\
\bigoplus\limits_{v\in N_{\mathcal{V}}} H_n(\mathcal{R}_v^{i}) \arrow[ur, "(\phi_n^i)_v"] \arrow[dd, dash, dashed] & & \bigoplus\limits_{e\in N_{\mathcal{V}}} H_n(\mathcal{R}_e^{i}) \arrow[ll, "\partial_n^{i}"'] \arrow[ur, "(\phi_n^i)_e"] \arrow[dd, dash, dashed] & \\
& \bigoplus\limits_{v\in N_{\mathcal{V}}} H_{n-1}(\mathcal{R}_v^{i+1}) & & \bigoplus\limits_{e\in N_{\mathcal{V}}} H_{n-1}(\mathcal{R}_e^{i+1}) \arrow[ll, "\partial_{n-1}^{i+1}"'] \\
\bigoplus\limits_{v\in N_{\mathcal{V}}} H_{n-1}(\mathcal{R}_v^{i}) \arrow[ur, "(\phi_{n-1}^i)_v"] & & \bigoplus\limits_{e\in N_{\mathcal{V}}} H_{n-1}(\mathcal{R}_e^{i}) \arrow[ll, "\partial_{n-1}^{i}"'] \arrow[ur, "(\phi_{n-1}^i)_e"] &
\end{tikzcd} \tag{4.19}$$

Now compute the homology with respect to the maps ∂_n^i. We then obtain the following diagram of cosheaf homologies. The front and back faces of the cube correspond to the E_2 pages of the spectral sequences illustrated in Diagram 4.5. Note that the only remaining maps are the ones induced by cosheaf morphisms.

$$\begin{tikzcd}
& H_0(C_\bullet \mathcal{F}_n^{i+1}) \arrow[rr, dash, dashed] \arrow[dd, dash, dashed] & & H_1(C_\bullet \mathcal{F}_n^{i+1}) \arrow[dd, dash, dashed] \\
H_0(C_\bullet \mathcal{F}_n^{i}) \arrow[ur, "H_0(\phi_n^i)"] \arrow[rr, dash, dashed] \arrow[dd, dash, dashed] & & H_1(C_\bullet \mathcal{F}_n^{i}) \arrow[ur, "H_1(\phi_n^i)"] \arrow[dd, dash, dashed] & \\
& H_0(C_\bullet \mathcal{F}_{n-1}^{i+1}) \arrow[rr, dash, dashed] & & H_1(C_\bullet \mathcal{F}_{n-1}^{i+1}) \\
H_0(C_\bullet \mathcal{F}_{n-1}^{i}) \arrow[ur, "H_0(\phi_{n-1}^i)"] \arrow[rr, dash, dashed] & & H_1(C_\bullet \mathcal{F}_{n-1}^{i}) \arrow[ur, "H_1(\phi_{n-1}^i)"] &
\end{tikzcd} \tag{4.20}$$

We now take the homology with respect to the cosheaf morphisms. We will show that there is an induced map from $\ker H_1(\phi^i_{n-1})$ to $\operatorname{coker} H_0(\phi^i_n)$ as shown in the following diagram.

$$
\begin{tikzcd}
 & \operatorname{coker} H_0(\phi^i_n) \arrow[rr, dash, dashed] & & \operatorname{coker} H_1(\phi^i_n) \\
\ker H_0(\phi^i_n) \arrow[ur, dash, dashed] \arrow[rr, dash, dashed] \arrow[dd, dash, dashed] & & \ker H_1(\phi^i_n) \arrow[ur, dash, dashed] \arrow[dd, dash, dashed] & \\
 & \operatorname{coker} H_0(\phi^i_{n-1}) \arrow[uu, dash, dashed] \arrow[rr, dash, dashed] & & \operatorname{coker} H_1(\phi^i_{n-1}) \arrow[uu, dash, dashed] \\
\ker H_0(\phi^i_{n-1}) \arrow[ur, dash, dashed] \arrow[rr, dash, dashed] & & \ker H_1(\phi^i_{n-1}) \arrow[ur, dash, dashed] \arrow[uuul] &
\end{tikzcd}
\tag{4.21}
$$

First, we establish some notation. Let $\langle\ \rangle$, $\{\ \}$, and $[\ ]$ each denote the homology classes that appear in diagrams 4.19, 4.20, and 4.21. For example, let $\gamma \in \bigoplus_{e\in N_v} C_{n-1}(\mathcal{R}^i_e)$.

- If $\partial\gamma = 0$, then $\langle\gamma\rangle$ denotes the homology class of γ in $\bigoplus_{e\in N_v} H_{n-1}(\mathcal{R}^i_e)$.
- If $\partial^i_{n-1}\langle\gamma\rangle = 0$, then $\{\langle\gamma\rangle\}$ denotes the homology class of $\langle\gamma\rangle$ in $H_1(C_\bullet\mathcal{F}^i_{n-1})$.
- If $H_1(\phi^i_{n-1})\{\langle\gamma\rangle\} = 0$, then $[\{\langle\gamma\rangle\}]$ denotes the homology class of $\{\langle\gamma\rangle\}$ in $\ker H_1(\phi^i_{n-1})$.

Let $[\{\langle\gamma\rangle\}]$ represent an element of $\ker H_1(\phi^i_{n-1})$. Then, $\gamma \in \bigoplus_{e\in N_v} C_{n-1}(\mathcal{R}^i_e)$ must satisfy the three conditions listed above.

The third condition, that $H_1(\phi^i_{n-1})\{\langle\gamma\rangle\} = 0$, implies that $(\phi^i_{n-1})_e\langle\gamma\rangle$ is trivial in $\bigoplus_{e\in N_v} H_{n-1}(\mathcal{R}^{i+1}_e)$, i.e., there exists $\alpha^{i+1} \in \bigoplus_{e\in N_v} C_n(\mathcal{R}^{i+1}_e)$ such that

$$\partial\alpha^{i+1} = \kappa^i_{n-1}\gamma. \tag{4.22}$$

The second condition, that $\partial^i_{n-1}\langle\gamma\rangle = 0$ in $\bigoplus_{v\in N_\mathcal{V}} H_{n-1}(\mathcal{R}^i_v)$, implies that there exists $\beta^i \in \bigoplus_{v\in N_\mathcal{V}} C_n(\mathcal{R}^i_v)$ such that

$$\partial\beta^i = e^i_{n-1}\gamma. \tag{4.23}$$

Define a map $\delta^i : \ker H_1(\phi^i_{n-1}) \to \operatorname{coker} H_0(\phi^i_n)$ by

$$\delta^i[\{\langle\gamma\rangle\}] = [\{\langle -e^{i+1}_n\alpha^{i+1} + \iota^i_n\beta^i\rangle\}]. \tag{4.24}$$

One can check that $-e^{i+1}_n\alpha^{i+1} + \iota^i_n\beta^i$ represents an element in $\operatorname{coker} H_0(\phi^i_n)$ and that δ^i is well defined. The proofs are in Appendix B.1. □

Lemma 14. *The map* $\delta^i : \ker H_1(\phi^i_{n-1}) \to \operatorname{coker} H_0(\phi^i_n)$ *extends to a map* $\psi^i : H_1(C_\bullet\mathcal{F}^i_{n-1}) \to H_0(C_\bullet\mathcal{F}^{i+1}_n)$.

Proof. Note that $\ker H_1(\phi^i_{n-1})$ is a subspace of $H_1(C_\bullet\mathcal{F}^i_{n-1})$ and that $\operatorname{coker} H_0(\phi^i_n)$ is a subspace of $H_0(C_\bullet\mathcal{F}^{i+1}_n)$. Since $H_1(C_\bullet\mathcal{F}^i_{n-1})$ and $H_0(C_\bullet\mathcal{F}^{i+1}_n)$ are finite dimensional vector spaces, we have the following decompositions

$$H_1(C_\bullet\mathcal{F}^i_{n-1}) = \ker H_1(\phi^i_{n-1}) \oplus A^i\,, \tag{4.25}$$

$$H_0(C_\bullet\mathcal{F}^{i+1}_n) = \operatorname{coker} H_0(\phi^i_n) \oplus B^i\,. \tag{4.26}$$

So every $u \in H_1(C_\bullet\mathcal{F}^i_{n-1})$ can be written uniquely as $u = (w_1, w_2)$, with $w_1 \in \ker H_1(\phi^i_{n-1})$ and $w_2 \in A^i$. Define $\psi^i : H_1(C_\bullet\mathcal{F}^i_{n-1}) \to H_0(C_\bullet\mathcal{F}^{i+1}_n)$ by

$$\psi^i(u) = \psi^i(w_1, w_2) = (\delta^i(w_1), 0)\,. \tag{4.27}$$

□

The following example illustrates the choice of α^{i+1} and β^i in the construction of δ^i.

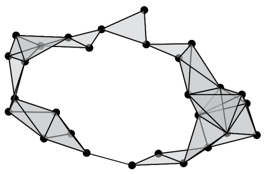

(A) Rips complex $\mathcal{R}^i$

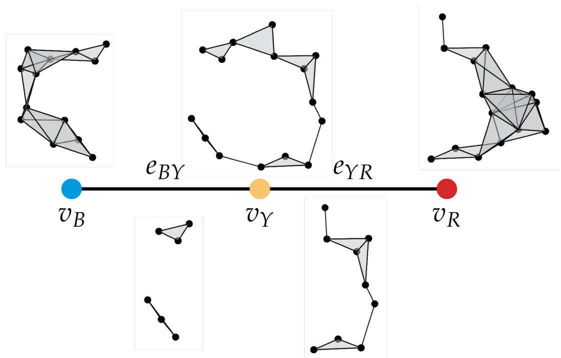

(B) Rips system for parameter ϵ_i

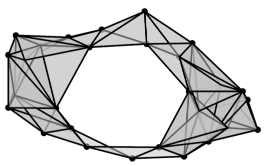

(C) Rips complex $\mathcal{R}^{i+1}$

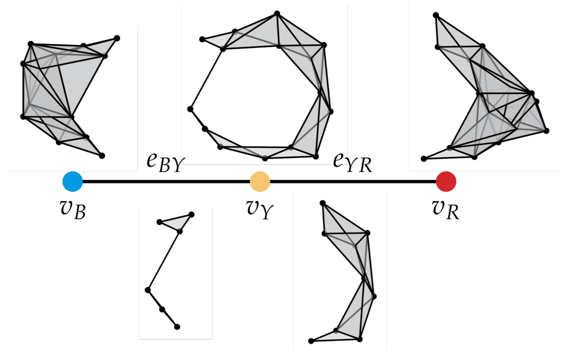

(D) Rips system for parameter ϵ_{i+1}

FIGURE 4.6: Rips complexes and the Rips systems for parameters ϵ_i and ϵ_{i+1}

Example 14. Consider the Rips complexes $\mathcal{R}^i$ and $\mathcal{R}^{i+1}$ built for parameters ϵ_i and ϵ_{i+1} illustrated in Figure 4.6a and Figure 4.6c. The Rips system for the two parameters are illustrated in Figure 4.6b and Figure 4.6d.

Note that

$$\begin{aligned} H_0(C_\bullet\mathcal{F}_1^i) = 0, \quad H_1(C_\bullet\mathcal{F}_0^i) = \mathbb{K} \\ H_0(C_\bullet\mathcal{F}_1^{i+1}) = \mathbb{K}, \quad H_1(C_\bullet\mathcal{F}_0^{i+1}) = 0. \end{aligned} \tag{4.28}$$

The map $H_1(\phi_0^i) : H_1(C_\bullet\mathcal{F}_0^i) \to H_1(C_\bullet\mathcal{F}_0^{i+1})$ is trivial, so $\ker H_1(\phi_0^i) = H_1(C_\bullet\mathcal{F}_0^i)$.

Let $[\{\langle\gamma\rangle\}] \in \ker H_1(\phi_0^i)$. The process of finding α^{i+1} is illustrated in Figure 4.7. The coset representative $\gamma \in \bigoplus_{e\in N_v} C_0(\mathcal{R}_e^i)$ is illustrated in Figure 4.7a. Note that $\kappa_{n-1}^i\gamma \in \bigoplus_{e\in N_v} C_0(\mathcal{R}_e^{i+1})$, so $\kappa_{n-1}^i\gamma$ is illustrated in a Rips system for parameter ϵ_{i+1} in Figure 4.7b. Recall that $\alpha^{i+1} \in \bigoplus_{e\in N_v} C_1(\mathcal{R}_e^{i+1})$ satisfies Equation 4.22, i.e., α^{i+1} is a 1-chain whose boundary equals $\kappa_{n-1}^i\gamma$. The element α^{i+1} is illustrated in Figure 4.7c. Finally, $e_n^{i+1}\alpha \in$

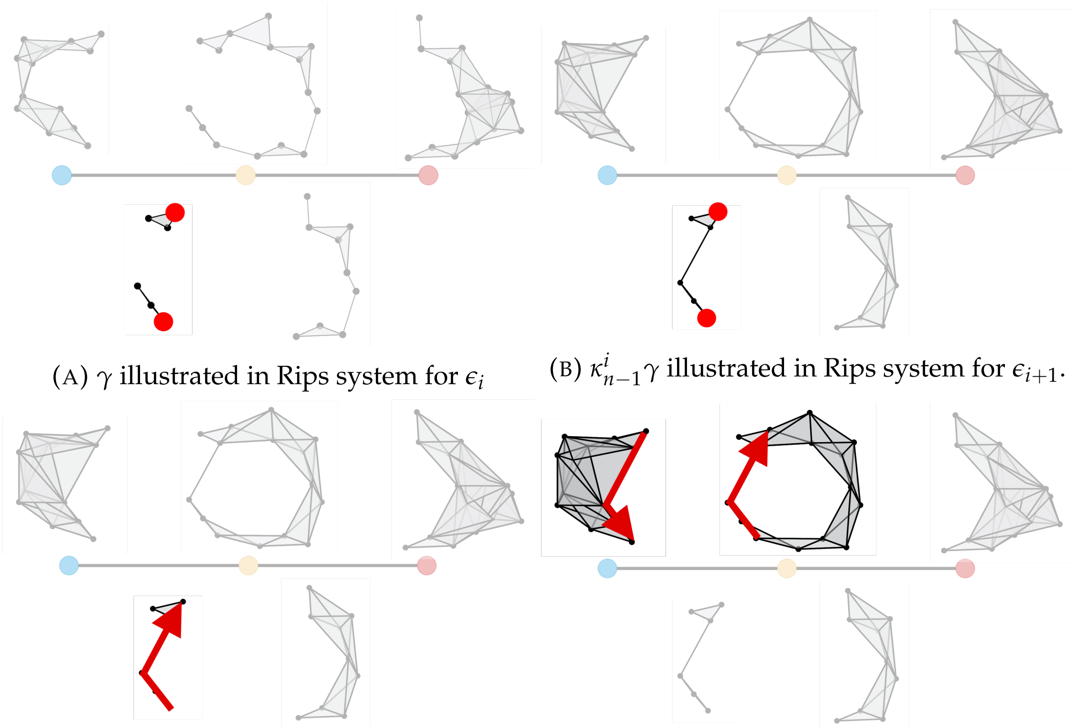

(A) γ illustrated in Rips system for ϵ_i (B) $\kappa^i_{n-1}\gamma$ illustrated in Rips system for ϵ_{i+1}.

(C) α^{i+1} illustrated in Rips system for ϵ_{i+1} (D) $e^{i+1}_n\alpha^{i+1}$ illustrated in Rips system for ϵ_{i+1}

FIGURE 4.7: Finding α^{i+1}

$\bigoplus_{v \in N_\mathcal{V}} C_1(\mathcal{R}^{i+1}_v)$ is illustrated in Figure 4.7d.

On the other hand, the process of finding β^i is illustrated in Figure 4.8. We start with the same coset representative $\gamma \in \bigoplus_{e \in N_\mathcal{V}} C_0(\mathcal{R}^i_v)$ illustrated in Figure 4.8a. Note that $e^i_{n-1}\gamma \in \bigoplus_{v \in N_\mathcal{V}} C_0(\mathcal{R}^i_v)$, which is illustrated in Figure 4.8b. The element $\beta^i \in \bigoplus_{v \in N_\mathcal{V}} C_1(\mathcal{R}^i_v)$ must satisfy Equation 4.23, i.e., $e^i_{n-1}\gamma$ must be the boundary of β^i. Such β^i is illustrated in Figure 4.8c. Lastly, $\iota^i_n\beta^i$ is illustrated in Figure 4.8d.

From Figures 4.7 and 4.8, one can now visualize the map $\delta^i[\{\langle\gamma\rangle\}] = [\{\langle -e^{i+1}_n\alpha^{i+1} + \iota^i_n\beta^i\rangle\}]$, as illustrated in Figure 4.9.

In Appendix A, we provide an alternate construction of map $\psi^i_* : H_1(C_\bullet\mathcal{F}^i_{n-1}) \to H_0(C_\bullet\mathcal{F}^{i+1}_n)$ via long exact sequences. We also show that the two maps ψ^i and ψ^i_* are the same maps up to a change of basis.

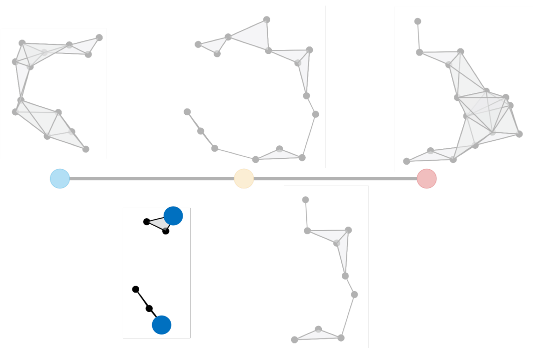

(A) An element $[\{\langle\gamma\rangle\}] \in \ker H_1(\phi_0^i)$

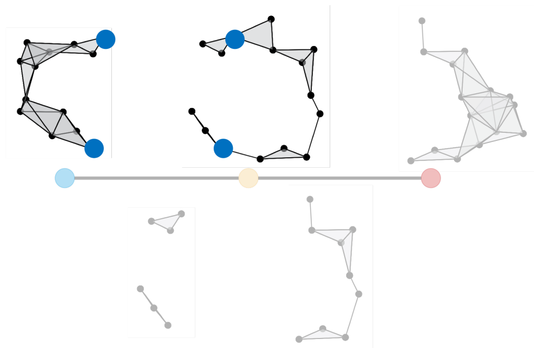

(B) $e^i_{n-1}\gamma$ illustrated in Rips system for ϵ_i

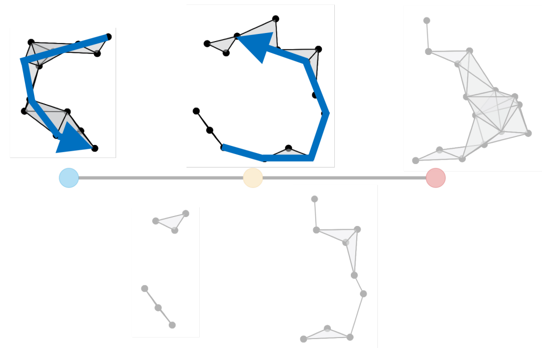

(C) β^i illustrated in Rips system for ϵ_i

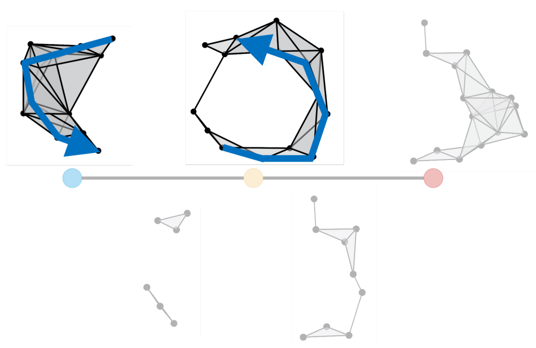

(D) $\iota^i_n\beta^i$ illustrated in Rips system for ϵ_{i+1}

FIGURE 4.8: Finding β

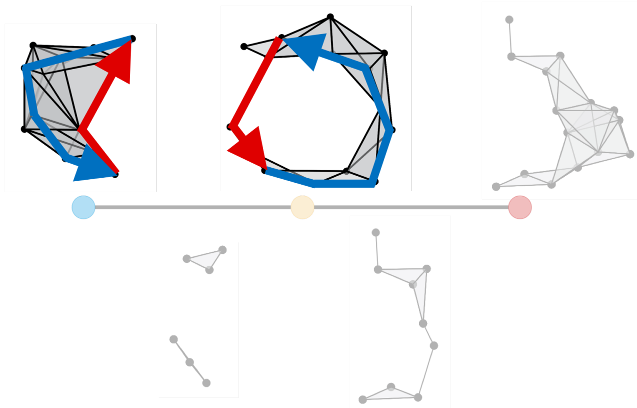

FIGURE 4.9: $-e_n^{i+1}\alpha^{i+1} + \iota_n^i\beta^i$ illustrated in Rips system for parameter ϵ_{i+1}

4.2.3 Construction of distributed persistence module

Given a family of parameters $(\epsilon_i)_{i=1}^N$ such that the isomorphism

$$H_n(\mathcal{R}^i) \cong H_0(C_\bullet \mathcal{F}_n^i) \oplus H_1(C_\bullet \mathcal{F}_{n-1}^i)$$

holds for each ϵ_i, we now construct maps

$$\Psi^i : H_0(C_\bullet \mathcal{F}_n^i) \oplus H_1(C_\bullet \mathcal{F}_{n-1}^i) \to H_0(C_\bullet \mathcal{F}_n^{i+1}) \oplus H_1(C_\bullet \mathcal{F}_{n-1}^{i+1})$$

such that the resulting persistence module

$$\mathbb{V}_\Psi : H_0(C_\bullet \mathcal{F}_n^1) \oplus H_1(C_\bullet \mathcal{F}_{n-1}^1) \xrightarrow{\Psi^1} \cdots \xrightarrow{\Psi^{N-1}} H_0(C_\bullet \mathcal{F}_n^N) \oplus H_1(C_\bullet \mathcal{F}_{n-1}^N)$$

is isomorphic to the persistence module

$$\mathbb{V} : H_n(\mathcal{R}^1) \xrightarrow{\iota_*^1} \cdots \xrightarrow{\iota_*^{N-1}} H_n(\mathcal{R}^N)$$

from Equation 4.14.

Recall the maps

$$\begin{aligned} H_0(\phi_n^i) :& H_0(C_\bullet \mathcal{F}_n^i) \to H_0(C_\bullet \mathcal{F}_n^{i+1}) \\ H_1(\phi_{n-1}^i) :& H_1(C_\bullet \mathcal{F}_{n-1}^i) \to H_1(C_\bullet \mathcal{F}_{n-1}^{i+1}) \end{aligned} \tag{4.29}$$

from Equation 4.16 and the map

$$\psi^i : H_1(C_\bullet \mathcal{F}_{n-1}^i) \to H_0(C_\bullet \mathcal{F}_n^{i+1})$$

from Equation 4.27. For each ϵ_i, it is possible to construct a map

$$\Psi^i : H_0(C_\bullet \mathcal{F}_n^i) \oplus H_1(C_\bullet \mathcal{F}_{n-1}^i) \to H_0(C_\bullet \mathcal{F}_n^{i+1}) \oplus H_1(C_\bullet \mathcal{F}_{n-1}^{i+1})$$

by

$$\Psi^i(\{\langle x \rangle\}, \{\langle y \rangle\}) = (H_0(\phi_n^i)\{\langle x \rangle\} + (-1)^{n+1}\psi^i\{\langle y \rangle\}, H_1(\phi_{n-1}^i)\{\langle y \rangle\}).$$

Given two parameters $\epsilon_i < \epsilon_{i+1}$, the persistence module

$$H_0(C_\bullet \mathcal{F}_n^i) \oplus H_1(C_\bullet \mathcal{F}_{n-1}^i) \xrightarrow{\Psi^i} H_0(C_\bullet \mathcal{F}_n^{i+1}) \oplus H_1(C_\bullet \mathcal{F}_{n-1}^{i+1})$$

can be shown to be isomorphic to the persistence module

$$H_n(\mathcal{R}^i) \xrightarrow{\iota_*^i} H_n(\mathcal{R}^{i+1}).$$

Given more than two parameters, the maps Ψ^i may define a persistence module that is different from the persistence module $\mathbb{V}$ that we are interested in. Thus, one should be mindful of the subtleties involved when constructing a persistence module for more than two parameters. Example 15 at the end of this chapter illustrates a situation where the maps Ψ^i lead to a persistence module that is not isomorphic to the persistence module of interest.

The subtlety arises from the fact that for each parameter ϵ_i, the cosheaf homology $H_1(C_\bullet \mathcal{F}_{n-1}^i)$ can potentially represent multiple cycles of $H_n(\mathcal{R}^i)$. When considering multiple ϵ_i parameters, the naive construction might force $H_1(C_\bullet\mathcal{F}^i_{n-1})$ to represent cycles that are not compatible with other parameters.

In this section, we construct morphisms Ψ^i that ensures that $H_1(C_\bullet\mathcal{F}^i_{n-1})$ represent cycles that are compatible across parameters. We achieve this goal by reconstructing morphisms

$$\psi^i : H_1(C_\bullet\mathcal{F}^i_{n-1}) \to H_0(C_\bullet\mathcal{F}^{i+1}_n).$$

Recall from Equations 4.24 and 4.27 that a map $\psi^i : H_1(C_\bullet\mathcal{F}^i_{n-1}) \to H_0(C_\bullet\mathcal{F}^{i+1}_n)$ has been defined by extending the map δ^i. The map δ^i was defined by

$$\delta^i[\{\langle\gamma\rangle\}] = [\{\langle -e^{i+1}_n\alpha^{i+1} + \iota^i_n\beta^i\rangle\}],$$

where α^{i+1} satisfies Equation 4.22 and β^i satisfies Equation 4.23.

Instead of extending the map δ^i, we will define the map $\psi^i : H_1(C_\bullet\mathcal{F}^i_{n-1}) \to H_0(C_\bullet\mathcal{F}^{i+1}_n)$ directly, as

$$\psi^i\{\langle\gamma\rangle\} = \{\langle -e^{i+1}_n\alpha^{i+1} + \iota^i_n\beta\rangle\}$$

for $\{\langle\gamma\rangle\} \in \ker H_1(\phi^i_{n-1})$.

When there are multiple candidates for α^{i+1} and β^i, the different choices of α^{i+1} and β^i can lead to different constructions of ψ^i. It turns out, the different choices for α^{i+1} do not affect the map ψ^i. It is the different choices of β^i that can lead to varying constructions of ψ^i. In particular, we want to choose elements β^i such that the maps ψ^i are compatible across parameters.

To that end, we construct the maps ψ^i on a fixed basis $\mathcal{B}^i$ of $H_1(C_\bullet\mathcal{F}^i_{n-1})$ in an inductive manner so that we can guarantee that choices of β^i for a parameter ϵ_i are compatible with the choices of β^{i-1} for parameter ϵ_{i-1}. Once we define the map ψ^i, we will be able to define Ψ^i.

The construction of map ψ^i will make use of Diagram 4.30. Note that while the previous commutative diagrams were constructed for two parameters $\epsilon_i < \epsilon_{i+1}$, the following diagram is constructed for the entire collection of ϵ parameters. Moreover, the following diagram is seen from a different perspective in three dimensions than the previous diagrams for display purposes. In this diagram, each horizontal face of the cube corresponds to the 0^{th} page of the spectral sequence from Diagram 4.3 for a fixed ϵ parameter.

Note that ∂ are the usual boundary maps and $e_n^i : \bigoplus\limits_{e\in N_{\mathcal{V}}} C_n(\mathcal{R}_e^i) \to \bigoplus\limits_{v\in N_{\mathcal{V}}} C_n(\mathcal{R}_v^i)$ is the inclusion of n-chains on the edges of $N_{\mathcal{V}}$ to the vertices of $N_{\mathcal{V}}$. The map $\iota_n^i : \bigoplus\limits_{v\in N_{\mathcal{V}}} C_n(\mathcal{R}_v^i) \to \bigoplus\limits_{v\in N_{\mathcal{V}}} C_n(\mathcal{R}_v^{i+1})$ and $\kappa_n^i : \bigoplus\limits_{e\in N_{\mathcal{V}}} C_n(\mathcal{R}_e^i) \to \bigoplus\limits_{e\in N_{\mathcal{V}}} C_n(\mathcal{R}_e^{i+1})$ are both inclusion maps.

$$\begin{tikzcd}
& \bigoplus\limits_{v\in N_{\mathcal{V}}} C_n(\mathcal{R}_v^1) \arrow[dl, "\partial"] \arrow[dd, "\iota_n^1"] & & \bigoplus\limits_{e\in N_{\mathcal{V}}} C_n(\mathcal{R}_e^1) \arrow[ll, "e_n^1"'] \arrow[dl, "\partial"] \arrow[dd, "\kappa_n^1"] \\
\bigoplus\limits_{v\in N_{\mathcal{V}}} C_{n-1}(\mathcal{R}_v^1) \arrow[dd, "\iota_{n-1}^1"] & & \bigoplus\limits_{e\in N_{\mathcal{V}}} C_{n-1}(\mathcal{R}_e^1) \arrow[ll, "e_{n-1}^1"] \arrow[dd, "\kappa_{n-1}^1"] & \\
& \bigoplus\limits_{v\in N_{\mathcal{V}}} C_n(\mathcal{R}_v^2) \arrow[dl, "\partial"] \arrow[dd, "\iota_n^2"] & & \bigoplus\limits_{e\in N_{\mathcal{V}}} C_n(\mathcal{R}_e^2) \arrow[ll, "e_n^2"'] \arrow[dl, "\partial"] \arrow[dd, "\kappa_n^2"] \\
\bigoplus\limits_{v\in N_{\mathcal{V}}} C_{n-1}(\mathcal{R}_v^2) \arrow[dd, "\iota_{n-1}^2"] & & \bigoplus\limits_{e\in N_{\mathcal{V}}} C_{n-1}(\mathcal{R}_e^2) \arrow[ll, "e_{n-1}^2"] \arrow[dd, "\kappa_{n-1}^2"] & \\
& \bigoplus\limits_{v\in N_{\mathcal{V}}} C_n(\mathcal{R}_v^3) \arrow[dl, "\partial"] \arrow[d, "\iota_n^3"] & & \bigoplus\limits_{e\in N_{\mathcal{V}}} C_n(\mathcal{R}_e^3) \arrow[ll, "e_n^3"'] \arrow[dl, "\partial"] \arrow[d, "\kappa_n^3"] \\
\bigoplus\limits_{v\in N_{\mathcal{V}}} C_{n-1}(\mathcal{R}_v^3) \arrow[d, "\iota_{n-1}^3"] & \vdots & \bigoplus\limits_{e\in N_{\mathcal{V}}} C_{n-1}(\mathcal{R}_e^3) \arrow[ll, "e_{n-1}^3"] \arrow[d, "\kappa_{n-1}^3"] & \vdots \\
\vdots & & \vdots &
\end{tikzcd} \tag{4.30}$$

For parameter ϵ_1, we will fix a basis $\mathcal{B}^1$ of $H_1(C_\bullet \mathcal{F}_{n-1}^1)$. We will define a linear map $\Gamma^1 : H_1(C_\bullet \mathcal{F}_{n-1}^1) \to \bigoplus\limits_{v\in N_{\mathcal{V}}} C_n(\mathcal{R}_v^1)$ and a linear map $\psi^1 : H_1(C_\bullet \mathcal{F}_{n-1}^1) \to H_0(C_\bullet \mathcal{F}_n^2)$ by defining the maps on the basis $\mathcal{B}^1$ and extending the maps linearly.

For each parameter ϵ_i, we will go through the following steps to construct the map ψ^i.

- **Step 1.** Fix a basis $\mathcal{C}^i$ of $H_1(C_\bullet \mathcal{F}^i_{n-1})$ that is compatible with the basis $\mathcal{B}^{i-1}$ of $H_1(C_\bullet \mathcal{F}^{i-1}_{n-1})$.
- **Step 2.** Define a map $\Gamma^i : H_1(C_\bullet \mathcal{F}^1_{n-1}) \to \bigoplus_{v \in N_\mathcal{V}} C_n(\mathcal{R}^i_v)$ by defining the map on $\mathcal{C}^i$ and extending linearly.
- **Step 3.** Fix a new basis $\mathcal{B}^i$ of $H_1(C_\bullet \mathcal{F}^i_{n-1})$.
- **Step 4.** Define the map $\psi^i : H_1(C_\bullet \mathcal{F}^i_{n-1}) \to H_0(C_\bullet \mathcal{F}^{i+1}_n)$ on basis $\mathcal{B}^i$ using the map Γ^i defined in Step 2.

The map $\Gamma^i : H_1(C_\bullet \mathcal{F}^i_{n-1}) \to \bigoplus_{v \in N_\mathcal{V}} (\mathcal{R}^i_v)$ defined in Step 2 will encode the choice of β^i for each basis vector $\{\langle b \rangle\} \in \mathcal{B}^i$. The basis $\mathcal{C}^i$ of $H_1(C_\bullet \mathcal{F}^i_{n-1})$ of Step 1 will allow us to define the map Γ^i in a manner compatible with map Γ^{i-1} from the previous parameter ϵ_{i-1}.

We proceed with the base case for parameter ϵ_1.

Base case

Recall from Equation 4.25 that

$$H_1(C_\bullet \mathcal{F}^1_{n-1}) = A^1 \oplus \ker H_1(\phi^1_{n-1}).$$

Let $\mathcal{B}^1_A$ be a basis of A^1, and let $\mathcal{B}^1_{\text{ker}}$ be a basis of $\ker H_1(\phi^1_{n-1})$. Then,

$$\mathcal{B}^1 = \mathcal{B}^1_A \cup \mathcal{B}^1_{\text{ker}}$$

is a basis of $H_1(C_\bullet \mathcal{F}^1_{n-1})$. For each basis vector $\{\langle b \rangle\} \in \mathcal{B}^1$, fix a coset representative b^* of $\langle b^* \rangle$. Thus, we can express the basis as

$$\mathcal{B}^1 = \{\, \{\langle b^*_1 \rangle\}, \dots, \{\langle b^*_m \rangle\} \,\}.$$

We will define $\Gamma^1 : H_1(C_\bullet \mathcal{F}^1_{n-1}) \to \bigoplus_{v \in N_\mathcal{V}} C_n(\mathcal{R}^1_v)$ on the basis $\mathcal{B}^1$. For a basis vector $\{\langle b^* \rangle\} \in \mathcal{B}^1$, we know from Equation 4.23 that there exists some $\beta^1 \in \bigoplus_{v \in N_\mathcal{V}} C_n(\mathcal{R}^1_v)$ such that

$$\partial \beta^1 = e^1_{n-1} b^*.$$

Among all possible candidates for β^1 that satisfy the above equation, choose any particular β^1, and denote the chosen element by β^1_*. For each $\{\langle b^* \rangle\} \in \mathcal{B}^1$, let

$$\Gamma^1\{\langle b^* \rangle\} = \beta^1_*. \tag{4.31}$$

Extend this map Γ^1 linearly to the vector space $H_1(C_\bullet \mathcal{F}^1_{n-1})$, i.e., define

$$\Gamma^1(\, a_1\{\langle b^*_1 \rangle\} + \cdots + a_m\{\langle b^*_m \rangle\}\,) = a_1\Gamma^1\{\langle b^*_1 \rangle\} + \cdots + a_m\Gamma^1\{\langle b^*_m \rangle\}.$$

We now define $\psi^1 : H_1(C_\bullet \mathcal{F}^1_{n-1}) \to H_0(C_\bullet \mathcal{F}^2_n)$ on the basis $\mathcal{B}^1$ and extend the map linearly. By construction, a basis vector $\{\langle b^* \rangle\} \in \mathcal{B}^1$ must satisfy either $\{\langle b^* \rangle\} \in \mathcal{B}^1_{\text{ker}}$ or $\{\langle b^* \rangle\} \in \mathcal{B}^1_A$. If $\{\langle b^* \rangle\} \in \mathcal{B}^1_{\text{ker}}$, recall from Equation 4.22 that there exists an $\alpha^2 \in \bigoplus_{e \in N_\mathcal{V}} C_n(\mathcal{R}^2_e)$ such that

$$\partial \alpha^2 = \kappa^1_{n-1} b^*. \tag{4.32}$$

Define ψ^1 for each $\{\langle b^* \rangle\} \in \mathcal{B}^1$ by

$$\psi^1\{\langle b^* \rangle\} = \begin{cases} \{\langle -e^2_n \alpha^2 + \iota^1_n \circ \Gamma^1\{\langle b^* \rangle\} \rangle\} & \text{if } \{\langle b^* \rangle\} \in \mathcal{B}^1_{\text{ker}} \\ 0 & \text{if } \{\langle b^* \rangle\} \in \mathcal{B}^1_A \end{cases} \tag{4.33}$$

where $\alpha^2 \in \bigoplus_{e \in N_\mathcal{V}} C_n(\mathcal{R}^2_e)$ can be any element satisfying Equation 4.32 and Γ^1 is the map defined in Equation 4.31.

Extend the map ψ^1 to the vector space $H_1(C_\bullet \mathcal{F}^1_{n-1})$, i.e., let

$$\psi^1(a_1\{\langle b^*_1 \rangle\} + \cdots + a_m\{\langle b^*_m \rangle\}) = a_1\psi^1\{\langle b^*_1 \rangle\} + \cdots + a_m\psi^1\{\langle b^*_m \rangle\}. \tag{4.34}$$

One can check that the map ψ^1 is well-defined (Appendix B.2).

Inductive step

Recall from Equation 4.25 that

$$H_1(C_\bullet \mathcal{F}_{n-1}^{i-1}) = A^{i-1} \oplus \ker H_1(\phi_{n-1}^{i-1}).$$

Assume that we are given a basis $\mathcal{B}^{i-1}$ of $H_1(C_\bullet \mathcal{F}_{n-1}^{i-1})$ that has the form

$$\mathcal{B}^{i-1} = \mathcal{B}_A^{i-1} \cup \mathcal{B}_{\ker}^{i-1},$$

where $\mathcal{B}_A^{i-1}$ is a basis of A^{i-1} and $\mathcal{B}_{\ker}^{i-1}$ is a basis of $\ker H_1(\phi_{n-1}^{i-1})$. Moreover, assume that for each basis vector $\{\langle b \rangle\} \in \mathcal{B}^{i-1}$, a coset representative b^* of $\langle b \rangle$ has been fixed, i.e., we can write the basis $\mathcal{B}^{i-1}$ as

$$\mathcal{B}^{i-1} = \{\, \{\langle b_1^* \rangle\}, \ldots, \{\langle b_{i-1_m}^* \rangle\} \,\}.$$

Lastly, assume that the map $\Gamma^{i-1} : H_1(C_\bullet \mathcal{F}_{n-1}^{i-1}) \to \bigoplus_{v \in N_\mathcal{V}} C_n(\mathcal{R}_v^{i-1})$ has been defined such that for every $\{\langle b^* \rangle\} \in \mathcal{B}^{i-1}$, we have

$$\partial \Gamma^{i-1}\{\langle b^* \rangle\} = e_{n-1}^{i-1} b^*. \tag{4.35}$$

- **Step 1.** We first fix a basis $\mathcal{C}^i$ of $H_1(C_\bullet \mathcal{F}_{n-1}^i)$. By assumption, the basis $\mathcal{B}^{i-1}$ of $H_1(C_\bullet \mathcal{F}_{n-1}^{i-1})$ has the form $\mathcal{B}^{i-1} = \mathcal{B}_A^{i-1} \cup \mathcal{B}_{\ker}^{i-1}$. Without loss of generality, assume that

  $$\mathcal{B}_A^{i-1} = \{\, \{\langle b_1^* \rangle\}, \ldots, \{\langle b_t^* \rangle\} \,\}.$$

  One can show that $\{\langle \kappa_{n-1}^{i-1} b_1^* \rangle\}, \ldots, \{\langle \kappa_{n-1}^{i-1} b_t^* \rangle\}$ are linearly independent in $H_1(C_\bullet \mathcal{F}_{n-1}^i)$ (Appendix B.3). Let

  $$\mathcal{C}_{\mathrm{im}}^i = \{\, \{\langle \kappa_{n-1}^{i-1} b_1^* \rangle\}, \ldots, \{\langle \kappa_{n-1}^{i-1} b_t^* \rangle\} \,\}.$$

Extend $\mathcal{C}^i_{\text{im}}$ to a basis $\mathcal{C}^i$ of $H_1(C_\bullet \mathcal{F}^i_{n-1})$. Let $\mathcal{C}^i_D$ denote the basis vectors of $\mathcal{C}^i$ that are not in $\mathcal{C}^i_{\text{im}}$, i.e.,

$$\mathcal{C}^i = \mathcal{C}^i_{\text{im}} \cup \mathcal{C}^i_D. \tag{4.36}$$

For each $\{\langle c \rangle\} \in \mathcal{C}^i$, fix a coset representative c^* of $\langle c \rangle$ as the following. If $\{\langle c \rangle\} \in \mathcal{C}^i_{\text{im}}$ such that $\{\langle c \rangle\} = \{\langle \kappa^{i-1}_{n-1} b^*_s \rangle\}$, then let $c^* = \kappa^{i-1}_{n-1} b^*_s$ be the coset representative of $\langle c \rangle$. If $\{\langle c \rangle\} \in \mathcal{C}^i_D$, fix any coset representative c^* of $\langle c \rangle$.

- **Step 2.** We will now define $\Gamma^i : H_1(C_\bullet \mathcal{F}^i_{n-1}) \to \bigoplus_{v \in N_\mathcal{V}} C_n(\mathcal{R}^i_v)$ on the basis $\mathcal{C}^i$. Given a basis vector $\{\langle c^* \rangle\} \in \mathcal{C}^i$, we know from Equation 4.23 that there exists some $\beta^i \in \bigoplus_{v \in N_\mathcal{V}} C_n(\mathcal{R}^i_v)$ such that

$$\partial \beta^i = e^i_{n-1} c^*. \tag{4.37}$$

If $\{\langle c^* \rangle\} = \{\langle \kappa^{i-1}_{n-1} b^* \rangle\} \in \mathcal{C}^i_{\text{im}}$, then by Equation 4.35 and commutativity of Diagram 4.30, one can check that $\iota^{i-1}_n \Gamma^{i-1}\{\langle b^* \rangle\}$ is a candidate for β^i that satisfies Equation 4.37. Define Γ^i on each $\{\langle c^* \rangle\} \in \mathcal{C}^i$ by

$$\Gamma^i\{\langle c^* \rangle\} = \begin{cases} \iota^{i-1}_n \Gamma^{i-1}\{\langle b^* \rangle\} & \text{if } \{\langle c^* \rangle\} = \{\langle \kappa^{i-1}_{n-1} b^* \rangle\} \in \mathcal{C}^i_{\text{im}} \\ \beta^i & \text{if } \{\langle c^* \rangle\} \in \mathcal{C}^i_D \end{cases} \tag{4.38}$$

where $\beta^i \in \bigoplus_{v \in N_\mathcal{V}} C_n(\mathcal{R}^i_v)$ is any element satisfying Equation 4.37. Note that by construction, for each $\{\langle c^* \rangle\} \in \mathcal{C}^i$, we defined $\Gamma^i c^*$ such that

$$\partial \Gamma^i\{\langle c^* \rangle\} = e^i_{n-1} c^*. \tag{4.39}$$

Extend the map Γ^i linearly to the vector space $H_1(C_\bullet \mathcal{F}^i_{n-1})$.

- **Step 3.** Recall from Equation 4.25 the decomposition

$$H_1(C_\bullet \mathcal{F}^i_{n-1}) = A^i \oplus \ker H_1(\phi^i_{n-1}).$$

Let $\mathcal{B}^i_A$ be a basis of A^i, and let $\mathcal{B}^i_{\ker}$ be a basis of $\ker H_1(\phi^i_{n-1})$. Then,

$$\mathcal{B}^i = \mathcal{B}^i_A \cup \mathcal{B}^i_{\ker}$$

is a basis of $H_1(C_\bullet \mathcal{F}^i_{n-1})$. Each basis vector $\{\langle b \rangle\} \in \mathcal{B}^i$ can be written as a linear combination of basis $\mathcal{C}^i = \{\, \{\langle c^*_1 \rangle\}, \ldots, \{\langle c^*_l \rangle\} \,\}$ as

$$\{\langle b \rangle\} = d_1\{\langle c^*_1 \rangle\} + \cdots + d_l\{\langle c^*_l \rangle\}.$$

Then, let

$$b^* = d_1 c^*_1 + \cdots + d_l c^*_l \tag{4.40}$$

be the coset representative of $\langle b \rangle$. We can express the basis $\mathcal{B}^i$ of $H_1(C_\bullet \mathcal{F}^i_{n-1})$ as

$$\mathcal{B}^i = \{\, \{\langle b^*_1 \rangle\}, \ldots, \{\langle b^*_k \rangle\} \,\}. \tag{4.41}$$

Note that by construction, for any basis vector $\{\langle b^* \rangle\} \in \mathcal{B}^i$, we have

$$\Gamma^i\{\langle b^* \rangle\} = d_1 \Gamma^i\{\langle c^*_1 \rangle\} + \cdots + d_l \Gamma^i\{\langle c^*_l \rangle\}$$

and

$$\partial \Gamma^i\{\langle b^* \rangle\} = e^i_{n-1} b^*,$$

which is a condition we need to pass on to the next inductive step.

- **Step 4.** We now define $\psi^i : H_1(C_\bullet \mathcal{F}^i_{n-1}) \to H_0(C_\bullet \mathcal{F}^{i+1}_n)$ by defining ψ^i on the basis $\mathcal{B}^i$ and extending the map linearly. If $\{\langle b^* \rangle\} \in \mathcal{B}^i_{\ker}$, recall from Equation 4.22 that there exists some $\alpha^{i+1} \in \bigoplus_{e \in N_\mathcal{V}} C_n(\mathcal{R}^{i+1}_e)$ such that

$$\partial \alpha^{i+1} = \kappa^i_{n-1} b^*. \tag{4.42}$$

Define ψ^i on each $\{\langle b^* \rangle\} \in \mathcal{B}^i$ by

$$\psi^i\{\langle b^*\rangle\} = \begin{cases} \{\langle -e^i_n \alpha^{i+1} + \iota^{i-1}_n \circ \Gamma^i\{\langle b^* \rangle\} \rangle\} & \text{if } \{\langle b^*\rangle\} \in \mathcal{B}^i_{\text{ker}} \\ 0 & \text{if } \{\langle b^*\rangle\} \in \mathcal{B}^i_A \end{cases}, \tag{4.43}$$

where $\alpha^{i+1} \in \bigoplus_{e \in N_\mathcal{V}} C_n(\mathcal{R}^{i+1}_e)$ is any element satisfying Equation 4.42 and Γ^i is the map defined in Equation 4.38. Define the linear map ψ^i by extending the above to the vector space $H_1(C_\bullet \mathcal{F}^i_{n-1})$ by

$$\psi^i(a_1\{\langle b_1^*\rangle\} + \cdots + a_l\{\langle b_l^*\rangle\}) = a_1\psi^i\{\langle b_1^*\rangle\} + \cdots + a_l\psi^i\{\langle b_l^*\rangle\}. \tag{4.44}$$

One can check that ψ^i is well-defined (Appendix B.2).

Once we define the maps $\psi^i : H_1(C_\bullet \mathcal{F}^i_{n-1}) \to H_0(C_\bullet \mathcal{F}^{i+1}_n)$ inductively, we can define

$$\Psi^i : H_0(C_\bullet \mathcal{F}^i_n) \oplus H_1(C_\bullet \mathcal{F}^i_{n-1}) \to H_0(C_\bullet \mathcal{F}^{i+1}_n) \oplus H_1(C_\bullet \mathcal{F}^{i+1}_{n-1})$$

by

$$\Psi^i(\{\langle x\rangle\}, \{\langle y \rangle\}) = (\, H_0(\phi^i_n)\{\langle x\rangle\} + (-1)^{n+1}\psi^i\{\langle y\rangle\}\,,\, H_1(\phi^i_{n-1})\{\langle y\rangle\}\,), \tag{4.45}$$

where $H_0(\phi^i_n)$ and $H_1(\phi^i_{n-1})$ are the maps defined in Equation 4.16.

Let $\mathbb{V}_\Psi$ denote the persistence module

$$\mathbb{V}_\Psi : H_0(C_\bullet \mathcal{F}^1_n) \oplus H_1(C_\bullet \mathcal{F}^1_{n-1}) \xrightarrow{\Psi^1} \cdots \xrightarrow{\Psi^{N-1}} H_0(C_\bullet \mathcal{F}^N_n) \oplus H_1(C_\bullet \mathcal{F}^N_{n-1}). \tag{4.46}$$

4.2.4 Isomorphism of persistence modules

We show that the persistence module $\mathbb{V}_\Psi$ constructed in Equation 4.46 is isomorphic to the persistence module

$$\mathbb{V} : H_n(\mathcal{R}^1) \xrightarrow{\iota^1_*} \cdots \xrightarrow{\iota^{N-1}_*} H_n(\mathcal{R}^N.)$$

To show that the persistence module $\mathbb{V}_\Psi$ is isomorphic to $\mathbb{V}$, we will show that both $\mathbb{V}_\Psi$ and $\mathbb{V}$ are isomorphic to a third persistence module

$$\mathbb{V}_{\text{Tot}} : H_n(\text{Tot}^1) \xrightarrow{\iota^1_{\text{Tot}}} H_n(\text{Tot}^2) \xrightarrow{\iota^2_{\text{Tot}}} \cdots \xrightarrow{\iota^{N-1}_{\text{Tot}}} H_n(\text{Tot}^N),$$

where each $H_n(\text{Tot}^i)$ is the homology of the double complex from Diagram 4.3 for parameter ϵ_i, and ι^i_{Tot} is the morphism induced by maps of double complexes. We will first show that $\mathbb{V}_{\text{Tot}}$ is isomorphic to the persistence module $\mathbb{V}$. This first step corresponds to constructing an isomorphism Φ^i_{Tot} for each ϵ_i that make the right half of Diagram 4.47 commute (Theorem 9). We will then show that $\mathbb{V}_\Psi$ is isomorphic to $\mathbb{V}_{\text{Tot}}$, by constructing maps Φ^i that make the left half of Diagram 4.47 commute (Theorem 10).

$$\begin{tikzcd}
H_0(C_\bullet\mathcal{F}^1_n) \oplus H_1(C_\bullet\mathcal{F}^1_{n-1}) \arrow[r, "\Phi^1"] \arrow[d, "\Psi^1"] & H_n(\text{Tot}^1) \arrow[r, "\Phi^1_{\text{Tot}}"] \arrow[d, "\iota^1_{\text{Tot}}"] & H_n(\mathcal{R}^1) \arrow[d, "\iota^1_*"] \\
H_0(C_\bullet\mathcal{F}^2_n) \oplus H_1(C_\bullet\mathcal{F}^2_{n-1}) \arrow[r, "\Phi^2"] \arrow[d, "\Psi^2"] & H_n(\text{Tot}^2) \arrow[r, "\Phi^2_{\text{Tot}}"] \arrow[d, "\iota^2_{\text{Tot}}"] & H_n(\mathcal{R}^2) \arrow[d, "\iota^2_*"] \\
\vdots \arrow[d, "\Psi^{N-1}"] & \vdots \arrow[d, "\iota^{N-1}_{\text{Tot}}"] & \vdots \arrow[d, "\iota^{N-1}_*"] \\
H_0(C_\bullet\mathcal{F}^N_n) \oplus H_1(C_\bullet\mathcal{F}^N_{n-1}) \arrow[r, "\Phi^N"] & H_n(\text{Tot}^N) \arrow[r, "\Phi^N_{\text{Tot}}"] & H_n(\mathcal{R}^N)
\end{tikzcd} \tag{4.47}$$

Before we proceed with the proof, we provide a summary of the construction of the homology of a double complex. For a fixed ϵ_i parameter, consider the 0^{th} page of the spectral sequence in Diagram 4.48.

$$
\begin{array}{ccc}
\vdots & & \vdots \\
\downarrow{\scriptstyle \partial} & & \downarrow{\scriptstyle \partial} \\
\bigoplus\limits_{v \in N_{\mathcal{V}}} C_2(\mathcal{R}_v^i) & \xleftarrow[e_2^i]{} & \bigoplus\limits_{e \in N_{\mathcal{V}}} C_2(\mathcal{R}_e^i) \\
\downarrow{\scriptstyle \partial} & & \downarrow{\scriptstyle \partial} \\
\bigoplus\limits_{v \in N_{\mathcal{V}}} C_1(\mathcal{R}_v^i) & \xleftarrow[e_1^i]{} & \bigoplus\limits_{e \in N_{\mathcal{V}}} C_1(\mathcal{R}_e^i) \\
\downarrow{\scriptstyle \partial} & & \downarrow{\scriptstyle \partial} \\
\bigoplus\limits_{v \in N_{\mathcal{V}}} C_0(\mathcal{R}_v^i) & \xleftarrow[e_0^i]{} & \bigoplus\limits_{e \in N_{\mathcal{V}}} C_0(\mathcal{R}_e^i)
\end{array}
\tag{4.48}
$$

Let

$$C_n^{\bullet,\bullet} = \bigoplus_{v \in N_{\mathcal{V}}} C_n(\mathcal{R}_v^i) \oplus \bigoplus_{e \in N_{\mathcal{V}}} C_{n-1}(\mathcal{R}_e^i),$$

and let $D_n : C_n^{\bullet,\bullet} \to C_{n-1}^{\bullet,\bullet}$ be defined by

$$D_n = \partial + (-1)^n e_{n-1}^i.$$

One can check that $D_{n-1} \circ D_n = 0$, and hence obtain the following chain complex, called total complex.

$$\mathrm{Tot}_\bullet^i : \qquad \cdots \xrightarrow{D_3} C_2^{\bullet,\bullet} \xrightarrow{D_2} C_1^{\bullet,\bullet} \xrightarrow{D_1} C_0^{\bullet,\bullet} \xrightarrow{D_0} 0$$

Let $H_n(\mathrm{Tot}^i)$ denote the homology of the total complex. Note that a coset of $H_n(\mathrm{Tot}^i)$ is represented by $[a, b]$, where $a \in \bigoplus\limits_{v \in N_{\mathcal{V}}} C_n(\mathcal{R}_v^i)$, $b \in \bigoplus\limits_{e \in N_{\mathcal{V}}} C_{n-1}(\mathcal{R}_e^i)$, $\partial b = 0$ and $\partial a = (-1)^{n-1} e_{n-1}^i b$.

A coset $[a, b]$ is trivial in $H_n(\mathrm{Tot}^i)$ if there exist $p_{n+1} \in \bigoplus\limits_{v \in N_{\mathcal{V}}} C_{n+1}(\mathcal{R}_v^i)$ and $q_n \in \bigoplus\limits_{e \in N_{\mathcal{V}}} C_n(\mathcal{R}_e^i)$ such that $\partial q_n = b$ and $\partial p_{n+1} + (-1)^{n+1} e_n^i(q_n) = a$.

Given increasing parameter values $(\epsilon_i)_{i=1}^N$, one can construct Diagram 4.48 for each parameter ϵ_i. There exists an inclusion map from double complex associated with parameter ϵ_i to that of parameter ϵ_{i+1}, as illustrated in Diagram 4.50. Each horizontal face of Diagram 4.50 corresponds to a double complex for a parameter ϵ_i. The vertical maps ι_n^i's and κ_n^i's constitute the inclusion maps of double complexes. Such inclusion of double complexes induces morphisms on the corresponding total complexes $\text{Tot}_\bullet^i \to \text{Tot}_\bullet^{i+1}$, which induces morphism $\iota_{\text{Tot}}^i : H_n(\text{Tot}^i) \to H_n(\text{Tot}^{i+1})$. The morphism ι_{Tot}^i can be written explicitly as

$$\iota_{\text{Tot}}([a, b]) = [\iota_n^i(a), \kappa_{n-1}^i(b)]. \tag{4.49}$$

$$\begin{tikzcd}
 & \bigoplus\limits_{v \in N_{\mathcal{V}}} C_n(\mathcal{R}_v^1) \arrow[dl, "\partial"] \arrow[dd, "\iota_n^1"] & & \bigoplus\limits_{e \in N_{\mathcal{V}}} C_n(\mathcal{R}_e^1) \arrow[ll, "e_n^1"'] \arrow[dl, "\partial"] \arrow[dd, "\kappa_n^1"] \\
\bigoplus\limits_{v \in N_{\mathcal{V}}} C_{n-1}(\mathcal{R}_v^1) \arrow[dd, "\iota_{n-1}^1"] & & \bigoplus\limits_{e \in N_{\mathcal{V}}} C_{n-1}(\mathcal{R}_e^1) \arrow[ll, "e_{n-1}^1"'] \arrow[dd, "\kappa_{n-1}^1"] & \\
 & \bigoplus\limits_{v \in N_{\mathcal{V}}} C_n(\mathcal{R}_v^2) \arrow[dl, "\partial"] \arrow[dd, "\iota_n^2"] & & \bigoplus\limits_{e \in N_{\mathcal{V}}} C_n(\mathcal{R}_e^2) \arrow[ll, "e_n^2"'] \arrow[dl, "\partial"] \arrow[dd, "\kappa_n^2"] \\
\bigoplus\limits_{v \in N_{\mathcal{V}}} C_{n-1}(\mathcal{R}_v^2) \arrow[dd, "\iota_{n-1}^2"] & & \bigoplus\limits_{e \in N_{\mathcal{V}}} C_{n-1}(\mathcal{R}_e^2) \arrow[ll, "e_{n-1}^2"'] \arrow[dd, "\kappa_{n-1}^2"] & \\
 & \bigoplus\limits_{v \in N_{\mathcal{V}}} C_n(\mathcal{R}_v^3) \arrow[dl, "\partial"] \arrow[d, "\iota_n^3"] & & \bigoplus\limits_{e \in N_{\mathcal{V}}} C_n(\mathcal{R}_e^3) \arrow[ll, "e_n^3"'] \arrow[dl, "\partial"] \arrow[d, "\kappa_n^3"] \\
\bigoplus\limits_{v \in N_{\mathcal{V}}} C_{n-1}(\mathcal{R}_v^3) \arrow[d, "\iota_{n-1}^3"] & \vdots & \bigoplus\limits_{e \in N_{\mathcal{V}}} C_{n-1}(\mathcal{R}_e^3) \arrow[ll, "e_{n-1}^3"'] \arrow[d, "\kappa_{n-1}^3"] & \vdots \\
\vdots & & \vdots &
\end{tikzcd} \tag{4.50}$$

We first show that the right half of Diagram 4.47 commutes.

Theorem 9. *There exist isomorphisms $\Psi^i_{\text{Tot}} : H_n(\text{Tot}^i) \to H_n(\mathcal{R}^i)$ such that the following diagram commutes.*

$$\begin{tikzcd}
H_n(\text{Tot}^1) \arrow[r, "\Psi^1_{\text{Tot}}"] \arrow[d, "\iota^1_{\text{Tot}}"] & H_n(\mathcal{R}^1) \arrow[d, "\iota^1_*"] \\
H_n(\text{Tot}^2) \arrow[r, "\Psi^2_{\text{Tot}}"] \arrow[d, "\iota^2_{\text{Tot}}"] & H_n(\mathcal{R}^2) \arrow[d, "\iota^2_*"] \\
\vdots \arrow[d, "\iota^{N-1}_{\text{Tot}}"] & \vdots \arrow[d, "\iota^{N-1}_*"] \\
H_n(\text{Tot}^N) \arrow[r, "\Psi^N_{\text{Tot}}"] & H_n(\mathcal{R}^N)
\end{tikzcd} \tag{4.51}$$

Proof. We first define isomorphisms $\Psi^i_{\text{Tot}} : H_n(\text{Tot}^i) \to H_n(\mathcal{R}^i)$. For each parameter ϵ_i, let $j^i_n : \bigoplus_{v \in N_\mathcal{V}} C_n(\mathcal{R}^i_v) \to C_n(\mathcal{R}^i)$ be a collection of inclusion maps. Define Ψ^i_{Tot} by

$$\Psi^i_{\text{Tot}}([x, y]) = [j^i_n(x)]. \tag{4.52}$$

One can check that Ψ^i_{Tot} is well-defined and bijective (Appendix B.4).

We now show that Diagram 4.51 commutes. Given $[x, y] \in H_n(\text{Tot}^i)$, we have

$$\iota^i_* \circ \Psi^i_{\text{Tot}}[x, y] = \iota^i_*[j^i_n(x)] = [\iota^i \circ j^i_n(x)],$$

and

$$\Psi^{i+1}_{\text{Tot}} \circ \iota^i_{\text{Tot}}[x, y] = \Psi^{i+1}_{\text{Tot}}[\iota^i_n(x), \kappa^i_{n-1}(y)] = [j^{i+1}_n \circ \iota^i_n(x)].$$

The following diagram commutes because all the maps involved are inclusion maps.

$$\begin{tikzcd}
\bigoplus_{v \in N_\mathcal{V}} C_n(\mathcal{R}^i_v) \arrow[r, "j^i_n"] \arrow[d, "\iota^i_n"] & C_n(\mathcal{R}^i) \arrow[d, "\iota^i"] \\
\bigoplus_{v \in N_\mathcal{V}} C_n(\mathcal{R}^{i+1}_v) \arrow[r, "j^{i+1}_n"] & C_n(\mathcal{R}^{i+1})
\end{tikzcd}$$

So we know that $\iota^i_* \circ \Psi^i_{\text{Tot}} = \Psi^{i+1}_{\text{Tot}} \circ \iota^i_{\text{Tot}}$. Thus, Diagram 4.51 commutes. $\square$

We now show that the left half of Diagram 4.47 commutes.

Theorem 10. *There exists an isomorphism $\Phi^i : H_0(C_\bullet \mathcal{F}^i_n) \oplus H_1(C_\bullet \mathcal{F}^i_{n-1}) \to H_n(\mathrm{Tot}^i)$ for every parameter ϵ_i such that the following diagram commutes.*

$$
\begin{tikzcd}
H_0(C_\bullet \mathcal{F}^1_n) \oplus H_1(C_\bullet \mathcal{F}^1_{n-1}) \arrow[r, "\Phi^1"] \arrow[d, "\Psi^1"] & H_n(\mathrm{Tot}^1) \arrow[d, "\iota^1_{\mathrm{Tot}}"] \\
H_0(C_\bullet \mathcal{F}^2_n) \oplus H_1(C_\bullet \mathcal{F}^2_{n-1}) \arrow[r, "\Phi^2"] \arrow[d, "\Psi^2"] & H_n(\mathrm{Tot}^2) \arrow[d, "\iota^2_{\mathrm{Tot}}"] \\
\vdots \arrow[d, "\Psi^{N-1}"] & \vdots \arrow[d, "\iota^{N-1}_{Tot}"] \\
H_0(C_\bullet \mathcal{F}^N_n) \oplus H_1(C_\bullet \mathcal{F}^N_{n-1}) \arrow[r, "\Phi^N"] & H_n(\mathrm{Tot}^N)
\end{tikzcd}
\tag{4.53}
$$

Proof. Note that Lemma 12 already tells us that there exists an isomorphism between $H_0(C_\bullet \mathcal{F}^i_n) \oplus H_1(C_\bullet \mathcal{F}^i_{n-1})$ and $H_n(\mathrm{Tot}^i)$ for parameter $\epsilon_i < K$. For clarity, we will define isomorphisms $\Phi^i : H_0(C_\bullet \mathcal{F}^i_n) \oplus H_1(C_\bullet \mathcal{F}^i_{n-1}) \to H_n(\mathrm{Tot}^i)$ explicitly on vectors of $H_0(C_\bullet \mathcal{F}^i_n)$ and $H_1(C_\bullet \mathcal{F}^i_{n-1})$.

For $\{\langle x \rangle\} \in H_0(C_\bullet \mathcal{F}^i_n)$, let

$$\Phi^i(\{\langle x \rangle\}, 0) = [x, 0]. \tag{4.54}$$

To define the map Φ^i on $H_1(C_\bullet \mathcal{F}^i_{n-1})$, recall the basis $\mathcal{B}^i$ of $H_1(C_\bullet \mathcal{F}^i_{n-1})$ from Equation 4.41. We will define Φ^i on each basis $\mathcal{B}^i$ as the following. Given $\{\langle b^* \rangle\} \in \mathcal{B}^i$, let

$$\Phi^i(0, \{\langle b^* \rangle\}) = [(-1)^{n+1}\Gamma^i\{\langle b^* \rangle\}, b^*], \tag{4.55}$$

where Γ^i is the map defined in Equation 4.38. Extend this map linearly to $H_1(C_\bullet \mathcal{F}^i_{n-1})$.

Note that given $(\{\langle x \rangle\}, \{\langle y \rangle\}) \in H_0(C_\bullet \mathcal{F}^i_n) \oplus H_1(C_\bullet \mathcal{F}^i_{n-1})$, the map Φ^i is

$$\Phi^i(\{\langle x \rangle\}, \{\langle y \rangle\}) = \Phi^i(\{\langle x \rangle\}, 0) + \Phi^i(0, \{\langle y \rangle\}).$$

One can check that Φ^i is well-defined and bijective (Appendix B.5).

We now show that Diagram 4.53 commutes. It suffices to show that each square of Diagram 4.53 commutes.

$$\begin{array}{ccc} H_0(C_\bullet \mathcal{F}_n^i) \oplus H_1(C_\bullet \mathcal{F}_{n-1}^i) & \xrightarrow{\Phi^i} & H_n(\mathrm{Tot}^i) \\ \downarrow{\Psi^i} & & \downarrow{\iota_{\mathrm{Tot}}^i} \\ H_0(C_\bullet \mathcal{F}_n^{i+1}) \oplus H_1(C_\bullet \mathcal{F}_{n-1}^{i+1}) & \xrightarrow{\Phi^{i+1}} & H_n(\mathrm{Tot}^{i+1}) \end{array} \tag{4.56}$$

We will show that the above diagram commutes for each vector of $H_0(C_\bullet \mathcal{F}_n^i)$ and $H_1(C_\bullet \mathcal{F}_{n-1}^i)$.

Case 1: Given $\{\langle x \rangle\} \in H_0(C_\bullet \mathcal{F}_n^i)$, we know that

$$\iota_{\mathrm{Tot}}^i \circ \Phi^i(\{\langle x \rangle\}, 0) = \iota_{\mathrm{Tot}}^i([x, 0]) = [\iota_n^i x, 0].$$

On the other hand, note that $\{\langle \iota_n^i x \rangle\} \in H_0(C_\bullet \mathcal{F}_n^{i+1})$, and

$$\Phi^{i+1} \circ \Psi^i(\{\langle x \rangle\}, 0) = \Phi^{i+1}(\{\langle \iota_n^i x \rangle\}, 0) = [\iota_n^i x, 0].$$

Thus, the diagram commutes for every $\{\langle x \rangle\} \in H_0(C_\bullet \mathcal{F}_n^i)$.

Case 2: To show that the diagram commutes for every vector in $H_1(C_\bullet \mathcal{F}_{n-1}^i)$, it suffices to show that the diagram commutes for the basis $\mathcal{B}^i$ of $H_1(C_\bullet \mathcal{F}_{n-1}^i)$ from Equation 4.41. We consider two cases separately: the first, if $\{\langle b^* \rangle\} \in \mathcal{B}_{\ker}^i$, and the second, if $\{\langle b^* \rangle\} \in \mathcal{B}_A^i$.

Case 2A: Assume $\{\langle b^* \rangle\} \in \mathcal{B}_{\ker}^i$. We know that

$$\iota_{\mathrm{Tot}}^i \circ \Phi^i(0, \{\langle b^* \rangle\}) = \iota_{\mathrm{Tot}}^i([(-1)^{n+1}\Gamma^i\{\langle b^* \rangle\}, b^*]) = [(-1)^{n+1}\iota_n^i \circ \Gamma^i\{\langle b^* \rangle\}, \kappa_{n-1}^i(b^*)].$$

On the other hand,

$$\begin{aligned}\Phi^{i+1} \circ \Psi^{i}(0, \{\langle b^* \rangle\}) &= \Phi^{i+1}((-1)^{n+1}\psi^{i}\{\langle b^* \rangle\}, \{\langle \kappa^{i}_{n-1} b^* \rangle\}) \\ &= \Phi^{i+1}((-1)^{n+1}\{\langle -e^{i+1}_{n}\alpha^{i+1} + \iota^{i}_{n} \circ \Gamma^{i}\{\langle b^* \rangle\}\rangle\}, 0) \\ &= [-(-1)^{n+1}e^{i+1}_{n}\alpha^{i+1} + (-1)^{n+1}\iota^{i}_{n} \circ \Gamma^{i}\{\langle b^* \rangle\}, 0]\end{aligned}$$

Then,

$$\iota^{i}_{\text{Tot}} \circ \Phi^{i}(0, \{\langle b^* \rangle\}) - \Phi^{i+1} \circ \Psi^{i}(0, \{\langle b^* \rangle\}) = [(-1)^{n+1}e^{i+1}_{n}\alpha^{i+1}, \kappa^{i}_{n-1}b^*].$$

Recall from Equation 4.43 that $\alpha^{i+1} \in \bigoplus_{e \in N_{\mathcal{V}}} C_n(\mathcal{R}^{i+1}_{e})$ satisfies $\kappa^{i}_{n-1}b^* = \partial\alpha^{i+1}$. Thus, $\iota^{i}_{\text{Tot}} \circ \Phi^{i}(0, \{\langle b^* \rangle\}) - \Phi^{i+1} \circ \Psi^{i}(0, \{\langle b^* \rangle\}) = 0$, and the diagram commutes for basis vectors $\{\langle b^* \rangle\} \in \mathcal{B}^{i}_{\text{ker}}$.

Case 2B: If $\{\langle b^* \rangle\} \in \mathcal{B}^{i}_{A}$, then again,

$$\iota^{i}_{\text{Tot}} \circ \Phi^{i}(0, \{\langle b^* \rangle\}) = \iota^{i}_{\text{Tot}}([(-1)^{n+1}\Gamma^{i}\{\langle b^* \rangle\}, b^*]) = [(-1)^{n+1}\iota^{i}_{n} \circ \Gamma^{i}\{\langle b^* \rangle\}, \kappa^{i}_{n-1}b^*].$$

On the other hand,

$$\begin{aligned}\Phi^{i+1} \circ \Psi^{i}(0, \{\langle b^* \rangle\}) &= \Phi^{i+1}(\psi^{i}\{\langle b^* \rangle\}, \{\langle \kappa^{i}_{n-1} b^* \rangle\}) \\ &= \Phi^{i+1}(0, \{\langle \kappa^{i}_{n-1} b^* \rangle\}) \\ &= [(-1)^{n+1}\Gamma^{i+1}\{\langle \kappa^{i}_{n-1} b^* \rangle\}, \kappa^{i}_{n-1}b^*] \\ &= [(-1)^{n+1}\iota^{i}_{n} \circ \Gamma^{i}\{\langle b^* \rangle\}, \kappa^{i}_{n-1}b^*].\end{aligned}$$

The third equality follows from the fact that Γ^{i+1} was defined in Equation 4.38 such that $\Gamma^{i+1}\{\langle \kappa^{i}_{n-1}b^* \rangle\} = \iota^{i}_{n}\Gamma^{i}\{\langle b^* \rangle\}$. Thus, the diagram commutes for basis vectors $\{\langle b^* \rangle\} \in \mathcal{B}^{i}_{A}$.

Thus, Diagram 4.53 commutes. □

The following immediate corollary tells us that the persistence module

$$\mathbb{V}_\Psi : H_0(C_\bullet\mathcal{F}_n^1) \oplus H_1(C_\bullet\mathcal{F}_{n-1}^1) \xrightarrow{\Psi^1} \cdots \xrightarrow{\Psi^{N-1}} H_0(C_\bullet\mathcal{F}_n^N) \oplus H_1(C_\bullet\mathcal{F}_{n-1}^N)$$

constructed via distributed computation is isomorphic to the persistence module

$$\mathbb{V} : H_n(\mathcal{R}^1) \xrightarrow{\iota_*^1} \cdots \xrightarrow{\iota_*^{N-1}} H_n(\mathcal{R}^N.)$$

Hence, $barcode(\mathbb{V}_\Psi) = barcode(\mathbb{V})$.

Corollary 2. *The maps Φ^i and Φ^i_{Tot} are isomorphisms that make the Diagram 4.47 commute.*

In §4.2.2, we defined the map $\psi^i : H_1(C_\bullet\mathcal{F}_{n-1}^i) \to H_0(C_\bullet\mathcal{F}_n^{i+1})$ in Equation 4.27 by extending a map δ^i constructed in Equation 4.24. In §4.2.3, we redefined the map $\psi^i : H_1(C_\bullet\mathcal{F}_{n-1}^i) \to H_0(C_\bullet\mathcal{F}_n^{i+1})$ explicitly on a basis $\mathcal{B}^i$ of $H_1(C_\bullet\mathcal{F}_{n-1}^i)$ in Equation 4.43. One might wonder why it was necessary for us to reconstruct the map ψ^i explicitly when we already had ψ^i defined in Equation 4.27.

To clarify the discussion, let

$$\psi^i : H_1(C_\bullet\mathcal{F}_{n-1}^i) \to H_0(C_\bullet\mathcal{F}_n^{i+1})$$

denote the map defined in Equation 4.27, and let

$$\psi^i_{\mathcal{B}} : H_1(C_\bullet\mathcal{F}_{n-1}^i) \to H_0(C_\bullet\mathcal{F}_n^{i+1})$$

denote the map constructed explicitly on a basis $\mathcal{B}^i$ in Equation 4.43. Let Ψ^i : $H_0(C_\bullet\mathcal{F}_n^i) \oplus H_1(C_\bullet\mathcal{F}_{n-1}^i) \to H_0(C_\bullet\mathcal{F}_n^{i+1}) \oplus H_1(C_\bullet\mathcal{F}_{n-1}^{i+1})$ be the map defined by

$$\Psi^i(\{\langle x\rangle\},\{\langle y\rangle\}) = (H_0(\phi_n^i)\{\langle x\rangle\} + (-1)^{n+1}\psi^i\{\langle y\rangle\}, H_1(\phi_{n-1}^i)\{\langle y\rangle\}), \tag{4.57}$$

and let $\Psi^i_{\mathcal{B}} : H_0(C_\bullet \mathcal{F}^i_n) \oplus H_1(C_\bullet \mathcal{F}^i_{n-1}) \to H_0(C_\bullet \mathcal{F}^{i+1}_n) \oplus H_1(C_\bullet \mathcal{F}^{i+1}_{n-1})$ be the map defined by

$$\Psi^i_{\mathcal{B}}(\{\langle x\rangle\}, \{\langle y\rangle\}) = (H_0(\phi^i_n)\{\langle x\rangle\} + (-1)^{n+1}\psi^i_{\mathcal{B}}\{\langle y\rangle\}, H_1(\phi^i_{n-1})\{\langle y\rangle\}). \tag{4.58}$$

When given just two parameters, say ϵ_i and ϵ_{i+1}, then the two maps Ψ^i and $\Psi^i_{\mathcal{B}}$ both define persistence modules

$$\begin{aligned}
\mathbb{V}_\Psi &: H_0(C_\bullet \mathcal{F}^i_n) \oplus H_1(C_\bullet \mathcal{F}^i_{n-1}) \xrightarrow{\Psi^i} H_0(C_\bullet \mathcal{F}^{i+1}_n) \oplus H_1(C_\bullet \mathcal{F}^{i+1}_{n-1}),\\
\mathbb{V}^{\mathcal{B}}_\Psi &: H_0(C_\bullet \mathcal{F}^i_n) \oplus H_1(C_\bullet \mathcal{F}^i_{n-1}) \xrightarrow{\Psi^i_{\mathcal{B}}} H_0(C_\bullet \mathcal{F}^{i+1}_n) \oplus H_1(C_\bullet \mathcal{F}^{i+1}_{n-1})
\end{aligned}$$

that are each isomorphic to the persistence module

$$\mathbb{V} : H_n(\mathcal{R}^i) \to H_n(\mathcal{R}^{i+1}).$$

However, given more than two parameters, the persistence module defined by the maps Ψ^i may not be isomorphic to the persistence module of interest. We provide an illustration of the disparity in the following example.

Example 15. Consider the following example point cloud P, a map $f : P \to \mathbb{R}$, and a cover $\mathcal{V}$ of $f(P)$ in Figure 4.10. The cover $\mathcal{V}$ consists of two intervals, V_B and V_R. Assume that we are given two parameters $\epsilon_1 < \epsilon_2$. The Rips complexes and the Rips systems

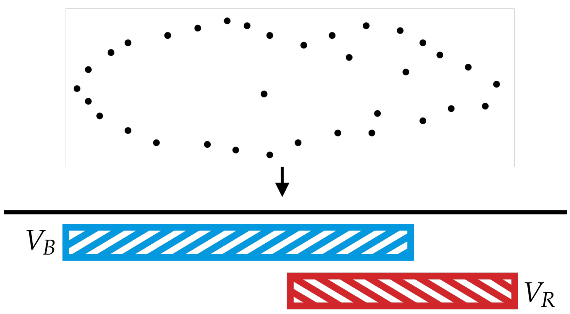

FIGURE 4.10: A point cloud P, map $f : P \to \mathbb{R}$, and a cover $\mathcal{V}$

for the two parameters are illustrated in Figure 4.11. The relevant cosheaf homologies

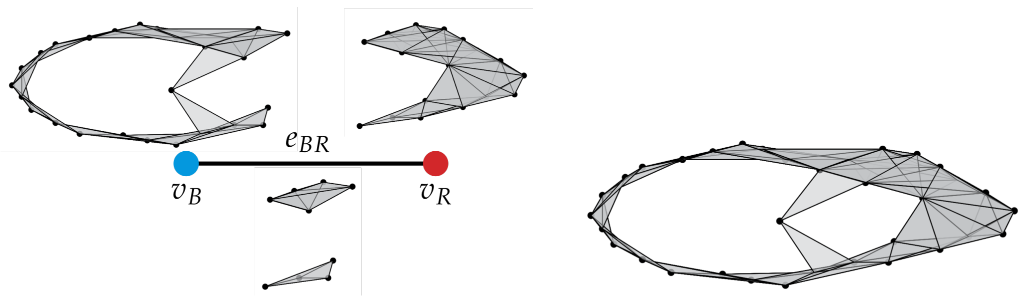

(A) Rips system for parameter ϵ_1 (B) Rips complex for parameter ϵ_1

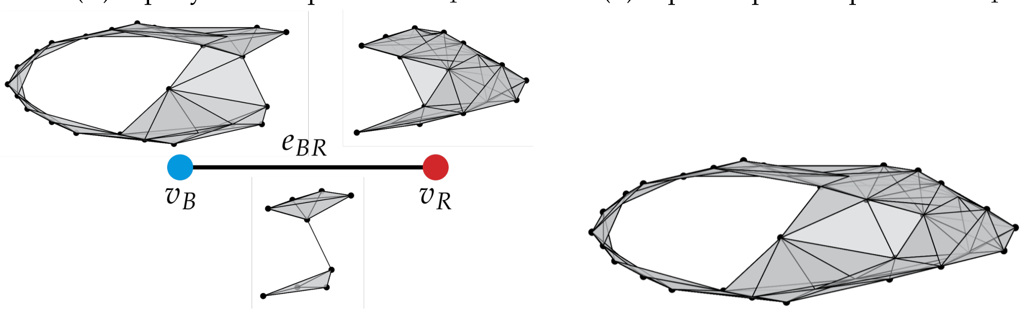

(C) Rips system for parameter ϵ_2 (D) Rips complex for parameter ϵ_2

FIGURE 4.11: Rips systems and Rips complexes for parameters ϵ_1 and ϵ_2

for computing $H_1(\mathcal{R}^i)$ are

$$H_0(C_\bullet \mathcal{F}_1^1) = \mathbb{K}, \quad H_1(C_\bullet \mathcal{F}_0^1) = \mathbb{K}$$
$$H_0(C_\bullet \mathcal{F}_1^2) = \mathbb{K}, \quad H_1(C_\bullet \mathcal{F}_0^2) = 0.$$

The map $H_0(\phi_1^1) : H_0(C_\bullet \mathcal{F}_1^1) \to H_0(C_\bullet \mathcal{F}_1^2)$ is the identity map, and the map $H_1(\phi_0^1) : H_1(C_\bullet \mathcal{F}_0^1) \to H_1(C_\bullet \mathcal{F}_0^2)$ is the trivial map. Then, we can construct a map $\delta^1 : \ker H_1(\phi_0^1) \to \operatorname{coker} H_0(\phi_1^1)$ as we have in Equation 4.24. Note that δ^1 is a trivial map since $\operatorname{coker} H_0(\phi_1^1)$ is trivial. Hence, when we extend δ^1 to ψ^1 as we have in Equation 4.27, we obtain a trivial map

$$\psi^1 : H_1(C_\bullet \mathcal{F}_0^1) \to H_0(C_\bullet \mathcal{F}_0^2).$$

When we define the map

$$\Psi^1 : H_0(C_\bullet \mathcal{F}_1^1) \oplus H_1(C_\bullet \mathcal{F}_0^1) \to H_0(C_\bullet \mathcal{F}_1^2) \oplus H_1(C_\bullet \mathcal{F}_0^2) \tag{4.59}$$

as in Equation 4.57, we obtain the following persistence module

$$\mathbb{V}_{\Psi^1} : \mathbb{K} \oplus \mathbb{K} \xrightarrow{\Psi^1} \mathbb{K},$$

where Ψ^1 can be expressed by the matrix

$$\begin{bmatrix} 1 & 0 \end{bmatrix}.$$

The persistence module $\mathbb{V}_{\Psi^1}$ is illustrated in Figure 4.12.

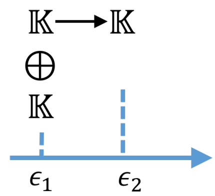

FIGURE 4.12: Persistence module Ψ^1

One can check that $\mathbb{V}_{\Psi^1}$ is isomorphic to the persistence module

$$\mathbb{V} : H_1(\mathcal{R}^1) \rightarrow H_1(\mathcal{R}^2).$$

The persistence module $\mathbb{V}$ is illustrated in Figure 4.13. The map between the left cycles represents the map $H_0(\phi_1^1) : H_0(C_\bullet\mathcal{F}_1^1) \rightarrow H_0(C_\bullet\mathcal{F}_1^2)$, and the map between the right cycles represents the map $H_1(\phi_0^1) : H_1(C_\bullet\mathcal{F}_0^1) \rightarrow H_1(C_\bullet\mathcal{F}_1^2)$. In particular, we can see that $H_1(C_\bullet\mathcal{F}_0^1)$ represents the right cycle in Figure 4.13.

Let's now consider what happens if we were given three parameters ϵ_0, ϵ_1, and ϵ_2. The Rips systems and the Rips complexes for the three parameters are illustrated in Figure 4.14.

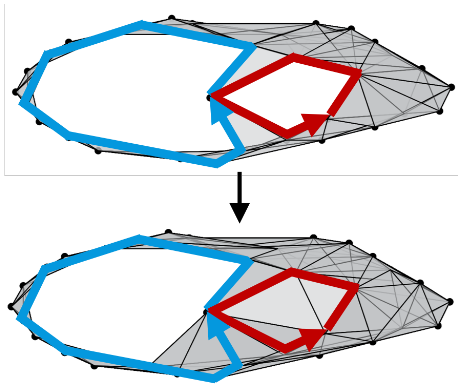

FIGURE 4.13: Rips complexes $\mathcal{R}^1 \hookrightarrow \mathcal{R}^2$

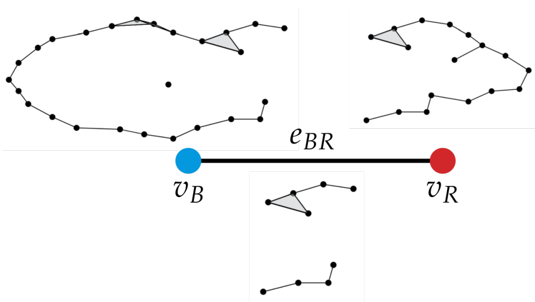

(A) Rips system for parameter ϵ_0

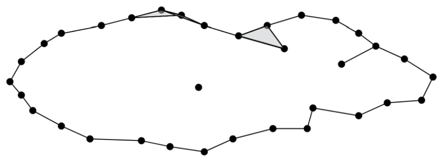

(B) Rips complex for parameter ϵ_0

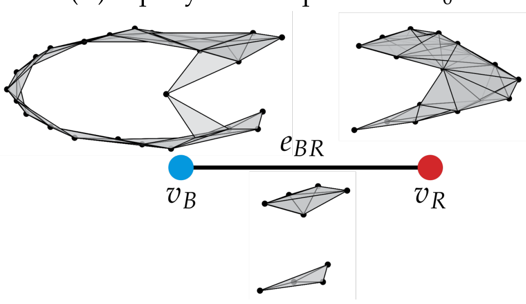

(C) Rips system for parameter ϵ_1

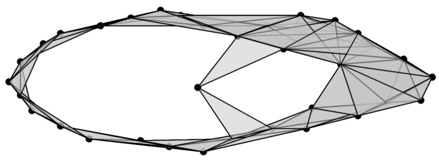

(D) Rips complex for parameter ϵ_1

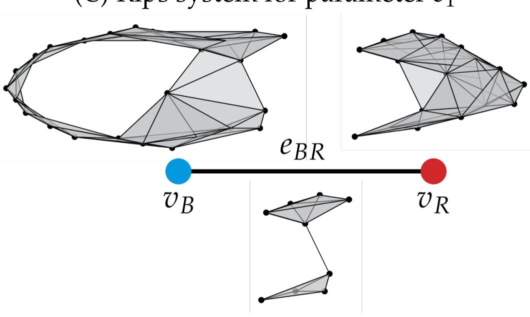

(E) Rips system for parameter ϵ_2

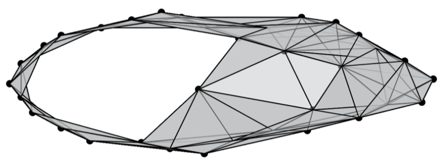

(F) Rips complex for parameter ϵ_2

FIGURE 4.14: Rips systems and Rips complexes for parameters ϵ_0, ϵ_1 and ϵ_2

The relevant cosheaf homologies for computing $H_1(\mathcal{R}^i)$ are

$$H_0(C_\bullet \mathcal{F}_1^0) = 0, \quad H_1(C_\bullet \mathcal{F}_0^0) = \mathbb{K}$$
$$H_0(C_\bullet \mathcal{F}_1^1) = \mathbb{K}, \quad H_1(C_\bullet \mathcal{F}_0^1) = \mathbb{K}$$
$$H_0(C_\bullet \mathcal{F}_1^2) = \mathbb{K}, \quad H_1(C_\bullet \mathcal{F}_0^2) = 0.$$

The map $\Psi^0 : H_0(C_\bullet \mathcal{F}_1^0) \oplus H_1(C_\bullet \mathcal{F}_0^0) \to H_0(C_\bullet \mathcal{F}_1^1) \oplus H_1(C_\bullet \mathcal{F}_0^1)$ maps $H_1(C_\bullet \mathcal{F}_0^0)$ identically to $H_1(C_\bullet \mathcal{F}_0^1)$. Note that the map Ψ^1 has been constructed in Equation 4.59. Then, we obtain a persistence module

$$\mathbb{V}_\Psi : \mathbb{K} \xrightarrow{\Psi^0} \mathbb{K} \oplus \mathbb{K} \xrightarrow{\Psi^1} \mathbb{K},$$

where Ψ^0 is represented by the matrix

$$\begin{bmatrix} 0 \\ 1 \end{bmatrix},$$

and Ψ^1 is represented by the matrix

$$\begin{bmatrix} 1 & 0 \end{bmatrix}.$$

Figure 4.15 illustrates the persistence module $\mathbb{V}_\Psi$.

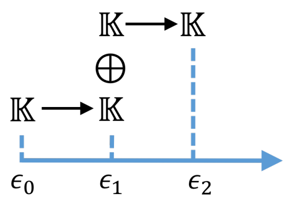

FIGURE 4.15: Persistence module $\mathbb{V}_\Psi$

Note that this persistence module is not isomorphic to the persistence module

$$\mathbb{V} : H_1(\mathcal{R}^0) \to H_1(\mathcal{R}^1) \to H_1(\mathcal{R}^2).$$

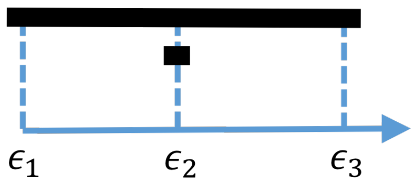

(A) Barcode for $\mathbb{V}_\Psi$

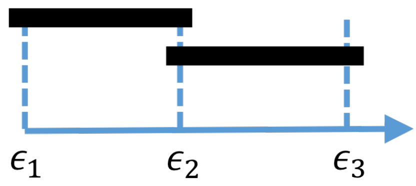

(B) Barcode for $\mathbb{V}$

FIGURE 4.16: Barcodes for persistence modules $\mathbb{V}_\Psi$ and $\mathbb{V}$

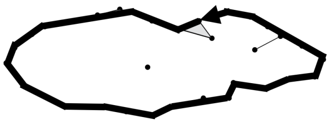

(A) Cycle represented by $\{\langle y \rangle\}$

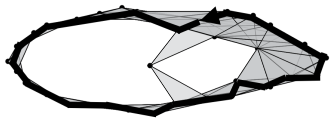

(B) Cycle that should be represented by $\Psi^0(0, \{\langle y \rangle\})$

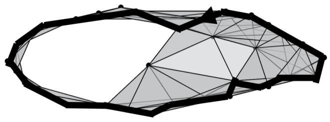

(C) Cycle that should be represented by $\Psi^1 \circ \Psi^0(0, \{\langle y \rangle\}$

FIGURE 4.17: Cycles that should be represented at parameters ϵ_0, ϵ_1, and ϵ_2

The difference between the two persistence modules $\mathbb{V}_\Psi$ and $\mathbb{V}$ are illustrated by the different barcodes in Figure 4.16.

The disparity occurs because the map Ψ^0 and Ψ^1 effectively determines the cycle of $\mathcal{R}^1$ represented by $H_1(C_\bullet \mathcal{F}_0^1)$. The construction of the maps Ψ^0 and Ψ^1 assume distinct cycle representations of $H_1(C_\bullet \mathcal{F}_0^1)$.

Let's start with a basis element $\{\langle y \rangle\} \in H_1(C_\bullet \mathcal{F}_0^0)$. This element $\{\langle y \rangle\}$ represents the cycle illustrated in Figure 4.17a. The image $\Psi^0(0, \{\langle y \rangle\}) = (0, H_1(\phi_0^0)\{\langle y \rangle\})$ must represent the cycle illustrated in Figure 4.17b, and the image $\Psi^1 \circ \Psi^0(0, \{\langle y \rangle\})$ must represent the cycle illustrated in Figure 4.17c.

In reality, we have seen in Figure 4.13 that $H_1(C_\bullet \mathcal{F}_0^1)$, and hence $\Psi^0(0, \{\langle y \rangle\}) = (0, H_1(\phi_0^0)\{\langle y \rangle\})$, represents a cycle illustrated in Figure 4.18. It is such inconsistency in the represented cycles that prevents $\mathbb{V}_\Psi$ from being isomorphic to the persistence module $\mathbb{V}$.

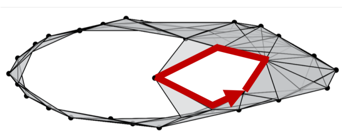

FIGURE 4.18: Cycle represented by $H_1(C_\bullet \mathcal{F}_0^1)$

The construction of §4.2.3 fixes this issue, by ensuring that $H_0(C_\bullet\mathcal{F}_0^1)$ actually represents the cycle in Figure 4.17b and not the cycle in Figure 4.18.

Chapter 5

Multiscale Persistent Homology

Data often comes with additional properties one might want to consider during the analysis process. For example, density estimate, coordinates, and time dependence of a point cloud are some of the factors that can affect one's analysis of a barcode. The goal of this chapter is to introduce a multiscale analysis framework for persistent homology using the distributed computation method from Chapter 4. The general structure for multiscale analysis is provided in §5.1. The result of this framework is a barcode annotated with the properties of interest. One can then use this annotated barcode for a finer analysis taking the characteristics into account. For example, one may analyze any trends in the barcode or if the significant features share a common property. In §5.2, we study a dataset in which the feature sizes depend on the density of the constituting points. In such situations, the annotated barcode allows the user to detect significant features that are overlooked by standard persistent homology methods.

5.1 Multiscale Persistent Homology

We provide a general schematic for using distributed persistent homology computation for multiscale analysis purposes. Our goal is to enrich the barcode so that it reflects properties of interest. In particular, given a point cloud P, let $f : P \to \mathbb{R}$ be a map that reflects some characteristic of the point cloud. For example, f can be a projection map to one of the coordinates, a density estimate, distance to a landmark, or any other characteristic of interest. Construct a cover $\mathcal{V}$ of $f(P)$ so that points $p \in P$ with similar

$f(p)$ values belong to the same member of $\mathcal{V}$. In particular, choose a cover $\mathcal{V}$ such that its nerve $N_{\mathcal{V}}$ is a compact subset of $\mathbb{R}$.

Let $\mathbb{V}$ denote the persistence module

$$\mathbb{V} : H_n(\mathcal{R}^1) \to H_n(\mathcal{R}^2) \to \cdots \to H_n(\mathcal{R}^N)$$

obtained by applying persistence to entire point cloud P in the usual sense. Let *barcode*$(\mathbb{V})$ denote the barcode of $\mathbb{V}$. Recall that each bar of a barcode represents a feature in the Rips complexes. If a bar with birth time ϵ_i represents a feature γ that consists of points in $f^{-1}(U)$ for some $U \in \mathcal{V}$, we say that the feature γ lives in U, and we annotate the corresponding bar with the set U. Our goal is to annotate the bars of *barcode*$(\mathbb{V})$ by such sets U of $\mathcal{V}$.

An algorithmic summary of the annotation process is provided, followed by a detailed explanation of each step.

Algorithm 1 Annotate *barcode*$(\mathbb{V})$.

1: Compute $\mathbb{V}_*$ using distributed computation.
2: Label vector spaces of $\mathbb{V}_*$.
3: For each persistence module $\mathbb{W}_s$ of $\mathbb{V}_* = \bigoplus_s \mathbb{W}_s$, annotate *barcode*$(\mathbb{W}_s)$.
4: From the annotated *barcode*$(\mathbb{V}_*)$, annotate *barcode*$(\mathbb{V})$.
5: Return annotated *barcode*$(\mathbb{V})$.

Step 1. Compute persistence module $\mathbb{V}_*$

Recall that $\mathbb{V}$ is the persistence module

$$\mathbb{V} : H_n(\mathcal{R}^1) \to H_n(\mathcal{R}^2) \to \cdots \to H_n(\mathcal{R}^N)$$

of interest. Let ϵ_L be the largest ϵ parameter such that

$$H_n(\mathcal{R}^\epsilon) \cong H_0(C_\bullet \mathcal{F}_n^\epsilon) \oplus H_1(C_\bullet \mathcal{F}_{n-1}^\epsilon),$$

i.e., $\epsilon_L < K$, where K is the upper bound from Lemma 13. Let $\mathbb{V}|_L$ denote the sequence of vector spaces and maps of $\mathbb{V}$ up to parameter ϵ_L:

$$\mathbb{V}|_L : H_n(\mathcal{R}^1) \to H_n(\mathcal{R}^2) \to \cdots \to H_n(\mathcal{R}^L).$$

We can compute the persistence module

$$\mathbb{V}|_L^{\Psi} : H_0(C_\bullet \mathcal{F}_n^1) \oplus H_1(C_\bullet \mathcal{F}_{n-1}^1) \xrightarrow{\Psi^1} \ldots \xrightarrow{\Psi^{L-1}} H_0(C_\bullet \mathcal{F}_n^L) \oplus H_1(C_\bullet \mathcal{F}_{n-1}^L), \tag{5.1}$$

that is isomorphic to $\mathbb{V}|_L$ using the distributed computation method from Chapter 4. Each map Ψ^i is defined in Equation 4.45.

In fact, instead of computing the persistence module $\mathbb{V}|_L^{\Psi}$, we will compute a persistence module $\mathbb{V}_*$ that is isomorphic to $\mathbb{V}|_L^{\Psi}$, and hence isomorphic to $\mathbb{V}|_L$, that can reveal some additional information about the features represented by the barcode. Recall from §2.2.5 that for each parameter ϵ_i, the cosheaf $\mathcal{F}_n^i$ can be decomposed as $\mathcal{F}_n^i \cong \oplus \mathcal{I}_n^i$, where each $\mathcal{I}_n^i$ is an indecomposable cosheaf over $N_{\mathcal{V}}$. In other words, there exists an isomorphism of cosheaves

$$D_n^i : \mathcal{F}_n^i \to \oplus \mathcal{I}_n^i. \tag{5.2}$$

For each parameter ϵ_i, let $\mathbb{V}_*^i$ denote the vector space

$$\mathbb{V}_*^i = H_0(C_\bullet \oplus \mathcal{I}_n^i) \oplus H_1(C_\bullet \mathcal{F}_{n-1}^i).$$

Let $(\mathbb{V}|_L^{\Psi})^i$ denote the i^{th} vector space of the persistence module $\mathbb{V}|_L^{\Psi}$ defined in Equation 5.1. Note the difference between $\mathbb{V}_*^i$ and $(\mathbb{V}|_L^{\Psi})^i$: we only replaced the cosheaf $\mathcal{F}_n^i$ by the direct sum of its indecomposables. Cosheaf $\mathcal{F}_{n-1}^i$ remains intact. The isomorphism D_n^i of cosheaves from Equation 5.2 induces an isomorphism $\alpha^i : (\mathbb{V}|_L^{\Psi})^i \to \mathbb{V}_*^i$ defined by

$$\alpha^i(\,\{\langle x\rangle\}, \{\langle y\rangle\}\,) = (\,H_0(D_n^i)\{\langle x\rangle\}, \{\langle y\rangle\}\,),$$

where $H_0(D_n^i) : H_0(C_\bullet \mathcal{F}_n^i) \to H_0(C_\bullet \oplus \mathcal{I}_n^i)$ is the map induced by D_n^i. Let $\mathbb{V}_*$ be the persistence module

$$\mathbb{V}_* : H_0(C_\bullet \oplus \mathcal{I}_n^1) \oplus H_1(C_\bullet \mathcal{F}_{n-1}^1) \xrightarrow{\Psi_*^1} \cdots \xrightarrow{\Psi_*^{N-1}} H_0(C_\bullet \oplus \mathcal{I}_n^N) \oplus H_1(C_\bullet \mathcal{F}_{n-1}^N),$$

where the map Ψ_*^i is defined by $\Psi_*^i = \alpha^{i+1} \circ \Psi^i \circ (\alpha^i)^{-1}$.

To write Ψ_*^i explicitly, recall from Equation 4.45 that given a pair of parameters $\epsilon_i < \epsilon_{i+1} < K$, the map $\Psi^i : H_0(C_\bullet \mathcal{F}_n^i) \oplus H_1(C_\bullet \mathcal{F}_{n-1}^i) \to H_0(C_\bullet \mathcal{F}_n^{i+1}) \oplus H_1(C_\bullet \mathcal{F}_{n-1}^{i+1})$ is defined by

$$\Psi^i(\,\{\langle x\rangle\}, \{\langle y\rangle\}\,) = (\, H_0(\phi_n^i)\{\langle x\rangle\} + (-1)^{n+1}\psi^i\{\langle y\rangle\}\,,\, H_1(\phi_{n-1}^i)\{\langle y\rangle\}\,),$$

where $H_0(\phi_n^i)$ and $H_1(\phi_{n-1}^i)$ are the maps defined in Equation 4.16 and ψ^i is the map defined in Equation 4.43. Then, $\Psi_*^i : H_0(C_\bullet \oplus \mathcal{I}_n^i) \oplus H_1(C_\bullet \mathcal{F}_{n-1}^i) \to H_0(C_\bullet \oplus \mathcal{I}_n^{i+1}) \oplus H_1(C_\bullet \mathcal{F}_{n-1}^{i+1})$ is defined by

$$\Psi_*^i(\,\{\langle x\rangle\}, \{\langle y\rangle\}\,) = (\, H_0(\phi_{n*}^i)\{\langle x\rangle\} + (-1)^{n+1}\psi_*^i\{\langle y\rangle\}\,,\, H_1(\phi_{n-1}^i)\{\langle y\rangle\}\,), \tag{5.3}$$

where $H_0(\phi_{n*}^i)$ is the map induced by

$$\phi_{n*}^i = D_n^{i+1} \circ \phi_n^i \circ (D_n^i)^{-1} \tag{5.4}$$

and ψ_*^i is defined by $\psi_*^i = H_0(D_n^{i+1}) \circ \psi$.

By construction, $\mathbb{V}_*$ is isomorphic to the persistence module $\mathbb{V}|_L^\Psi$ and hence isomorphic to $\mathbb{V}|_L$. Even though $\mathbb{V}_*$ is isomorphic to $\mathbb{V}|_L$, the reason we prefer to compute via $\mathbb{V}_*$ is because the persistence module $\mathbb{V}_*$ allows us to understand the cosheaf homologies in terms of the indecomposable cosheaves $\mathcal{I}_n^i$.

Step 2. Label the vector spaces of $\mathbb{V}_*$

For any parameter ϵ_i, recall that

$$\mathbb{V}^i_* = H_0(C_\bullet \oplus \mathcal{I}^i_n) \oplus H_1(C_\bullet \mathcal{F}^i_{n-1}).$$

Recall from Lemma 6 that $H_0(C_\bullet \oplus \mathcal{I}^i_n) \cong H_0(C_\bullet \oplus \mathcal{I}^i_{[-]})$, where $\oplus \mathcal{I}^i_{[-]}$ is a direct sum of indecomposables of the form $\mathcal{I}^i_{[-]}$. Moreover, $H_0(C_\bullet \oplus \mathcal{I}^i_{[-]}) = \oplus H_0(C_\bullet \mathcal{I}^i_{[-]})$. Thus, each component of $H_0(C_\bullet \oplus \mathcal{I}^i_n)$ corresponds to an indecomposable cosheaf of the form $\mathcal{I}^i_{[-]}$. We will annotate each component of $H_0(C_\bullet \oplus \mathcal{I}^i_n)$ by examining the support of the corresponding indecomposable cosheaf $\mathcal{I}^i_{[-]}$.

Note that the left and rightmost supports of an indecomposable cosheaf $\mathcal{I}^i_{[-]}$ are the vertices of $N_\mathcal{V}$. Let $v_j \in N_\mathcal{V}$ be the leftmost support of $\mathcal{I}^i_{[-]}$ and let $v_k \in N_\mathcal{V}$ be the rightmost support of $\mathcal{I}^i_{[-]}$. We will call such a cosheaf as being supported over $[v_j, v_k]$, and we will denote the cosheaf by $\mathcal{I}^i_{[v_j,v_k]}$. Recall that a vertex v_j of $N_\mathcal{V}$ correspond to member U_j of the cover $\mathcal{V}$. If $v_j, v_{j+1}, \ldots, v_k$ represent all the vertices of $N_\mathcal{V}$ between vertices v_j and v_k, then a cosheaf $\mathcal{I}^i_{[v_j,v_k]}$ supported over $[v_j, v_k]$ represents a feature that lives in all $U_j, U_{j+1}, \ldots, U_k$. Thus, we can annotate the component of $H_0(C_\bullet \oplus \mathcal{I}^i_n)$ that corresponds to $H_0(C_\bullet \mathcal{I}^i_{[v_j,v_k]})$ by its support $[U_j, U_k]$. Since this component represents a feature that lives in all $U_j, U_{j+1}, \ldots, U_k$, the user may choose to annotate this component by U_j or U_k depending on the user's goal.

For example, assume that

$$\mathbb{V}^i_* = H_0(C_\bullet \oplus \mathcal{I}^i_n) \oplus H_1(C_\bullet \mathcal{F}^i_{n-1}) = \mathbb{K} \oplus \mathbb{K} \oplus \mathbb{K} \oplus \mathbb{K},$$

where the first three components come from $H_0(C_\bullet \oplus \mathcal{I}^i_n)$ and the last component $\mathbb{K}$ comes from $H_1(C_\bullet \mathcal{F}^i_{n-1})$. An example of cosheaf $\oplus \mathcal{I}^i_n$ is illustrated in Figure 5.1.

Note that

$$\oplus \mathcal{I}^i_n \cong \mathcal{I}^i_{[v_B,v_B]} \oplus \mathcal{I}^i_{[v_R,v_R]} \oplus \mathcal{I}^i_{[v_B,v_R]}.$$

Then, each component of $H_0(C_\bullet \oplus \mathcal{I}^i_n) = \mathbb{K} \oplus \mathbb{K} \oplus \mathbb{K}$ can be labeled as $H_0(C_\bullet \oplus \mathcal{I}^i_n) =$

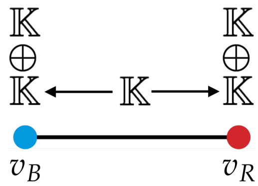

FIGURE 5.1: An example decomposition of a cosheaf $\mathcal{F}_n^i \cong \oplus \mathcal{I}_n^i$

$\mathbb{K}_B \oplus \mathbb{K}_R \oplus \mathbb{K}_{BR}$, where each label corresponds to the support of the indecomposable cosheaf in Figure 5.1. Then, the vector space $\mathbb{V}_*^i$ can be labeled as $\mathbb{K}_B \oplus \mathbb{K}_R \oplus \mathbb{K}_{BR} \oplus \mathbb{K}$. Depending on the user's interest, one can choose to label the component $\mathbb{K}_{BR}$ by either $\mathbb{K}_B$ or $\mathbb{K}_R$.

Our mechanism of decomposing the cosheaf $\mathcal{F}_n^i$ into indecomposable cosheaves may seem like a cumbersome step. However, such decomposition allows us to label components of cosheaf homologies according to properties of the features represented by the indecomposable cosheaves.

The labels of vector spaces $\mathbb{V}_*^i$ will allow us to enrich the barcode $barcode(\mathbb{V}_*)$ of the persistence module $\mathbb{V}_*$, which will then allow us to annotate the barcode $barcode(\mathbb{V})$ of the persistence module $\mathbb{V}$.

Step 3. Annotate the barcode of each $\mathbb{W}_s$ of $\mathbb{V}_* = \bigoplus_s \mathbb{W}_s$

Note that $\mathbb{V}_*$ can be expressed naturally as a sum of persistence modules as

$$\mathbb{V}_* = \bigoplus_s \mathbb{W}_s.$$

Moreover, $barcode(\mathbb{V}_*)$ is the same as the collection of barcodes $barcode(\mathbb{W}_s)$. Thus, for each $\mathbb{W}_s$, we will compute $barcode(\mathbb{W}_s)$ and annotate bars of $barcode(\mathbb{W}_s)$.

Compute $barcode(\mathbb{W}_s)$. If a bar $\overline{b}$ is born at parameter ϵ_i, consider the vector space $\mathbb{W}_s^i$ and the labeling of its components from Step 2. The bar $\overline{b}$ of $barcode(\mathbb{W}_s^i)$ with birth time ϵ_i corresponds to a linear combination of the components of $\mathbb{W}_s^i$. If all components of $\mathbb{W}_s^i$ were annotated as living in a unique set $U \in \mathcal{V}$ inStep 2, then $\overline{b}$, representing some linear combination of features that live in U, must also represent a feature that lives in U. We can thus annotate $\overline{b}$ by U. If some components of $\mathbb{W}_s^i$ were annotated as living in U_j and some were annotated as living in U_k, then $\overline{b}$ can represent a linear combination of features among points in U_j and U_k. At this point, depending on the user's goal, the user can decide to either not annotate the bars at all, to annotate the bars as U_j, or to annotate the bars as U_k, depending on the question of interest.

After repeating the above process for each bar in *barcode*$(\mathbb{W}_s)$, one can proceed to analogously annotate bars from *barcode*$(\mathbb{W}_s)$ for every $\mathbb{W}_s$ of $\mathbb{V} = \bigoplus_s \mathbb{W}_s$.

Step 4. Annotate the barcode of $\mathbb{V}$

So far, we have enriched *barcode*$(\mathbb{V}_*)$. We now explore how *barcode*$(\mathbb{V}_*)$ and *barcode*$(\mathbb{V})$ are related so that we can enrich *barcode*$(\mathbb{V})$ accordingly. Note that *barcode*$(\mathbb{V}_*)$ can be obtained from *barcode*$(\mathbb{V})$ by truncating *barcode*$(\mathbb{V})$ at parameter ϵ_L, i.e., a bar $[b, d]$ of barcode$(\mathbb{V})$ with $b \leq \epsilon_L$ corresponds to a bar $[b, \min\{d, \epsilon_L\}]$ of barcode$(\mathbb{V}')$.

If a bar $[b, d]$ of *barcode*$(\mathbb{V}_*)$ with $d < \epsilon_L$ has been annotated by a particular set U in Step 3, then we can find a bar $[b, d]$ with the same birth and death time in *barcode*$(\mathbb{V})$ and annotate it using the same set U. If a bar $[b, \epsilon_L]$ of *barcode*$(\mathbb{V}_*)$ is annotated by U, then it is possible that this bar is a truncated version of a longer bar $[b, d]$ of *barcode*$(\mathbb{V})$ with $d > \epsilon_L$. Hence, we use the birth time b to identify the corresponding bar in *barcode*$(\mathbb{V})$. If $[b, \epsilon_L]$, annotated by U, is the unique bar with birth time b in *barcode*$(\mathbb{V}_*)$, then there exists a unique bar $[b, d]$ with the same birth time b in *barcode*$(\mathbb{V})$. We can then annotate the bar $[b, d]$ of *barcode*$(\mathbb{V})$ by U.

The result is a barcode of persistence module $\mathbb{V}$ with bars annotated by properties of the corresponding features. This annotated barcode can then be used in various ways to perform finer data analysis. For example, one can select the bars that are annotated by a particular set, say U, and analyze only those chosen bars to determine significant features. In the following section, we provide an explicit example of multiscale analysis for point cloud with varying density.

5.2 Data with Varying Density

We now use the framework developed in §5.1 to study variable-density point cloud. Consider a situation where the size of a feature depends on the density of the constituting points. In such situation, using a uniform metric to analyze the data can lead to loss of information.

For example, consider a point cloud in Figure 5.2 where the sparse points constitute a large feature and the dense points constitute a small feature. In such situation, apply-

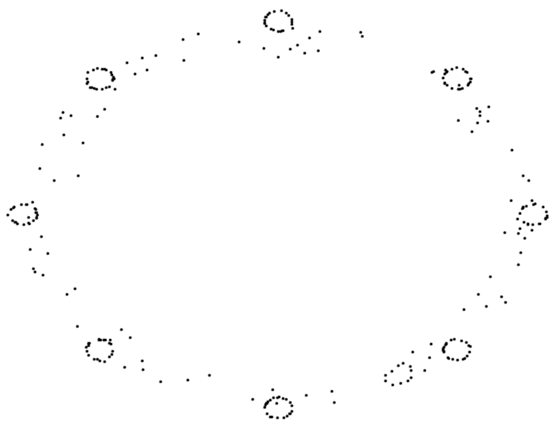

FIGURE 5.2: A point cloud with varying density

ing the standard persistent homology method results in an analysis where the small, but densely sampled features become overlooked. For example, Figure 5.3 illustrates the barcode in dimension 1. By observing this barcode, one would conclude that there is one significant feature, disregarding the small but densely sampled features as being insignificant. The multiscale framework from §5.1 can give insight into which bars of the barcode correspond to small but densely sampled features and annotate them as being significant.

Recall that the multiscale framework in §5.1 involved a choice of map $f : P \to \mathbb{R}^d$ from the point cloud that reflects some property of interest and a choice of covering $\mathcal{V}$ of $f(P)$. For the point cloud P in Figure 5.2, we will let $f : P \to \mathbb{R}$ be the function mapping each point to its estimated density value. Note that there are multiple methods for computing the density of each point. One option computes density of a point p by

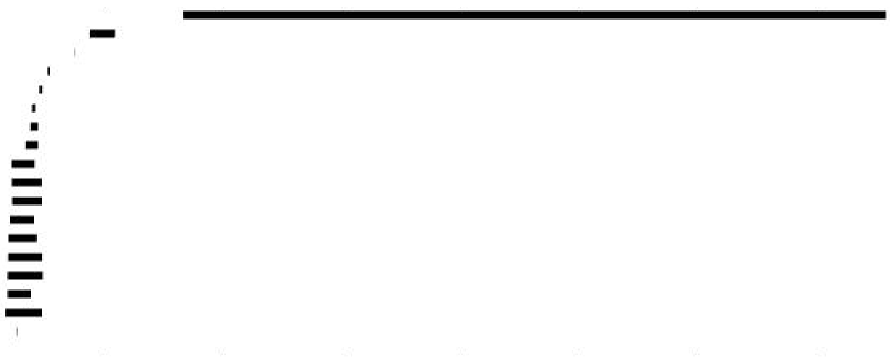

FIGURE 5.3: Barcode from standard persistent homology in dimension 1

computing the number of points whose Euclidean distance to p is less than a user specified parameter r. For our example, we used such density computation with $r = 0.1$.

The covering $\mathcal{V}$ of $f(P)$ should be chosen so that distinct members U_i, U_j of $\mathcal{V}$ reflect different ranges of the property of interest. For our example, we use a histogram to plot the number of points p for each density value to gain some insight into the distribution of density values. Figure 5.4 shows the histogram.

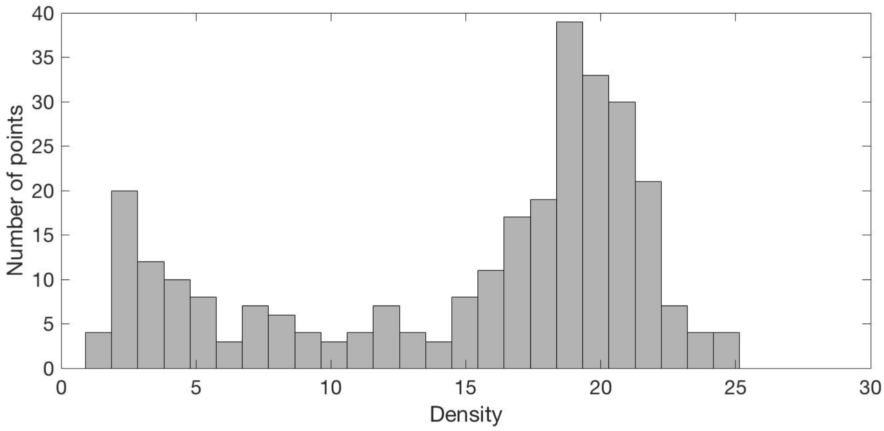

FIGURE 5.4: Histogram plot of estimated density values

Let $\mathcal{V} = \{U_s, U_d\}$ be a covering of $f(p)$, where $U_s = (0, 18)$ and $U_d = (8, 26)$. We will refer to points in $f^{-1}(U_s)$, which are the points whose density values are between 0 and 18, as the sparse points, and we will denote $S = f^{-1}(U_s)$. Similarly, we will refer to points in $f^{-1}(U_d)$ as the dense points, and we will denote the collection by D.

Figures 5.5a and 5.5b illustrate the sparse and dense points.

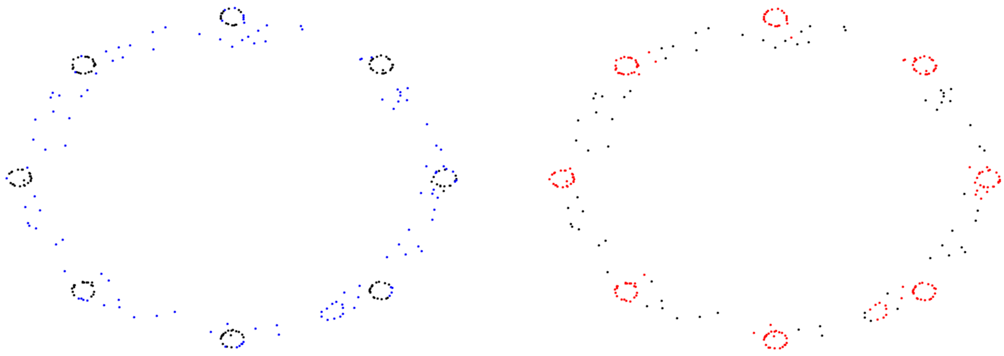

(A) Sparse points (B) Dense points

FIGURE 5.5: Sparse and dense points

Let

$$\mathbb{V} : H_1(\mathcal{R}^1) \to \cdots \to H_1(\mathcal{R}^N)$$

be the persistence module obtained from the point cloud P. For this example, the maximum parameter is $\epsilon_N = 1.6$. Let K be the upper bound of the parameter ϵ from Lemma 13 for which the isomorphism

$$H_n(\mathcal{R}^\epsilon) \cong H_0(C_\bullet \mathcal{F}_n^\epsilon) \oplus H_1(C_\bullet \mathcal{F}_{n-1}^\epsilon)$$

holds. Compute the persistence module

$$\mathbb{V}_* : H_0(C_\bullet \oplus \mathcal{J}_1^1) \oplus H_1(C_\bullet \mathcal{F}_0^1) \to \cdots \to H_0(C_\bullet \oplus \mathcal{J}_1^K) \oplus H_1(C_\bullet \mathcal{F}_0^K) \tag{5.5}$$

up to $\epsilon = K$ following Step 1 of Algorithm 1. For this example, the upper bound K is $K = 0.0719$.

Step 2 of Algorithm 1 labels the components of vector space $H_0(C_\bullet \mathcal{J}_0^i)$ by D or S according to the support of the indecomposable $\mathcal{J}_{[-]}^i$. Let v_d and v_s denote the vertices of $N_{\mathcal{V}}$ that each corresponds to sets U_d and U_s of $\mathcal{V}$. For each cosheaf $\mathcal{J}_{[v_d,v_d]}^i$ with support $v_d \in N_{\mathcal{V}}$, label the component $H_0(C_\bullet \mathcal{J}_{[v_d,v_d]}^i)$ of $H_0(C_\bullet \mathcal{J}_1^i)$ by D. Similarly, for a cosheaf $\mathcal{J}_{[v_s,v_s]}^i$ with support $v_s \in N_{\mathcal{V}}$, label the component $H_0(C_\bullet \mathcal{J}_{[v_s,v_s]}^i)$ of $H_0(C_\bullet \mathcal{J}_1^i)$ by S. Given a cosheaf of the form $\mathcal{I}^i_{[v_s,v_d]}$, such cosheaf represents a feature that lives in both U_s and U_d. In our example, we decided to interpret such a cosheaf as representing a feature that lives in U_d. Thus, we can annotate the component $H_0(C_\bullet\mathcal{I}^i_{[v_s,v_d]})$ of $H_0(C_\bullet\mathcal{I}^i_1)$ by D.

Step 3 of Algorithm 1 results in an annotated version of *barcode*$(\mathbb{V}_*)$, illustrated in Figure 5.6. The top two bars colored in blue correspond to bars annotated by S and the remaining red bars correspond to bars annotated by D.

FIGURE 5.6: Annotated *barcode*$(\mathbb{V}_*)$

Step 4 of Algorithm 1 allows us to transfer the annotation of *barcode*$(\mathbb{V}_*)$ to *barcode*$(\mathbb{V})$ resulting in an annotated version of *barcode*$(\mathbb{V})$ illustrated in 5.7. The two bars enclosed by the blue box are annotated by S, and the bars enclosed by red box are annotated by D.

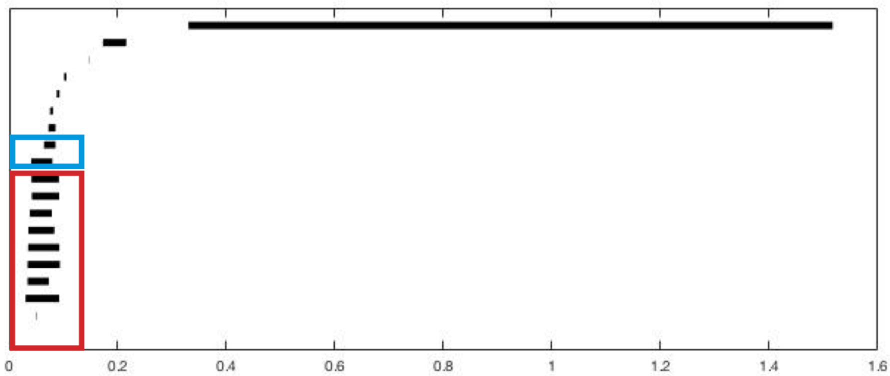

FIGURE 5.7: Annotated *barcode*$(\mathbb{V})$

What one can do with such annotated barcode depends on the problem of interest. In our example, the goal is to determine small but significant features that consist of the denser points. Thus, we focus on the bars of Figure 5.7 that have been annotated by

D, which are illustrated in Figure 5.8. By restricting our attention to only the bars that represent features in U_d, we are able to determine the significant features built among the denser points. From Figure 5.8, one can conclude that there are eight significant bars.

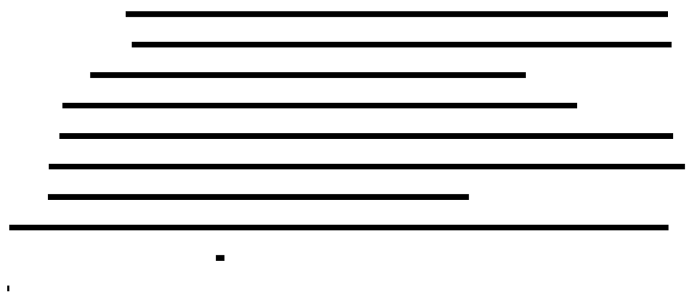

FIGURE 5.8: The dense bars

Lastly, we return to *barcode*$(\mathbb{V})$ and annotate significant bars of Figure 5.8 as being significant. We then obtain barcode in Figure 5.9, where the red bars are annotated as being significant. Note that we have one long red bar, which is deemed significant because of its length. We have eight additional shorter significant bars which were identified via Algorithm 1.

FIGURE 5.9: Final annotation of *barcode*$(\mathbb{V})$

Using the persistent homology computation software Eirene [17], we were able to identify the points of P that constitute each significant feature. The newly determined eight significant short bars indeed correspond to the eight small but densely sampled features in Figure 5.2.

Appendix A

Alternate Construction to §4.2.2

In Chapter 4, we constructed a morphism $\psi^i : H_1(C_\bullet \mathcal{F}^i_{n-1}) \to H_0(C_\bullet \mathcal{F}^{i+1}_n)$ using a spectral sequence type argument. Recall that in §4.2.2, computing the homology of the commutative cube 4.18 allowed us to construct the map δ^i. Once we reached Diagram 4.19, we decided to take the homology with respect to the maps ∂_n. Note that we could have taken the homology with respect to maps ϕ^i_n instead of maps ∂^i_n in Diagram 4.19. In this section, we explore the outcome of taking homology with respect to the maps ϕ^i_{n-1} instead of the maps ∂_n. When we take this alternative route, we end up constructing a map $\delta^i_* : H_1(C_\bullet \ker \phi^i_{n-1}) \to H_0(C_\bullet \operatorname{coker} \phi^i_n)$ while emphasizing the perspective of long exact sequence of pairs.

We start with the same commutative diagram as we have in §4.2.2.

$$
\begin{tikzcd}
 & {} \arrow[d] & & {} \arrow[d] \\
{} \arrow[d] & \bigoplus\limits_{v\in N_{\mathcal{V}}} C_n(\mathcal{R}_v^{i+1}) \arrow[dd, "\partial"] & {} \arrow[d] & \bigoplus\limits_{e\in N_{\mathcal{V}}} C_n(\mathcal{R}_e^{i+1}) \arrow[ll, "e_n^{i+1}"'] \arrow[dd, "\partial"] \\
\bigoplus\limits_{v\in N_{\mathcal{V}}} C_n(\mathcal{R}_v^{i}) \arrow[ur, "\iota_n^i"] \arrow[dd, "\partial"] & & \bigoplus\limits_{e\in N_{\mathcal{V}}} C_n(\mathcal{R}_e^{i}) \arrow[ll, "e_n^i"'] \arrow[ur, "\kappa_n^i"] \arrow[dd, "\partial"] & \\
 & \bigoplus\limits_{v\in N_{\mathcal{V}}} C_{n-1}(\mathcal{R}_v^{i+1}) \arrow[d] & & \bigoplus\limits_{e\in N_{\mathcal{V}}} C_{n-1}(\mathcal{R}_e^{i+1}) \arrow[ll, "e_{n-1}^{i+1}"'] \arrow[d] \\
\bigoplus\limits_{v\in N_{\mathcal{V}}} C_{n-1}(\mathcal{R}_v^{i}) \arrow[ur, "\iota_{n-1}^i"] \arrow[d] & {} & \bigoplus\limits_{e\in N_{\mathcal{V}}} C_{n-1}(\mathcal{R}_e^{i}) \arrow[ll, "e_{n-1}^i"'] \arrow[ur, "\kappa_{n-1}^i"] \arrow[d] & {} \\
{} & & {} &
\end{tikzcd}
\tag{A.1}
$$

Taking the homology with respect to the boundary maps ∂, we obtain the same diagram as Diagram 4.19. Note that in Diagram 4.19, the terms on the right and left faces of the cube are related by relative homology as illustrated in Diagram A.2.

$$\begin{tikzcd}
 & & \bigoplus\limits_{v\in N_\mathcal{V}} H_n(\mathcal{R}_v^{i+1}) \arrow[ddl, "j^0"] \arrow[ddd, dash, dashed] & & & \bigoplus\limits_{e\in N_\mathcal{V}} H_n(\mathcal{R}_e^{i+1}) \arrow[lll, "\partial_n^{i+1}"'] \arrow[ddl, "j^1"] \arrow[ddd, dash, dashed] \\
\bigoplus\limits_{v\in N_\mathcal{V}} H_n(\mathcal{R}_v^{i}) \arrow[urr, "(\phi_n^i)_v"] \arrow[ddd, dash, dashed] & & & \bigoplus\limits_{e\in N_\mathcal{V}} H_n(\mathcal{R}_e^{i}) \arrow[lll, "\partial_n^{i}"'] \arrow[urr, "(\phi_n^i)_e"] \arrow[ddd, dash, dashed] & & \\
 & \bigoplus\limits_{v\in N_\mathcal{V}} H_n(\mathcal{R}_v^{i+1}, \mathcal{R}_v^{i}) \arrow[ddl, "\partial^0"] & & & \bigoplus\limits_{e\in N_\mathcal{V}} H_n(\mathcal{R}_e^{i+1}, \mathcal{R}_e^{i}) \arrow[lll, "j"] \arrow[ddl, "\partial^1"] & \\
 & & \bigoplus\limits_{v\in N_\mathcal{V}} H_{n-1}(\mathcal{R}_v^{i+1}) & & & \bigoplus\limits_{e\in N_\mathcal{V}} H_{n-1}(\mathcal{R}_e^{i+1}) \arrow[lll, "\partial_{n-1}^{i+1}"'] \\
\bigoplus\limits_{v\in N_\mathcal{V}} H_{n-1}(\mathcal{R}_v^{i}) \arrow[urr, "(\phi_{n-1}^i)_v"] & & & \bigoplus\limits_{e\in N_\mathcal{V}} H_{n-1}(\mathcal{R}_e^{i}) \arrow[lll, "\partial_{n-1}^{i}"'] \arrow[urr, "(\phi_{n-1}^i)_e"] & &
\end{tikzcd} \tag{A.2}$$

Diagram A.2 can be laid out in a more familiar long exact sequence form as the following.

$$\begin{tikzcd}
\cdots \bigoplus\limits_{e\in N_\mathcal{V}} H_n(\mathcal{R}_e^{i}) \arrow[r, "(\phi_n^i)_e"] \arrow[d] & \bigoplus\limits_{e\in N_\mathcal{V}} H_n(\mathcal{R}_e^{i+1}) \arrow[r, "j^1"] \arrow[d, "\partial_n^{i+1}"] & \bigoplus\limits_{e\in N_\mathcal{V}} H_n(\mathcal{R}_e^{i+1}, \mathcal{R}_e^{i}) \arrow[r, "\partial^1"] \arrow[d, "j"] & \bigoplus\limits_{e\in N_\mathcal{V}} H_{n-1}(\mathcal{R}_e^{i}) \arrow[r, "(\phi_{n-1}^i)_e"] \arrow[d, "\partial_{n-1}^i"] & \bigoplus\limits_{e\in N_\mathcal{V}} H_{n-1}(\mathcal{R}_e^{i+1}) \cdots \arrow[d] \\
\cdots \bigoplus\limits_{v\in N_\mathcal{V}} H_n(\mathcal{R}_v^{i}) \arrow[r, "(\phi_n^i)_v"] & \bigoplus\limits_{v\in N_\mathcal{V}} H_n(\mathcal{R}_v^{i+1}) \arrow[r, "j^0"] & \bigoplus\limits_{v\in N_\mathcal{V}} H_n(\mathcal{R}_v^{i+1}, \mathcal{R}_v^{i}) \arrow[r, "\partial^0"] & \bigoplus\limits_{v\in N_\mathcal{V}} H_{n-1}(\mathcal{R}_v^{i}) \arrow[r, "(\phi_{n-1}^i)_v"] & \bigoplus\limits_{v\in N_\mathcal{V}} H_{n-1}(\mathcal{R}_v^{i+1}) \cdots
\end{tikzcd}$$

The top and bottom sequences are direct sums of long exact sequence of pairs. The diagram commutes by naturality of long exact sequences. Taking the homology with respect to ∂_n's from Diagram A.2, we obtain Diagram A.3.

$$\begin{tikzcd}
 & & \operatorname{coker}(\phi^i_n)_v \arrow[dll, dash, dashed] \arrow[ddl, "j^0_*"] \arrow[ddd, dash, dashed] & & & \operatorname{coker}(\phi^i_n)_e \arrow[lll, "\overline{\partial^{i+1}_n}"'] \arrow[dll, dash, dashed] \arrow[ddl, "j^1_*"] \arrow[ddd, dash, dashed] \\
\ker(\phi^i_n)_v \arrow[ddd, dash, dashed] & & & \ker(\phi^i_n)_e \arrow[lll, "\overline{\partial^i_n}"'] \arrow[ddd, dash, dashed] & & \\
 & \bigoplus\limits_{v\in N_{\mathcal{V}}} H_n(\mathcal{R}^{i+1}_v, \mathcal{R}^i_v) \arrow[ddl, "\partial^0_*"'] & & & \bigoplus\limits_{e\in N_{\mathcal{V}}} H_n(\mathcal{R}^{i+1}_e, \mathcal{R}^i_e) \arrow[lll, "j"'] \arrow[ddl, "\partial^1_*"] & \\
 & & \operatorname{coker}(\phi^i_{n-1})_v \arrow[dll, dash, dashed] & & & \operatorname{coker}(\phi^i_{n-1})_e \arrow[lll, "\overline{\partial^{i+1}_{n-1}}"'] \arrow[dll, dash, dashed] \\
\ker(\phi^i_{n-1})_v & & & \ker(\phi^i_{n-1})_e \arrow[lll, "\overline{\partial^i_{n-1}}"'] & &
\end{tikzcd} \tag{A.3}$$

Note that $\ker(\phi^i_n)_v$ and $\ker(\phi^i_n)_e$ are the collections of local sections of the cosheaf $\ker\phi^i_n$ on the 0-simplices and 1-simplices of $N_{\mathcal{V}}$, i.e., $\ker(\phi^i_n)_v = \bigoplus\limits_{v\in N_{\mathcal{V}}} \ker\phi^i_n(v)$, and $\ker(\phi^i_n)_e = \bigoplus\limits_{e\in N_{\mathcal{V}}} \ker\phi^i_n(e)$. Similarly, $\operatorname{coker}(\phi^i_n)_v$ and $\operatorname{coker}(\phi^i_n)_e$ are the collections of local sections of cosheaf $\operatorname{coker}\phi^i_n$ on the 0-simplices and 1-simplices of $N_{\mathcal{V}}$.

After taking the homology with respect to the maps $\overline{\partial^i_n}$'s, a diagram chase will allow us to construct a map $\delta^i : \ker\overline{\partial^i_{n-1}} \to \operatorname{coker}\overline{\partial^{i+1}_n}$ as shown in Diagram A.4.

$$\begin{tikzcd}
 & \operatorname{coker}\overline{\partial^{i+1}_n} \arrow[rr, dash, dashed] \arrow[dl, dash, dashed] \arrow[dd, dash, dashed] & & \ker\overline{\partial^{i+1}_n} \arrow[dl, dash, dashed] \arrow[dd, dash, dashed] \\
\operatorname{coker}\overline{\partial^i_n} \arrow[rr, dash, dashed] \arrow[dd, dash, dashed] & & \ker\overline{\partial^i_n} \arrow[dd, dash, dashed] & \\
 & \operatorname{coker}\overline{\partial^{i+1}_{n-1}} \arrow[rr, dash, dashed] \arrow[dl, dash, dashed] & & \ker\overline{\partial^{i+1}_{n-1}} \arrow[dl, dash, dashed] \\
\operatorname{coker}\overline{\partial^i_{n-1}} \arrow[rr, dash, dashed] & & \ker\overline{\partial^i_{n-1}} \arrow[uuul] &
\end{tikzcd} \tag{A.4}$$

As we will show in the following theorem, $\delta^i_* : \ker \overline{\partial^i_{n-1}} \to \operatorname{coker} \overline{\partial^{i+1}_n}$ is actually a map from $H_1(C_\bullet \ker \phi^i_{n-1})$ to $H_0(C_\bullet \operatorname{coker} \phi^i_n)$.

Theorem 11. *Let P be a point cloud. Let $f : P \to \mathbb{R}^d$ be any map. Let $\mathcal{V}$ be a cover of $f(P) \subset \mathbb{R}^d$ such that $N_\mathcal{V}$ is one dimensional. Let $\phi^i_n : \mathcal{F}^i_n \to \mathcal{F}^{i+1}_n$ be the cosheaf morphism induced by inclusion maps of the Rips system. Then ϕ^i_n, ϕ^i_{n-1} induce a morphism $\delta^i_* : H_1(C_\bullet \ker \phi^i_{n-1}) \to H_0(C_\bullet \operatorname{coker} \phi^i_n)$.*

The induced morphism δ^i_* extends to a map $\psi^i_* : H_1(C_\bullet \mathcal{F}^i_{n-1}) \to H_0(C_\bullet \mathcal{F}^{i+1}_n)$ (Lemma 15), which is an equivalent map to ψ^i constructed in Lemma 14.

Proof. Let $\langle\ \rangle$, $\{\ \}$, and $[\ ]$ each denote the homology classes that appear in diagrams A.2, A.3, and A.4. Consider Diagram A.3 that has been laid out as the following.

$$\begin{tikzcd}
0 \arrow[r] & \operatorname{coker}(\phi^i_n)_e \arrow[r, "j^1_*"] \arrow[d, "\overline{\partial^{i+1}_n}"] & \bigoplus_{e\in N_\mathcal{V}} H_n(\mathcal{R}^{i+1}_e, \mathcal{R}^i_e) \arrow[r, "\partial^1_*"] \arrow[d, "j"] & \ker(\phi^i_{n-1})_e \arrow[r] \arrow[d, "\overline{\partial^i_{n-1}}"] & 0 \\
0 \arrow[r] & \operatorname{coker}(\phi^i_n)_v \arrow[r, "j^0_*"] & \bigoplus_{v\in N_\mathcal{V}} H_n(\mathcal{R}^{i+1}_v, \mathcal{R}^i_v) \arrow[r, "\partial^0_*"] & \ker(\phi^i_{n-1})_v \arrow[r] & 0
\end{tikzcd} \tag{A.5}$$

Note that the top and bottom sequences of the above diagram are exact. Let $[\{\langle\gamma\rangle\}]$ in $\ker \overline{\partial^i_{n-1}}$. Then, $\{\langle\gamma\rangle\} \in \ker(\phi^i_{n-1})_e$, and

$$\overline{\partial^i_{n-1}}\{\langle\gamma\rangle\} = 0. \tag{A.6}$$

By exactness of the top sequence of Diagram A.5, there exists $\langle|\gamma'|\rangle$ in $\bigoplus_{e\in N_\mathcal{V}} H_n(\mathcal{R}^{i+1}_e, \mathcal{R}^i_e)$ such that

$$\partial^1_*\langle|\gamma'|\rangle = \{\langle\gamma\rangle\}. \tag{A.7}$$

Here, $\gamma' \in \bigoplus_{e\in N_\mathcal{V}} C_n(\mathcal{R}^{i+1}_e)$ whose boundary is in $\bigoplus_{e\in N_\mathcal{V}} C_{n-1}(\mathcal{R}^i_e)$. We use $|\gamma'|$ to represent the coset $\gamma' + \bigoplus_{e\in N_\mathcal{V}} C_n(\mathcal{R}^i_e)$, and we use $\langle|\gamma'|\rangle$ to denote the homology class of $|\gamma'|$ in $\bigoplus_{e\in N_\mathcal{V}} H_n(\mathcal{R}^{i+1}_e, \mathcal{R}^i_e)$.

By commutativity of Diagram A.5, Equations A.6 and A.7, we have

$$\partial_*^0 \circ j\langle|\gamma'|\rangle = \overline{\partial_{n-1}^i} \circ \partial_*^1\langle|\gamma'|\rangle = \overline{\partial_{n-1}^i}\{\langle\gamma\rangle\} = 0.$$

Thus, $j\langle|\gamma'|\rangle \in \ker \partial_*^0$. By exactness of the bottom sequence of Diagram A.5, there exists $\{\langle\gamma''\rangle\} \in \operatorname{coker}(\phi_n^i)_v$ such that

$$j_*^0\{\langle\gamma''\rangle\} = j\langle|\gamma'|\rangle. \tag{A.8}$$

Recall that $[\{\langle\gamma''\rangle\}]$ denotes the coset $\{\langle\gamma''\rangle\} + \operatorname{im} \overline{\partial_n^{i+1}}$. Define $\delta_*^i : \ker \overline{\partial_{n-1}^i} \to \operatorname{coker} \overline{\partial_n^{i+1}}$ by

$$\delta_*^i[\{\langle\gamma\rangle\}] = [\{\langle\gamma''\rangle\}]. \tag{A.9}$$

We now check that δ_*^i is well-defined by considering different candidates γ' and γ'' that satisfy Equations A.7 and A.8.

Since j_*^0 is injective, $\{\langle\gamma''\rangle\}$ that satisfies Equation A.8 is uniquely determined once $j\langle|\gamma'|\rangle$ is determined. In other words, if $\{\langle\eta''\rangle\}$ also satisfies $j_*^0\{\langle\eta''\rangle\} = j\langle|\gamma'|\rangle$, then $\{\langle\eta''\rangle\} = \{\langle\gamma''\rangle\}$.

Let's now consider a different choice of γ' that satisfies Equation A.7. Let $\langle|\eta'|\rangle \in \bigoplus_{e\in N_\nu} H_n(\mathcal{R}_e^{i+1}, \mathcal{R}_e^i)$ satisfy

$$\partial_*^1\langle|\eta'|\rangle = \{\langle\gamma\rangle\}. \tag{A.10}$$

Let $\{\langle\eta''\rangle\} \in \operatorname{coker}(\phi_n^i)_v$ be an element that satisfies

$$j_*^0\{\langle\eta''\rangle\} = j\langle|\eta'|\rangle. \tag{A.11}$$

Then, one would define $\delta_*^i[\{\langle\gamma\rangle\}] = [\{\langle\eta''\rangle\}$.

From Equations A.7 and A.10, one can check that $\langle|\eta' - \gamma'|\rangle \in \ker \partial_*^1$. By exactness of the top sequence of Diagram A.5, there exists some $\{\langle\omega\rangle\} \in \operatorname{coker}(\phi_n^i)_e$ such that $\langle|\eta' - \gamma'|\rangle = j_*^1\{\langle\omega\rangle\}$. Note $j_*^1\{\langle\omega\rangle\} = j^1\langle\omega\rangle = \langle|\omega|\rangle$, where $j^1 : \bigoplus_{e\in N_\nu} H_n(\mathcal{R}_e^{i+1}) \to$

$\bigoplus_{e \in N_\mathcal{V}} H_n(\mathcal{R}_e^{i+1}, \mathcal{R}_e^i)$ from Diagram A.2. So

$$\langle|\omega|\rangle = \langle|\eta' - \gamma'|\rangle. \tag{A.12}$$

Note that

$$j_*^0 \circ \overline{\partial_n^{i+1}}\{\langle\omega\rangle\} = j \circ j_*^1\{\langle\omega\rangle\} = j\langle|\eta' - \gamma'|\rangle \tag{A.13}$$

from commutativity of Diagram A.5. Moreover,

$$\partial_*^0 \circ j\langle|\eta' - \gamma'|\rangle = \overline{\partial_{n-1}^i} \circ \partial_*^1\langle|\eta' - \gamma'|\rangle = 0$$

from commutativity of Diagram A.5 and Equations A.7 and A.10. Thus, $j\langle|\eta' - \gamma'|\rangle \in \ker \partial_*^0$, and by exactness of the bottom sequence of Diagram A.5, there exists $\{\langle\rho\rangle\} \in \operatorname{coker}(\phi_n^i)_v$ such that

$$j_*^0\{\langle\rho\rangle\} = j\langle|\eta' - \gamma'|\rangle.$$

Furthermore, since j_*^0 is injective, this $\{\langle\rho\rangle\}$ must be unique. Note that

$$j_*^0(\,\{\langle\eta''\rangle\} - \{\langle\gamma''\rangle\}\,) = j\langle|\eta' - \gamma'|\rangle$$

from Equations A.8 and A.11. Recall from Equation A.13 that

$$j_*^0 \circ \overline{\partial_n^{i+1}}\{\langle\omega\rangle\} = j\langle|\eta' - \gamma'|\rangle.$$

By uniqueness of $\{\langle\rho\rangle\}$, we thus have

$$\{\langle\eta''\rangle\} - \{\langle\gamma''\rangle\} = \overline{\partial_n^{i+1}}\{\langle\omega\rangle\},$$

and $[\{\langle\eta''\rangle\}] = [\{\langle\gamma''\rangle\}]$. Thus, the map δ_*^i is well-defined.

Note that $\ker(\phi_{n-1}^i)_e = \bigoplus_{e \in N_\mathcal{V}} \ker \phi_{n-1}^i(e)$ and $\ker(\phi_{n-1}^i)_v = \bigoplus_{v \in N_\mathcal{V}} \ker \phi_{n-1}(v)$. Moreover, the map $\overline{\partial_{n-1}^i}$ in Diagram A.3 is the boundary map of the chain complex of the cosheaf $\ker \phi^i_{n-1}$. Thus,

$$\ker \overline{\partial^i_{n-1}} = H_1(C_\bullet \ker \phi^i_{n-1}).$$

Similarly, $\overline{\partial^{i+1}_n}$ is the boundary map of the chain complex of cosheaf $\operatorname{coker} \phi^i_n$. Thus,

$$\operatorname{coker} \overline{\partial^{i+1}_n} = H_0(C_\bullet \operatorname{coker} \phi^i_n).$$

Thus, the map $\delta^i_* : \ker \overline{\partial^i_{n-1}} \to \operatorname{coker} \overline{\partial^{i+1}_n}$ is, in fact, a map from $H_1(C_\bullet \ker \phi^i_{n-1})$ to $H_0(C_\bullet \operatorname{coker} \phi^i_n)$.

□

Lemma 15. *The map* $\delta^i_* : \ker H_1(C_\bullet \ker \phi^i_{n-1}) \to H_0(C_\bullet \operatorname{coker} \phi^i_n)$ *extends to a map* $\psi^i_* : H_1(C_\bullet \mathcal{F}^i_{n-1}) \to H_0(C_\bullet \mathcal{F}^{i+1}_n)$.

Proof. We first show that $H_1(C_\bullet \ker \phi^i_{n-1})$ is a direct summand of $H_1(C_\bullet \mathcal{F}^i_{n-1})$ and that $H_0(C_\bullet \operatorname{coker} \phi^i_n)$ is a direct summand of $H_0(C_\bullet \mathcal{F}^{i+1}_n)$. Given cosheaf morphisms $\phi^i_n : \mathcal{F}^i_n \to \mathcal{F}^{i+1}_n$ and $\phi^i_{n-1} : \mathcal{F}^i_{n-1} \to \mathcal{F}^{i+1}_{n-1}$, there exist a pair of short exact sequences of cellular cosheaves

$$0 \to \ker \phi^i_{n-1} \to \mathcal{F}^i_{n-1} \to \operatorname{coim} \phi^i_{n-1} \to 0,$$

$$0 \to \mathcal{F}^i_n \to \mathcal{F}^{i+1}_n \to \operatorname{coker} \phi^i_n \to 0.$$

The exactness is enforced cell-by-cell.

This leads to the following pair of long exact sequences of cosheaf homology

$$0 \to H_1(C_\bullet \ker \phi^i_{n-1}) \to H_1(C_\bullet \mathcal{F}^i_{n-1}) \xrightarrow{h_{n-1}} H_1(C_\bullet \operatorname{coim} \phi^i_{n-1}) \to \cdots \to 0,$$

$$0 \to \cdots \to H_0(C_\bullet \mathcal{F}_n) \xrightarrow{H_0(\phi^i_n)} H_0(C_\bullet \mathcal{F}^{i+1}_n) \to H_0(C_\bullet \operatorname{coker} \phi^i_n) \to 0.$$

We then obtain the following short exact sequence of vector spaces

$$0 \to H_1(C_\bullet \ker \phi^i_{n-1}) \to H_1(C_\bullet \mathcal{F}^i_{n-1}) \to \operatorname{im} h_{n-1} \to 0,$$

$$0 \to \operatorname{coim} H_0(\phi^i_n) \to H_0(C_\bullet \mathcal{F}^{i+1}_n) \to H_0(C_\bullet \operatorname{coker} \phi^i_n) \to 0.$$

The above short exact sequences split, so

$$H_1(C_\bullet \mathcal{F}^i_{n-1}) \cong H_1(C_\bullet \ker \phi^i_{n-1}) \oplus A^i_*. \tag{A.14}$$

$$H_0(C_\bullet \mathcal{F}^{i+1}_n) \cong H_0(C_\bullet \operatorname{coker} \phi^i_n) \oplus B^i_*, \tag{A.15}$$

where $A^i_* = \operatorname{im} h_{n-1}$ and $B^i_* = \operatorname{coim} H_0(\phi^i_n)$. Given $u \in H_1(C_\bullet \mathcal{F}^i_{n-1})$, we can write u uniquely as $u = (w_1, w_2)$, with $w_1 \in H_1(C_\bullet \ker \phi^i_{n-1})$ and $w_2 \in \operatorname{im} A^i_*$. Define $\psi^i_* : H_1(C_\bullet \mathcal{F}^i_{n-1}) \to H_0(C_\bullet \mathcal{F}^{i+1}_n)$ by $\psi^i_*(u) = \psi^i_*(w_1, w_2) = (\delta^i_*(w_1), 0)$. $\square$

A.1 Equivalence of maps ψ^i and ψ^i_*

We will show that ψ^i from Lemma 14 and ψ^i_* from Lemma 15 are the same linear transformations up to a change of basis. Recall that ψ^i was obtained by extending $\delta^i : \ker H_1(\phi^i_{n-1}) \to \operatorname{coker} H_0(\phi^i_n)$, and that ψ^i_* was obtained by extending $\delta^i_* : H_1(C_\bullet \ker \phi^i_{n-1}) \to H_0(C_\bullet \operatorname{coker} \phi^i_n)$. We will first show that δ^i and δ^i_* have the same domain and isomorphic codomain in the following lemmas.

Lemma 16. *The maps δ^i and δ^i_* have the same domain.*

Proof. consider the following commutative diagram.

$$\begin{array}{ccc} \bigoplus_{v \in N_\mathcal{V}} H_{n-1}(\mathcal{R}^i_v) & \xrightarrow{(\phi^i_{n-1})_v} & \bigoplus_{v \in N_\mathcal{V}} H_{n-1}(\mathcal{R}^{i+1}_v) \\ \partial^i_{n-1}\big\uparrow & & \partial^{i+1}_{n-1}\big\uparrow \\ \bigoplus_{e \in N_\mathcal{V}} H_{n-1}(\mathcal{R}^i_e) & \xrightarrow{(\phi^i_{n-1})_e} & \bigoplus_{e \in N_\mathcal{V}} H_{n-1}(\mathcal{R}^{i+1}_e) \end{array}$$

Let $\overline{\partial^i_{n-1}} : \ker(\phi^i_{n-1})_e \to \ker(\phi^i_{n-1})_v$ be the map induced by ∂^i_{n-1}. Then, $H_1(C_\bullet \ker \phi^i_{n-1}) = \ker \overline{\partial^i_{n-1}} = \{x \in \ker(\phi^i_{n-1})_v | \partial^i_{n-1}(x) = 0\} = \ker(\phi^i_{n-1})_e \cap \ker \partial^i_{n-1}$.

Similarly, let $H_1(\phi^i_{n-1}) : \ker \partial^i_{n-1} \to \ker \partial^{i+1}_{n-1}$ be the map induced by $(\phi^i_{n-1})_e$. Then, $\ker H_1(\phi^i_{n-1}) = \{x \in \ker \partial^i_{n-1} | (\phi^i_{n-1})_e(x) = 0\} = \ker \partial^i_{n-1} \cap \ker(\phi^i_{n-1})_e$. Thus, $H_1(C_\bullet \ker \phi^i_{n-1}) = \ker H_1(\phi^i_{n-1})$.

$\square$

To show that δ^i and δ^i_* have isomorphic codomains, we will show that both codomains are isomorphic to

$$M = \bigoplus_{v \in N_V} H_n(\mathcal{R}_v^{i+1}) / (\operatorname{im}(\phi_n^i)_v + \operatorname{im} \partial_n^{i+1}),$$

where $(\phi_n^i)_v : \bigoplus_{v \in N_V} H_n(\mathcal{R}_v^i) \to \bigoplus_{v \in N_V} H_n(\mathcal{R}_v^{i+1})$ and $\partial_n^{i+1} : \bigoplus_{e \in N_V} H_n(\mathcal{R}_e^{i+1}) \to \bigoplus_{v \in N_V} H_n(\mathcal{R}_v^{i+1})$. Recall the coset notations $\langle\ \rangle$, $\{\ \}$, and $[\ ]$ from the proof of Theorem 8. Because we will be using multiple coset notations, we will denote the notations from Theorem 8 by $\{\ \}_1$ and $[\ ]_1$. Given $\langle c \rangle$ that represents the homology class of c in $\bigoplus_{v \in N_V} H_n(\mathcal{R}_v^{i+1})$, let $\|\langle c \rangle\|$ represent the coset $\langle c \rangle + (\operatorname{im}(\phi_n^i)_v + \operatorname{im} \partial_n^{i+1})$.

Define a map $\chi_1 : \operatorname{coker} H_0(\phi_n^i) \to M$ by

$$\chi_1[\{\langle c \rangle\}_1]_1 = \|\langle c \rangle\| \tag{A.16}$$

To define a map from $H_0(C_\bullet \operatorname{coker} \phi_n^i)$ to M, recall the notations $\langle\ \rangle$, $\{\ \}$, and $[\ ]$ from proof of Theorem 11. Note that the coset notations $\{\ \}$ and $[\ ]$ in Theorem 8 and 11 are not the same. In order to distinguish the two coset notations, we will denote $\{\ \}$ and $[\ ]$ from Theorem 11 by $\{\ \}_2$ and $[\ ]_2$.

Define a map $\chi_2 : H_0(C_\bullet \operatorname{coker} \phi_n^i) \to M$ by

$$\chi_2[\{\langle c \rangle\}_2]_2 = \|\langle -c \rangle\|. \tag{A.17}$$

Note that χ_1 and χ_2 are linear.

Lemma 17. *The maps χ_1 and χ_2 are each isomorphisms.*

Proof. We first check that the map χ_1 is well defined. Assume $[\{\langle c \rangle\}_1]_1 = [\{\langle c' \rangle\}_1]_1$ in $\operatorname{coker} H_0(\phi_n^i)$. Then, there exists $\{\langle a \rangle\}_1 \in H_0(C_\bullet \mathcal{F}_n^i)$ such that $\{\langle c - c' \rangle\}_1 = H_0(\phi_n^i)\{\langle a \rangle\}_1$, i.e., $\{\langle c - c' \rangle\}_1 = \{(\phi_n^i)_v \langle a \rangle\}_1$. So there exists $\langle b \rangle \in \bigoplus_{e \in N_V} H_n(\mathcal{R}_e^{i+1})$ such that $\langle c - c' \rangle = (\phi_n^i)_v \langle a \rangle + \partial_n^{i+1} \langle b \rangle$. Note that $\|\langle c - c' \rangle\| = \|(\phi_n^i)_v \langle a \rangle + \partial_n^{i+1} \langle b \rangle\|$ is trivial by definition of the coset represented by $\|\ \|$. Thus, $\chi_1[\{\langle c \rangle\}_1]_1 = \chi_1[\{\langle c' \rangle\}_1]_1$.

We now check that χ_1 is bijective. Note that if $[\{\langle c\rangle\}_1]_1 \in \ker \chi_1$, then $\langle c\rangle \in \operatorname{im}(\phi^i_n)_v + \operatorname{im}\partial^{i+1}_n$, i.e., there exists $\langle x\rangle \in \bigoplus_{e\in N_\gamma} H_n(\mathcal{R}^{i+1}_e)$ and $\langle y\rangle \in \bigoplus_{v\in N_\gamma} H_n(\mathcal{R}^i_v)$ such that $\langle c\rangle = (\phi^i_n)_v\langle x\rangle + \partial^{i+1}_n\langle y\rangle$. Then, $\{\langle c\rangle\}_1 = \{(\phi^i_n)_v\langle x\rangle\}_1 = H_0(\phi^i_n)\{\langle x\rangle\}_1$, and $[\{\langle c\rangle\}_1]_1$ is trivial. So χ_1 is injective. One can also check that χ_1 is surjective.

One can similarly show that χ_2 is well-defined and bijective. $\square$

We will use the following Lemma to show that ψ^i and ψ^i_* are the same linear transformations up to a change of basis.

Lemma 18. *The maps $\chi_2 \circ \delta^i_*$ and $\chi_1 \circ \delta^i$ are the same maps.*

Proof. Let $\langle\gamma\rangle \in \bigoplus_{e\in N_\gamma} H_{n-1}(\mathcal{R}^i_e)$ be such that $\langle\gamma\rangle \in \ker(\phi^i_{n-1})_v \cap \ker\partial^i_{n-1}$, where

$$\begin{aligned} (\phi^i_{n-1})_e &: \bigoplus_{e\in N_\gamma} H_{n-1}(\mathcal{R}^i_e) \to \bigoplus_{e\in N_\gamma} H_{n-1}(\mathcal{R}^{i+1}_e) \\ \partial^i_{n-1} &: \bigoplus_{e\in N_\gamma} H_{n-1}(\mathcal{R}^i_e) \to \bigoplus_{v\in N_\gamma} H_{n-1}(\mathcal{R}^i_v). \end{aligned} \tag{A.18}$$

Using notations from Theorem 8, we know that $[\{\langle\gamma\rangle\}_1]_1 \in \ker H_1(\phi^i_{n-1})$, and using notations from Theorem 11, we know that $[\{\langle\gamma\rangle\}_2]_2 \in H_1(C_\bullet \ker\phi^i_{n-1})$. Recall from Equation 4.24 that $\delta^i[\{\langle\gamma\rangle\}_1]_1 = [\{\langle -e^{i+1}_n\alpha + \iota^i_n\beta\rangle\}_1]_1$, where α and β can be any elements satisfying Equations 4.22 and 4.23. From the construction of δ^i_* in Theorem 11, we will provide explicit choices for α and β that will allows us to show that $\chi_2\circ\delta^i_* = \chi_1\circ\delta^i$.

Recall from Equation A.9 that $\delta^i_*[\{\langle\gamma\rangle\}_2]_2 = [\{\langle\gamma''\rangle\}_2]_2$, where δ^i_* was constructed by

- first finding $\gamma' \in \bigoplus_{e\in N_\gamma} C_n(\mathcal{R}^{i+1}_e)$ that satisfies Equation A.7, and
- finding $\gamma'' \in \bigoplus_{v\in N_\gamma} C_n(\mathcal{R}^{i+1}_v)$ that satisfies Equation A.8.

The first step of finding γ' will allow us to choose an explicit α, and the second step of finding γ'' will allow us to choose an explicit β.

In the first step, we found $\gamma' \in \bigoplus_{e \in N_v} C_n(\mathcal{R}_e^{i+1})$ with $\partial\gamma' \in \bigoplus_{e \in N_v} C_{n-1}(\mathcal{R}_e^i)$ that satisfies Equation A.7, which, using the fact that $\partial_*^1 \langle|\gamma'|\rangle = \{\langle\partial\gamma'\rangle\}$, one can express as

$$\langle\partial\gamma'\rangle = \langle\gamma\rangle$$

in $\bigoplus_{e \in N_v} H_{n-1}(\mathcal{R}_e^i)$. So there exists $\rho \in \bigoplus_{e \in N_v} C_n(\mathcal{R}_e^i)$ such that

$$\partial\gamma' - \gamma = \partial\rho. \tag{A.19}$$

Note that in the above equation, we considered $\partial\gamma'$ as living in $\bigoplus_{e \in N_v} C_{n-1}(\mathcal{R}_e^i)$. Technically, $\partial\gamma'$ refers to an element in $\bigoplus_{e \in N_v} C_{n-1}(\mathcal{R}_e^i)$. In terms of elements in $\bigoplus_{e \in N_v} C_{n-1}(\mathcal{R}_e^i)$, the above equation can be expressed as

$$\partial\gamma' - \kappa_{n-1}^i \gamma = \kappa_{n-1}^i \circ \partial\rho. \tag{A.20}$$

The right hand side of the above equation is equal to $\partial \circ \kappa_n^i \rho$ by commutativity of Diagram A.1. Thus,

$$\partial(\gamma' - \kappa_n^i \rho) = \kappa_{n-1}^i \gamma.$$

This implies that $\gamma' - \kappa_n^i$ is a candidate for α that satisfies Equation 4.22.

Given such γ', the fact that $\gamma'' \in \bigoplus_{v \in N_v} C_n(\mathcal{R}_v^{i+1})$ satisfies Equation A.8 can be expressed by

$$\langle|\gamma''|\rangle = \langle|e_n^{i+1}\gamma'|\rangle,$$

where $|\gamma''|$ denote the coset $\gamma'' + \bigoplus_{v \in N_v} C_n(\mathcal{R}_v^i)$ and $\langle|\gamma''|\rangle$ represents the homology class of $|\gamma''|$ in $\bigoplus_{v \in N_v} H_n(\mathcal{R}_v^{i+1}, \mathcal{R}_v^i)$. Since $\langle|e_n^{i+1}\gamma' - \gamma''|\rangle$ is trivial in $\bigoplus_{v \in N_v} H_n(\mathcal{R}_v^{i+1}, \mathcal{R}_v^i)$, there exists a $\mu \in \bigoplus_{v \in N_v} C_{n+1}(\mathcal{R}_v^{i+1})$ and $\eta \in \bigoplus_{v \in N_v} C_n(\mathcal{R}_v^i)$ such that

$$e_n^{i+1}\gamma' - \gamma'' = \partial\mu + \iota_n^i \eta. \tag{A.21}$$

Recall $\rho \in \bigoplus_{e \in N_v} C_n(\mathcal{R}_e^i)$ that satisfies Equation A.19. We will show that $-e_n^i \rho + \eta$

is a choice for β. By taking the boundary of Equation A.21 and using the fact that $\partial \circ \iota_n^i \eta = \partial \eta$, we obtain

$$\partial \circ e_n^{i+1} \gamma' = \partial \eta. \tag{A.22}$$

Then,

$$\begin{aligned}
\partial(-e_n^i \rho + \eta) &= -\partial \circ e_n^i \rho + \partial \eta \\
&= -e_{n-1}^i \circ \partial \rho + \partial \circ e_n^{i+1} \gamma' \\
&= -e_{n-1}^i (\partial \gamma' - \gamma) + \partial \circ e_n^{i+1} \gamma' \\
&= -e_{n-1}^i \circ \partial \gamma' + e_{n-1}^i \gamma + \partial \circ e_n^{i+1} \gamma' \\
&= e_{n-1}^i \gamma.
\end{aligned}$$

The second equality follows from Equation A.22 and the commutativity of Diagram 4.18. The third equality follows from Equation A.19. Since $\gamma' \in \bigoplus_{e \in N_\nu} C_n(\mathcal{R}_e^{i+1})$ such that $\partial \gamma' \in \bigoplus_{e \in N_\nu} C_{n-1}(\mathcal{R}_e^i)$, the boundary of $e_n^{i+1}\gamma'$, denoted $\partial e_n^{i+1}\gamma'$, lives in $\bigoplus_{v \in N_\nu} C_{n-1}(\mathcal{R}_v^i)$ and $\partial \circ e_n^{i+1} \gamma' = e_{n-1}^i \circ \partial \gamma'$. The last equality follows from the fact that $\partial \circ e_n^{i+1} \gamma' = e_{n-1}^i \circ \partial \gamma'$. Recall that in the construction of δ in Theorem 8, we found an element β such that $\partial \beta = e_{n-1}^i \gamma$. Thus, $-e_n^i \rho + \eta$ is a choice of β that satisfies Equation 4.23.

With the choice of $\alpha = \gamma' - \kappa_n^i \rho$ and $\beta = -e_n^i \rho + \eta$, consider

$$\begin{aligned}
\chi_1 \circ \delta^i[\{\langle \gamma \rangle\}_1]_1 - \chi_2 \circ \delta_*^i[\{\langle \gamma \rangle\}_2]_2 =& \chi_1[\{\langle -e_n^{i+1}(\gamma' - \kappa_n^i \rho) + \iota_n^i(-e_n^i \rho + \eta) \rangle\}_1]_1 \\
&- \chi_2[\{\langle \gamma'' \rangle\}_2]_2 \\
=& \| \langle -e_n^{i+1} \gamma' + e_n^{i+1} \circ \kappa_n^i \rho - \iota_n^i \circ e_n^i \rho + \iota_n^i \eta \rangle \| + \| \langle \gamma'' \rangle \| \\
=& \| \langle -e_n^{i+1} \gamma' + \iota_n^i \eta + \gamma'' \rangle \| \\
=& \| \langle -\partial \mu \rangle \|.
\end{aligned}$$

The third equality follows from commutativity of Diagram 4.18. The last equality follows from Equation A.21. Thus, $\chi_2 \circ \delta_*^i[\{\langle \gamma \rangle\}_2]_2 = \chi_1 \circ \delta^i[\{\langle \gamma \rangle\}_1]_1$.

□

We now show that ψ^i and ψ^i_* are the same map under different choices of basis of $H_1(C_\bullet \mathcal{F}^i_{n-1})$ and $H_0(C_\bullet \mathcal{F}^{i+1}_n)$.

Theorem 12. *There exist isomorphisms* $\Lambda_1 : H_1(C_\bullet \mathcal{F}^i_{n-1}) \to H_1(C_\bullet \mathcal{F}^i_{n-1})$ *and* $\Lambda_2 : H_0(C_\bullet \mathcal{F}^{i+1}_n) \to H_0(C_\bullet \mathcal{F}^{i+1}_n)$ *such that* $\psi^i = \Lambda_2 \circ \psi^{i+1} \circ \Lambda_1$.

Proof. Recall that we defined $\psi^i : \ker H_1(\phi^i_{n-1}) \oplus A^i \to \operatorname{coker} H_0(\phi^i_n) \oplus B^i$ by $\psi^i(u) = \psi^i(w_1, w_2) = (\delta^i(w_1), 0)$ in Lemma 14. Similarly, we defined $\psi^i_* : H_1(C_\bullet \ker \phi^i_{n-1}) \oplus A^i_* \to H_0(C_\bullet \operatorname{coker} \phi^i_n) \oplus B^i_*$ by $\psi^i_*(u) = \psi^i_*(w_1, w_2) = (\delta^i_*(w_1), 0)$ in Lemma 15.

Recall that $\ker H_1(\phi^i_{n-1}) \oplus A^i \cong H_1(C_\bullet \mathcal{F}^i_{n-1}) \cong H_1(C_\bullet \ker \phi^i_{n-1}) \oplus A^i_*$ from Equation A.14 and Equation 4.25. Define $\Lambda_1 : \ker H_1(\phi^i_{n-1}) \oplus A^i \to H_1(C_\bullet \ker \phi^i_{n-1}) \oplus A^i_*$ by

$$\Lambda_1(w_1, w_2) = (w_1, g_1(w_2)),$$

where $g_1 : A^i \to A^i_*$ is an isomorphism. One can check that Λ_1 is an isomorphism.

Similarly, we know that $\operatorname{coker} H_0(\phi^i_n) \oplus B^i \cong H_0(C_\bullet \mathcal{F}^{i+1}_n) \cong H_0(C_\bullet \operatorname{coker} \phi^i_n) \oplus B^i_*$ from Equation A.15 and Equation 4.26. From Lemma 17, we know that $\operatorname{coker} H_0(\phi^i_n) \cong H_0(C_\bullet \operatorname{coker} \phi^i_n)$. Define $\Lambda_2 : H_0(C_\bullet \operatorname{coker} \phi^i_n) \oplus B^i_* \to \operatorname{coker} H_0(\phi^i_n) \oplus B^i$ by

$$\Lambda_2(u_1, u_2) = (\chi_1^{-1} \circ \chi_2(u_1), g_2(u_2)),$$

where χ_1 and χ_2 are defined in Equations A.16, A.17, and $g_2 : B^i \to B^i_*$ is an isomorphism. Since $\chi_1^{-1} \circ \chi_2$ and g_2 are isomorphisms, Λ_2 is an isomorphism as well.

From Lemma 18, we know that $\delta^i = \chi_1^{-1} \circ \chi_2 \circ \delta^i_*$. Thus,

$$\begin{aligned}
\Lambda_2 \circ \psi^i_* \circ \Lambda_1(w_1, w_2) &= \Lambda_2 \circ \psi^i_*(w_1, g_1(w_2)) \\
&= \Lambda_2(\delta^i_*(w_1), 0) \\
&= (\chi_1^{-1} \circ \chi_2 \circ \delta^i_*(w_1), 0) \\
&= (\delta^i(w_1), 0) \\
&= \psi^i(w_1, w_2),
\end{aligned}$$

i.e., the following diagram commutes.

$$\begin{tikzcd}
\ker H_1(\phi^i_{n-1}) \oplus A^i \arrow[r, "\psi^i"] \arrow[d, "\Lambda_1"] & \operatorname{coker} H_0(\phi^i_n) \oplus B^i \\
H_1(C_\bullet \ker \phi^i_{n-1}) \oplus A^i_* \arrow[r, "\psi^i_*"] & H_0(C_\bullet \operatorname{coker} \phi^i_n) \oplus B^i_* \arrow[u, "\Lambda_2"']
\end{tikzcd}$$

Thus, regardless of which homology we take first from Diagram 4.19, we end up constructing the same maps ψ^i and ψ^i_* under different choices of basis of $H_1(C_\bullet \mathcal{F}^i_{n-1})$ and $H_0(C_\bullet \mathcal{F}^{i+1}_n)$.

$\square$

Appendix B

Details of Proofs

B.1 Details of proof for Theorem 8

For the proof, we drop the superscripts for α^{i+1} and β^i. It should be understood that $\alpha = \alpha^{i+1}$ and $\beta = \beta^i$.

We will first check that $-e_n^{i+1}\alpha + \iota_n^i\beta$ represents an element in $\operatorname{coker} H_0(\phi_n^i)$. Note that

$$
\begin{aligned}
\partial(-e_n^{i+1}\alpha + \iota_n^i\beta) &= -e_{n-1}^{i+1} \circ \partial\alpha + \iota_{n-1}^i \circ \partial\beta \\
&= -e_{n-1}^{i+1} \circ \kappa_{n-1}^i\gamma + \iota_{n-1}^i \circ e_{n-1}^i\gamma \\
&= 0,
\end{aligned}
$$

which follows from Equation 4.22, Equation 4.23, and the commutativity of Diagram 4.18. Thus, $-e_n^{i+1}\alpha + \iota_n^i\beta$ represents an element in $\bigoplus_{v\in N_\mathcal{V}} H_n(\mathcal{R}_v^{i+1})$, and $[\{\langle -e_n^{i+1}\alpha + \iota_n^i\beta\rangle\}]$ represents an element in $\operatorname{coker} H_0(\phi_n^i)$.

We now show that δ^i (Equation 4.24) is well defined. Let $\alpha' \in \bigoplus_{e\in N_\mathcal{V}} C_n(\mathcal{R}_e^{i+1})$ be a different choice of α that satisfies Equation 4.22:

$$\partial\alpha' = \kappa_{n-1}^i\gamma.$$

Note that $\partial(\alpha - \alpha') = \kappa_{n-1}^i\gamma - \kappa_{n-1}^i\gamma = 0$. So $\langle \alpha - \alpha' \rangle$ represents an element in $\bigoplus_{e\in N_\mathcal{V}} H_n(\mathcal{R}_e^{i+1})$. Then, $\langle e_n^{i+1}(\alpha - \alpha')\rangle = \partial_n^{i+1}\langle \alpha - \alpha'\rangle \in \operatorname{im} \partial_n^{i+1}$. So $\{\langle e_n^{i+1}(\alpha - \alpha')\rangle\}$ is trivial in $H_0(C_\bullet\mathcal{F}_n^{i+1})$. Hence, $\{\langle -e_n^{i+1}\alpha + \iota_n^i\beta\rangle\}$ and $\{\langle -e_n^{i+1}\alpha' + \iota_n^i\beta\rangle\}$ represent homologous elements in $H_0(C_\bullet\mathcal{F}_n^{i+1})$. Thus, $[\{\langle -e_n^{i+1}\alpha + \iota_n^i\beta\rangle\}] = [\{\langle -e_n^{i+1}\alpha' + \iota_n^i\beta\rangle\}]$ in $\operatorname{coker} H_0(\phi_n^i)$.

Similarly, let $\beta' \in \bigoplus_{v\in N_\mathcal{V}} C_n(\mathcal{R}_v^i)$ be a different choice of β that satisfies Equation 4.23:

$$\partial\beta' = e_{n-1}^i\gamma.$$

Note that $\partial(\beta - \beta') = e_{n-1}^i(\gamma - \gamma) = 0$, and $\langle\beta - \beta'\rangle$ represents an element of $\bigoplus_{v\in N_\mathcal{V}} H_n(\mathcal{R}_v^i)$. Then, $\{\langle\iota_n^i(\beta - \beta')\rangle\} = \{(\phi_n^i)_v\langle\beta - \beta'\rangle\} = H_0(\phi_n^i)\{\langle\beta - \beta'\rangle\} \in \operatorname{im} H_0(\phi_n^i)$. Thus, $[\{\langle\iota_n^i(\beta - \beta')\rangle\}]$ is trivial in $\operatorname{coker} H_0(\phi_n^i)$. Hence, $[\{\langle -e_n^{i+1}\alpha + \iota_n^i\beta\rangle\}] = [\{\langle -e_n^{i+1}\alpha + \iota_n^i\beta'\rangle\}]$ in $\operatorname{coker} H_0(\phi_n)$. Thus, given different choices β' and α', we have $[\{\langle -e_n^{i+1}\alpha + \iota_n^i\beta\rangle\}] = [\{\langle -e_n^{i+1}\alpha' + \iota_n^i\beta'\rangle\}]$.

Lastly, consider a different coset representative $\gamma' \in \bigoplus_{e\in N_\mathcal{V}} C_{n-1}(\mathcal{R}_e^i)$ of $[\{\langle\gamma\rangle\}]$, i.e., $[\{\langle\gamma\rangle\}] = [\{\langle\gamma'\rangle\}]$. Then, there exists $\omega \in \bigoplus_{e\in N_\mathcal{V}} C_n(\mathcal{R}_e^i)$ such that

$$\gamma - \gamma' = \partial\omega. \tag{B.1}$$

Assume that

$$\begin{aligned} \delta^i[\{\langle\gamma\rangle\}] &= [\{\langle -e_n^{i+1}\alpha + \iota_n^i\beta\rangle\}] \\ \delta^i[\{\langle\gamma'\rangle\}] &= [\{\langle -e_n^{i+1}\alpha' + \iota_n^i\beta'\rangle\}] \end{aligned} \tag{B.2}$$

for some $\alpha, \alpha' \in \bigoplus_{e\in N_\mathcal{V}} C_n(\mathcal{R}_e^{i+1})$, $\beta, \beta' \in \bigoplus_{v\in N_\mathcal{V}} C_n(\mathcal{R}_v^i)$. We will use the following fact that $\alpha - \alpha' - \kappa_n^i\omega$ and $\beta - \beta' - e_n^i\omega$ are cycles, which can be shown from Equations 4.22, 4.23, B.1, and Diagram 4.18.

$$\begin{aligned} \partial(\alpha - \alpha' - \kappa_n^i\omega) &= \kappa_{n-1}^i(\gamma - \gamma' - \partial\omega) = 0, \\ \partial(\beta - \beta' - e_n^i\omega) &= e_{n-1}^i(\gamma - \gamma' - \partial\omega) = 0. \end{aligned} \tag{B.3}$$

One can show that

$$
\begin{aligned}
[\{\langle -e_n^{i+1}(\alpha-\alpha')+\iota_n^i(\beta-\beta')\rangle\}] =&[\{\langle -e_n^{i+1}(\alpha-\alpha')+\iota_n^i(\beta-\beta') \\
&+\iota_n^i\circ e_n^i\omega-\iota_n^i\circ e_n^i\omega\rangle\}] \\
=&[\{\langle -e_n^{i+1}(\alpha-\alpha')+\iota_n^i(\beta-\beta') \\
&+e_n^{i+1}\circ\kappa_n^i\omega-\iota_n^i\circ e_n^i\omega\rangle\}] \\
=&[\{\langle -e_n^{i+1}(\alpha-\alpha'-\kappa_n^i\omega)\rangle\}]+[\{\langle \iota_n^i(\beta-\beta'-e_n^i\omega)\rangle\}] \\
=&[\{\langle 0\rangle\}].
\end{aligned} \tag{B.4}
$$

The second equality follows from commutativity of Diagram 4.18. The third equality follows from the fact that $e_n^{i+1}(\alpha-\alpha'-\kappa_n^i\omega)$ and $\iota_n^i(\beta-\beta'-e_n^i\omega)$ are cycles, which follows from Equation B.3 and Diagram 4.18. To show the last equality of Equation B.4, note that

$$
\begin{aligned}
\langle e_n^{i+1}(\alpha-\alpha'-\kappa_n^i\omega)\rangle &= \partial_n^{i+1}\langle \alpha-\alpha'-\kappa_n^i\omega\rangle \in \operatorname{im}\partial_n^{i+1}, \\
\{\langle \iota_n^i(\beta-\beta'-e_n^i\omega)\rangle\} &= H_0(\phi_n^i)\{\langle \beta-\beta'-e_n^i\omega\rangle\} \in \operatorname{im} H_0(\phi_n^i).
\end{aligned} \tag{B.5}
$$

Thus, both $[\{\langle e_n^{i+1}(\alpha-\alpha'-\kappa_n^i\omega)\rangle\}]$ and $[\{\langle \kappa_n^i(\beta-\beta'-e_n^i\omega)\rangle\}]$ are trivial in $\operatorname{coker} H_0(\phi_n^i)$. This shows that $\delta^i[\{\langle\gamma\rangle\}]=\delta^i[\{\langle\gamma'\rangle\}]$. Thus, the map δ^i is well defined.

B.2 Proof of well-definedness of map ψ^i

We show that the maps $\psi^i : H_1(C_\bullet\mathcal{F}_{n-1}^i)\to H_0(C_\bullet\mathcal{F}_n^{i+1})$ defined in Equations 4.34 and 4.44 are well-defined maps.

Proof. We omit the superscripts for α^{i+1} and β^i.

Recall that for each basis $\{\langle b^*\rangle\}\in\mathcal{B}^i$, the map ψ^i was defined as

$$\psi^i\{\langle b^*\rangle\}=\{\langle -e_n^{i+1}\alpha+\iota_n^i\beta^*\rangle\},$$

where $\alpha \in \bigoplus_{e \in N_{\mathcal{V}}} C_n(\mathcal{R}_e^{i+1})$ satisfies

$$\partial \alpha = \kappa_{n-1}^i b^*,$$

and β^* is the element defined by

$$\beta^* = \Gamma^i\{\langle b^* \rangle\}.$$

Recall that β^* satisfies

$$\partial \beta^* = e_{n-1}^i b^*.$$

We first show that $-e_n^{i+1}\alpha + \iota_n^i \beta^*$ actually defines an element in $H_0(C_\bullet \mathcal{F}_n^{i+1})$. One can check that

$$\begin{aligned}
\partial(-e_n^{i+1}\alpha + \iota_n^i \beta^*) &= -e_{n-1}^{i+1} \circ \partial \alpha + \iota_{n-1}^i \circ \partial \beta^* \\
&= -e_{n-1}^{i+1} \circ \kappa_{n-1}^i b^* + \iota_{n-1}^i \circ e_{n-1}^i b^* \\
&= 0
\end{aligned}$$

from the commutativity of Diagram 4.30. Thus, $\{\langle -e_n^{i+1}\alpha + \iota_n^i \beta^* \rangle\}$ does represent an element of $H_0(C_\bullet \mathcal{F}_n^{i+1})$.

We now show that the map ψ^i is well-defined. By construction, it suffices to show that ψ^i is well-defined on each basis $\{\langle b^* \rangle\} \in \mathcal{B}^i$. When defining

$$\psi^i\{\langle b^* \rangle\} = \{\langle -e_n^{i+1}\alpha + \iota_n^i \beta^* \rangle\},$$

note that β^* was a fixed element given by $\Gamma^i\{\langle b^* \rangle\} = \beta^*$. However, there may be other choices of $\alpha' \in \bigoplus_{e \in N_{\mathcal{V}}} C_n(\mathcal{R}_e^{i+1})$ that satisfy $\partial \alpha = \kappa_{n-1}^i b^*$. Note that

$$\partial(\alpha' - \alpha) = \kappa_{n-1}^i b^* - \kappa_{n-1}^i b^* = 0,$$

i.e., $\langle \alpha' - \alpha \rangle$ represents an element in $\bigoplus_{e \in N_{\mathcal{V}}} H_n(\mathcal{R}_e^{i+1})$.

Then,

$$\begin{aligned}\langle -e_n^{i+1}\alpha + \iota_n^i \beta^* \rangle - \langle -e_n^{i+1}\alpha' + \iota_n^i \beta^* \rangle &= \langle e_n^{i+1}(\alpha' - \alpha) \rangle \\ &= \partial_n^{i+1} \langle \alpha' - \alpha \rangle\end{aligned}$$

Since $\partial_n^{i+1}\langle \alpha' - \alpha \rangle \in \operatorname{im} \partial_n^{i+1}$, then $\{\langle -e_n^{i+1}\alpha + \iota_n^i \beta^* \rangle - \langle -e_n^{i+1}\alpha' + \iota_n^i \beta^* \rangle\}$ is trivial in $H_0(C_\bullet \mathcal{F}_n^{i+1})$. Thus, $\{\langle -e_n^{i+1}\alpha + \iota_n^i \beta^* \rangle\}$ and $\{\langle -e_n^{i+1}\alpha' + \iota_n^i \beta^* \rangle\}$ represent homologous elements in $H_0(C_\bullet \mathcal{F}_n^{i+1})$, and $\psi^i\{\langle b^* \rangle\}$ is well-defined for each basis $\{\langle b^* \rangle\} \in \mathcal{B}^i$. Thus, ψ^i is well-defined. □

B.3 Obtaining basis $\mathcal{C}_{\mathbf{im}}^i$ from basis $\mathcal{B}_A^{i-1}$ of A^{i-1}.

Lemma 19. *Let $\mathcal{B}^{i-1} = \mathcal{B}_A^{i-1} \oplus \mathcal{B}_{\ker}^{i-1}$ be a basis of $H_1(C_\bullet \mathcal{F}_{n-1}^{i-1}) = A^{i-1} \oplus \ker H_1(\phi_{n-1}^{i-1})$. Let $\mathcal{B}_A^{i-1} = \{\{\langle b_1 \rangle\}, \ldots, \{\langle b_m \rangle\}\}$ be the basis of A^{i-1}. Then, $\{\langle \kappa_{n-1}^{i-1} b_1 \rangle\}, \ldots, \{\langle \kappa_{n-1}^{i-1} b_m \rangle\}$ is linearly independent in $H_1(C_\bullet \mathcal{F}_{n-1}^i)$.*

Proof. Assume not, i.e., assume that

$$c_1\{\langle \kappa_{n-1}^{i-1} b_1 \rangle\} + \cdots + c_m\{\langle \kappa_{n-1}^{i-1} b_m \rangle\} = \{\langle 0 \rangle\}$$

for some $c_1, \ldots, c_m$ that are not all zero. By construction, this implies that

$$c_1\langle \kappa_{n-1}^{i-1} b_1 \rangle + \cdots + c_m\langle \kappa_{n-1}^{i-1} b_m \rangle = \langle 0 \rangle$$

for some $c_1, \ldots, c_m$ that are not all zero. Then, $\langle c_1 b_1 + \ldots c_m b_m \rangle \in \ker H_1(\phi_{n-1}^{i-1})$. Note that $\langle c_1 b_1 + \ldots c_m b_m \rangle \in A^{i-1}$ as well since A^{i-1} is a subspace of $H_1(C_\bullet \mathcal{F}_{n-1}^{i-1})$. This contradicts the fact that $H_1(C_\bullet \mathcal{F}_{n-1}^{i-1})$ is a direct sum of $\ker H_1(\phi_{n-1})$ and A. Thus, $\{\langle \kappa_{n-1}^{i-1} b_1 \rangle\}, \ldots, \{\langle \kappa_{n-1}^{i-1} b_m \rangle\}$ are linearly independent. □

B.4 Details of proof of Theorem 9

We show that the map $\Psi^i_{\text{Tot}} : H_n(\text{Tot}^i) \to H_n(\mathcal{R}^i)$ is well-defined and bijective. For the proof, we omit the superscript i indicating the parameter ϵ_i.

Proof. We first show that Ψ_{Tot} is a well-defined map. Assume that $[x_1, y_1] = [x_2, y_2]$ in $H_n(\text{Tot})$. Recall that $j_n : \bigoplus_{v \in N_\mathcal{V}} C_n(\mathcal{R}_v) \to C_n(\mathcal{R})$ is the map into the left column in Diagram 4.2. Recall from Diagram 4.2 that the following rows are exact.

$$\begin{tikzcd}
0 & C_{n+1}(\mathcal{R}) \arrow[l] \arrow[d, "\partial"] & \bigoplus_{v \in N_\mathcal{V}} C_{n+1}(\mathcal{R}_v) \arrow[l, "j_{n+1}"'] \arrow[d, "\partial"] & \bigoplus_{e \in N_\mathcal{V}} C_{n+1}(\mathcal{R}_e) \arrow[l] \arrow[d, "\partial"] & 0 \arrow[l] \\
0 & C_n(\mathcal{R}) \arrow[l] & \bigoplus_{v \in N_\mathcal{V}} C_n(\mathcal{R}_v) \arrow[l, "j_n"'] & \bigoplus_{e \in N_\mathcal{V}} C_n(\mathcal{R}_e) \arrow[l, "e_n"'] & 0 \arrow[l]
\end{tikzcd} \tag{B.6}$$

Since $[x_1, y_1] = [x_2, y_2]$ in $H_n(\text{Tot})$, there exists $p_{n+1} \in \bigoplus_{v \in N_\mathcal{V}} C_{n+1}(\mathcal{R}_v)$ and $q_n \in \bigoplus_{e \in N_\mathcal{V}} C_n(\mathcal{R}_e)$ such that $y_2 - y_1 = \partial q_n$ and $x_2 - x_1 = \partial p_{n+1} + (-1)^{n+1} e_n q$. Then,

$$\begin{aligned}
j_n(x_2 - x_1) =& j_n(\partial p_{n+1} + (-1)^{n+1} e_n q) \\
=& j_n(\partial p_{n+1}) \\
=& \partial(j_{n+1}(p_{n+1})).
\end{aligned}$$

The second equality follows from the fact that $j_n \circ e_n(q) = 0$, which follows from exactness of Diagram B.6. Thus, $[j_n(x_2)] = [j_n(x_1)]$, and the map Ψ_{Tot} is well-defined.

We now show that Ψ_{Tot} is surjective. Let $[\gamma] \in H_n(\mathcal{R})$. Recall from Diagram 4.2 that the following rows are exact.

$$\begin{tikzcd}
0 & C_n(\mathcal{R}) \arrow[l] \arrow[d, "\partial"] & \bigoplus_{v\in N_{\mathcal{V}}} C_n(\mathcal{R}_v) \arrow[l, "j_n"'] \arrow[d, "\partial"] & \bigoplus_{e\in N_{\mathcal{V}}} C_n(\mathcal{R}_e) \arrow[l] \arrow[d, "\partial"] & 0 \arrow[l] \\
0 & C_{n-1}(\mathcal{R}) \arrow[l] \arrow[d, "\partial"] & \bigoplus_{v\in N_{\mathcal{V}}} C_{n-1}(\mathcal{R}_v) \arrow[l, "j_{n-1}"'] \arrow[d, "\partial"] & \bigoplus_{e\in N_{\mathcal{V}}} C_{n-1}(\mathcal{R}_e) \arrow[l, "e_{n-1}"'] \arrow[d, "\partial"] & 0 \arrow[l] \\
0 & C_{n-2}(\mathcal{R}) \arrow[l] & \bigoplus_{v\in N_{\mathcal{V}}} C_{n-2}(\mathcal{R}_v) \arrow[l, "j_{n-2}"'] & \bigoplus_{e\in N_{\mathcal{V}}} C_{n-2}(\mathcal{R}_e) \arrow[l, "e_{n-2}"'] & 0 \arrow[l]
\end{tikzcd} \tag{B.7}$$

Then, there exists $\gamma_n \in \bigoplus_{v\in N_{\mathcal{V}}} C_n(\mathcal{R}_v)$ such that $\gamma = j_n(\gamma_n)$. Then,

$$j_{n-1} \circ \partial\gamma_n = \partial \circ j_n(\gamma_n) = \partial\gamma = 0.$$

So $\partial\gamma_n \in \ker j_{n-1}$, and by exactness, there exists $\gamma_{n-1} \in \bigoplus_{e\in N_{\mathcal{V}}} C_{n-1}(\mathcal{R}_e^{\epsilon})$ such that $e_{n-1}(\gamma_{n-1}) = \partial\gamma_n$. Moreover,

$$e_{n-2} \circ \partial\gamma_{n-1} = \partial \circ e_{n-1}\gamma_{n-1} = \partial\partial\gamma_n = 0.$$

Since e_{n-2} is injective, we know that $\partial\gamma_{n-1} = 0$. Then, $\Psi_{\text{Tot}}[\gamma_n, \gamma_{n-1}] = [\gamma]$. Thus, Ψ_{Tot} is surjective.

Lastly, we show that Ψ_{Tot} is injective. Assume that $\Psi_{\text{Tot}}([x, y]) = 0$. Then, there exists $p_{n+1} \in C_{n+1}(\mathcal{R})$ such that $\partial p_{n+1} = j_n(x)$. Since the rows of Diagram B.6 are exact, j_n and j_{n+1} are surjective maps. Thus, there exists $p'_{n+1} \in \bigoplus_{v\in N_{\mathcal{V}}} C_{n+1}(\mathcal{R}_v)$ such that $p_{n+1} = j_{n+1}(p'_{n+1})$. Then,

$$
\begin{aligned}
j_n(\partial p'_{n+1} - x) &= j_n \circ \partial p'_{n+1} - j_n(x) \\
&= \partial \circ j_{n+1}(p'_{n+1}) - j_n(x) \\
&= \partial p_{n+1} - j_n(x) \\
&= 0.
\end{aligned}
$$

Thus, $\partial p'_{n+1} - x \in \ker j_n$. Again, from exactness of the rows of Diagram B.6, there exists $q_n \in \bigoplus_{e \in N_\mathcal{V}} C_n(\mathcal{R}_e)$ such that $\partial p'_{n+1} - x = e_n(q_n)$.

Note that

$$\partial(\partial p'_{n+1} - x) = \partial e_n(q_n),$$

while the left hand side of above is equal to $-\partial x = -(-1)^{n+1} e_n(y)$ by definition. Then, $e_n \partial q_n = \partial e_n(q_n) = -\partial x = -(-1)^{n+1} e_n(y)$. Since e_n is injective, this implies that $\partial q_n = -(-1)^{n+1} y$. Let $q'_n = -(-1)^{n+1} q_n$, so that $\partial q'_n = y$.

Thus, we have $p'_{n+1} \in \bigoplus_{v \in N_\mathcal{V}} C_{n+1}(\mathcal{R}_v)$ and $q'_n \in \bigoplus_{e \in N_\mathcal{V}} C_n(\mathcal{R}_e)$ such that

$$\partial q'_n = y$$

and

$$x = \partial p'_{n+1} - e_n(q_n) = \partial p'_{n+1} - e_n(-(-1)^{n+1} q'_n) = \partial p'_{n+1} + (-1)^{n+1} e_n q'_n.$$

Thus, $[x, y] = 0$ in $H_n(\mathrm{Tot})$, and Ψ_{Tot} is injective. □

B.5 Details of proof of Theorem 10

We provide proofs that the map $\Phi^i : H_0(C_\bullet \mathcal{F}^i_n) \oplus H_1(C_\bullet \mathcal{F}^i_{n-1}) \to H_n(\mathrm{Tot}^i)$ defined in Theorem 10 is well-defined and bijective. For the remainder of the proof, we omit the superscript i indicating the parameter ϵ_i.

Proof. We first show that Φ is well-defined. Assume that $(\{\langle x\rangle\},\{\langle y\rangle\}) = (\{\langle x'\rangle\},\{\langle y'\rangle\})$ in $H_0(C_\bullet\mathcal{F}_n)\oplus H_1(C_\bullet\mathcal{F}_{n-1})$, i.e., $\{\langle x\rangle\} = \{\langle x'\rangle\}$ in $H_0(C_\bullet\mathcal{F}_n)$ and $\{\langle y\rangle\} = \{\langle y'\rangle\}$ in $H_1(C_\bullet\mathcal{F}_{n-1})$.

Let $\mathcal{B}$ be the fixed basis of $H_1(C_\bullet\mathcal{F}_{n-1})$ given by

$$\mathcal{B} = \{\{\langle b_1^*\rangle\},\dots,\{\langle b_m^*\rangle\}\}.$$

We can express $\{\langle y\rangle\}$ and $\{\langle y'\rangle\}$ in terms of the basis $\mathcal{B}^i$, as

$$\{\langle y\rangle\} = \{\langle y'\rangle\} = \{\langle c_1b_1^* + \cdots + c_mb_m^*\rangle\}.$$

Then, by construction,

$$\begin{aligned}\Phi(\{\langle y\rangle\}) &= [(-1)^{n+1}(c_1\beta_1^* + \cdots + c_m\beta_m^*), c_1b_1^* + \cdots + c_mb_m^*] \\ &= \Phi(\{\langle y'\rangle\})\end{aligned}$$

Then,

$$\begin{aligned}\Phi(\{\langle x\rangle\},\{\langle y\rangle\}) - \Phi(\{\langle x'\rangle\},\{\langle y'\rangle\}) &= \Phi(\{\langle x\rangle\}) - \Phi(\{\langle x'\rangle\}) \\ &= [x - x', 0].\end{aligned}$$

Since $\{\langle x\rangle\} = \{\langle x'\rangle\}$ in $H_0(C_\bullet\mathcal{F}_n)$, there exists $p_{n+1} \in \bigoplus_{v\in N_\mathcal{V}} C_{n+1}(\mathcal{R}_v)$ such that $\partial p_{n+1} = x - x'$. Thus, $[x - x', 0]$ is trivial in $H_n(\mathrm{Tot})$, and Φ is a well-defined map.

We now show that Φ is surjective. Given $[x, y] \in H_n(\mathrm{Tot})$, we know that $\partial(y) = 0$, so $\{\langle y\rangle\}$ is an element of $H_1(C_\bullet\mathcal{F}_{n-1})$. In terms of this fixed basis $\mathcal{B}^i$ of $H_1(C_\bullet\mathcal{F}_{n-1})$, we can express $\{\langle y\rangle\}$ as

$$\{\langle y\rangle\} = \{\langle c_1b_1^* + \cdots + c_mb_m^*\rangle\}.$$

Then, there exists $q_n \in \bigoplus_{e\in N_\mathcal{V}} C_n(\mathcal{R}_e)$ such that

$$c_1b_1^* + \cdots + c_mb_m^* - y = \partial q_n. \tag{B.8}$$

Recall from Equation 4.55 that $\Phi\{\langle b_j^* \rangle\} = [(-1)^{n+1}\beta_j^*, b_j^*]$, where $\beta_j^* \in \bigoplus_{v \in N_\mathcal{V}} C_n(\mathcal{R}_v)$ satisfies

$$\partial \beta_j^* = e_{n-1} b_j^*, \tag{B.9}$$

where $e_n : \bigoplus_{e \in N_\mathcal{V}} C_n(\mathcal{R}_e) \to \bigoplus_{v \in N_\mathcal{V}} C_n(\mathcal{R}_v)$ is an inclusion map.

Let

$$r_n = x - (-1)^{n+1}(c_1\beta_1^* + \cdots + c_m\beta_m^*) + (-1)^{n+1}e_n(q_n).$$

Note that

$$\begin{aligned}
\partial r_n &= \partial x - (-1)^{n+1}\partial(c_1\beta_1^* + \cdots + c_m\beta_m^*) + (-1)^{n+1}\partial e_n(q_n) \\
&= (-1)^{n-1}e_{n-1}(y) - (-1)^{n+1}e_{n-1}(c_1 b_1^* + \cdots + c_m b_m^*) + (-1)^{n+1}e_{n-1}\partial q_n \\
&= (-1)^{n+1}e_{n-1}(y) - (-1)^{n+1}e_{n-1}(c_1 b_1^* + \cdots + c_m b_m^*) + (-1)^{n+1}e_{n-1}\partial q_n \\
&= 0,
\end{aligned}$$

which follows from commutativity of Diagram 4.30, Equation B.9, and Equation B.8. Thus, $\{\langle r_n \rangle\}$ represents an element of $H_0(C_\bullet \mathcal{F}_n)$. Then,

$$\begin{aligned}
\Phi(\{\langle r_n \rangle\} + \{\langle y \rangle\}) &= [r_n, 0] + [(-1)^{n+1}(c_1\beta_1^* + \cdots + c_m\beta_m^*), c_1 b_1^* + \cdots + c_m b_m^*] \\
&= [x + (-1)^{n+1}e_n(q_n), y + \partial q_n] \\
&= [x, y] + [(-1)^{n+1}e_n(q_n), \partial q_n] \\
&= [x, y]
\end{aligned}$$

Thus, Φ is surjective.

Lastly, we show that Φ is injective. Let $(\{\langle x \rangle\}, \{\langle y \rangle\}) \in H_0(C_\bullet \mathcal{F}_n) \oplus H_1(C_\bullet \mathcal{F}_{n-1})$. Assume that $\Phi(\{\langle x \rangle\}, \{\langle y \rangle\}) = 0$. Again, in terms of the fixed basis $\mathcal{B}$ of $H_1(C_\bullet \mathcal{F}_{n-1})$, we can express $\{\langle y \rangle\}$ as

$$\{\langle y \rangle\} = \{\langle c_1 b_1^* + \cdots + c_m b_m^* \rangle\}.$$

Then $\Phi(\{\langle y\rangle\}) = [(-1)^{n+1}(c_1\beta_1^* + \cdots + c_m\beta_m^*), c_1b_1^* + \cdots + c_mb_m^*]$, and

$$\Phi(\{\langle x\rangle\}, \{\langle y\rangle\}) = [x + (-1)^{n+1}(c_1\beta_1 + \cdots + c_m\beta_m), c_1b_1^* + \cdots + c_mb_m^*].$$

If $\Phi(\{\langle x\rangle\}, \{\langle y\rangle\}) = 0$, then there exists $q_n \in \bigoplus_{e\in N_\mathcal{V}} C_n(\mathcal{R}_e)$ and $p_{n+1} \in \bigoplus_{v\in N_\mathcal{V}} C_{n+1}(\mathcal{R}_v)$ such that

$$\partial q_n = c_1b_1^* + \cdots + c_mb_m^*, \tag{B.10}$$

$$(-1)^{n-1}e_nq_n + \partial p_{n+1} = x + c_1\beta_1^* + \cdots + c_m\beta_m^*. \tag{B.11}$$

Then, from Equation B.10, we know that $\{\langle c_1b_1^* + \cdots + c_mb_m^*\rangle\} = \{\langle y\rangle\}$ is trivial in $H_1(C_\bullet\mathcal{F}_{n-1})$. Thus, $\Phi(\{\langle x\rangle\}, \{\langle y\rangle\}) = \Phi(\{\langle x\rangle\}) = [x, 0]$.

If $[x, 0]$ is trivial in $H_n(\mathrm{Tot})$, then there exists $q_n \in \bigoplus_{e\in N_\mathcal{V}} C_n(\mathcal{R}_e)$ and $p_{n+1} \in \bigoplus_{v\in N_\mathcal{V}} C_{n+1}(\mathcal{R}_v)$ such that

$$\partial q_n = 0,$$

$$(-1)^{n-1}e_nq_n + \partial p_{n+1} = x.$$

The above two equations imply that $\{\langle x\rangle\}$ is trivial in $H_0(C_\bullet\mathcal{F}_n)$. Thus, Φ is injective.

□

Bibliography

[1] S. Abramsky et al. “Contextuality, cohomology and paradox”. In: *24th EACSL Annual Conference on Computer Science Logic (CSL 2015)*. Ed. by Stephan Kreutzer. Vol. 41. Leibniz International Proceedings in Informatics (LIPIcs). Dagstuhl, Germany: Schloss Dagstuhl – Leibniz-Zentrum für Informatik, 2015, pp. 211–228.

[2] H. Adamns and G. Carlsson. “Evasion paths in mobile sensor networks”. In: *The International Journal of Robotics Research* 34.1 (2014), pp. 90–104.

[3] E. Begle. “The Vietoris mapping theorem for bigompact spaces”. In: *Annals of Mathematics* 51.3 (1950).

[4] K. Borsuk. “On the imbedding of systems of compacta in simplicial complexes”. In: *Fundamenta Mathematicae* 35 (1948), pp. 217–234.

[5] R. Bott and L. W. Tu. *Differential forms in algebraic topology*. Springer New York, 1995.

[6] G. E. Bredon. *Sheaf theory*. Springer-Verlag New York, 1997.

[7] G. Carlsson. “Topology and data”. In: *Bulletin of the American Mathematical Society* 46 (2009), pp. 255–308.

[8] G. Carlsson and V. de Silva. “Zigzag persistence”. In: *Foundations of Computational Mathematics* 10.4 (2010), pp. 367–405.

[9] D. Cohen-Steiner et al. “Stability of persistence diagrams”. In: *Discrete & Computational Geometry* 37.1 (2007), pp. 103–120.

[10] J. Curry. “Sheaves, cosheaves and applications”. PhD thesis. University of Pennsylvania, 2014.

[11] J. Curry, R. Ghrist, and V. Nanda. “Discrete Morse theory for computing cellular sheaf cohomology”. In: *Foundations of Computational Mathematics* (2015).

[12] H. Derksen and J. Weyman. “Quiver representations”. In: *Notices of the AMS* 52.2 (2005), pp. 200–206.

[13] H. Edelsbrunner et al. “Topological persistence and simplification”. In: *Discrete & Computational Geometry* 28.4 (2002), pp. 511–533.

[14] R. Ghrist. “Barcodes: the persistent topology of data”. In: *Bulletin of the American Mathematical Society* 45 (2008), pp. 61–75.

[15] R. Ghrist and S. Krishnan. “Positive alexander duality for pursuit and evasion”. In: *SIAM Journal on Applied Algebra and Geometry* 1.1 (2017), pp. 308–327.

[16] C. Giusti et al. “Clique topology reveals intrinsic geometric structure in neural correlations”. In: *Proceedings of the National Academy of Sciences USA* 112.44 (2015), pp. 13455–13460.

[17] G. Henselman and R. Ghrist. “Matroid filtrations and computational persistent homology”. In: *arXiv:1606.00199* (2016).

[18] D. König. *Theorei der endlichen und unendlichen Graphen: kombinatorische Topologie der Streckenkomplexe*. Akademische Verlagsgesellschaft, 1936.

[19] S. Mac Lane. *Categories for the working mathematician*. Springer-Verlag New York, 1971.

[20] J. Leray. “L’anneau spectral et l’anneau filtré d’homologie d’un espace localement compact et d’une application continue”. In: *J. Math. Pures Appl* 29 (1950), pp. 1–139.

[21] John McCleary. *A user’s guide to spectral sequences*. Cambridge University Press, 2000.

[22] M. Nicolau, A. J. Levine, and G. Carlsson. "Topology based data analysis identifies a subgroup of breast cancers with a unique mutational profile and excellent survival". In: *Proceedings of the National Academy of Sciences of the United States of America* 108.17 (2011), pp. 7265–7270.

[23] N. Otter et al. "A roadmap for the computation of persistent homology". In: *EPJ Data Science* 6.1 (2017).

[24] A. Shepard. "A cellular description of the derived category of a stratified space". PhD thesis. Brown University, 1985.

[25] V. de Silva and R. Ghrist. "Coordinate-free coverage in sensor networks with controlled boundaries via Homology". In: *International Journal of Robotics Research* 25.12 (2006), pp. 1205–1222.

[26] V. de Silva and R. Ghrist. "Coverage in sensor networks via persistent homology". In: *Algebraic & Geometric Topology* 7 (2007), pp. 339–358.

[27] L. Vietoris. "Über den höheren Zusammenhang kompakter Räume und eine Klasse von zusammenhangstreuen Abbildungen". In: *Mathematische Annalen* 97.1 (1927), pp. 454–472.

[28] A. Zomorodian and G. Carlsson. "Computing persistent homology". In: *Discrete & Computational Geometry* 33.2 (2005), pp. 249–274.